POLITECNICO DI MILANO

SCHOOL OF INDUSTRIAL AND INFORMATION ENGINEERING

Master of science program Nuclear engineering

ANALYSIS OF MODIFIED PASSIVE SAFETY SYSTEM IN FAST REACTOR

Relatore: Antonio Cammi

Master thesis:
Carlo Oggioni
Matr. 875683

Academic Year 2019 - 2020

Abstract

This Internship was performed at the Department of Nuclear Engineering at the University of California Berkeley. My project was to analyze a modified nuclear passive safety system, called ARC system, into Sodium-cooled Fast Reactors (SFR). The modifications of the system have been proposed to reduce the oscillation behavior witness in previous work [5]. The first months of this project were based on the coupling of two nuclear codes. I used an external coupling paradigm. I wrote a Python script that exchanges data by performing input/output on files specific to each code. Ones the coupling was finished, I simulate different accidents for two SFRs evaluating the results. In all the transient tested during this work the modifications have provided remarkable benefits and they have reduce the oscillation behavior

Keyword: Nuclear energy, Passive safety system, ARC system, Coupling of codes, Sodium-cooled Fast Reactors.

Estratto

Il progetto di tesi si è svolto presso il dipartimento di ingegneria nucleare all'università di Berkeley, in California. Il lavoro si è focalizzato sullo studio di un sistema di sicurezza passivo soggetto ad alcune modifiche. Queste modifiche sono state proposte per ridurre un fenomeno oscillatorio evidenziato in precedenti studi [5]. Durante questo lavoro due codici nucleari sono stati utilizzati. Una parte importante di questo progetto è stata l'accoppiamento dei due codici. Dopo aver varato varie possibilità, si è scelto di adottare un accoppiamento esterno realizzato medianto un script di Phyton. Questo script ha coordinato lo scambio di dati mediante un approcio ingresso/uscita nei file specifici per ogni codice. Pertanto, lo script Python è stato utilizzato per lo scambio di dati tra SAS e SAM per ogni passo temporale. Per essere certi della convergenza dei due codici, delle iterazione Picard sono state implementate nello script di Phyton. Successivamente si sono simulati diversi incidenti per due reattori a neutroni veloci di riferimento. Dai risultati ottenuti si è potuto constatare che le modifiche apportate al sistema forniscono notevoli benefici e riducono il comportamento oscillatorio.

Parole chiave : Energia nucleare, sistema di sicurezza passiva, sistema ARC, accoppiamento di codici, reattori veloce raffreddato al sodio

Ampio estratto della tesi in lingua italiana

Presentazione del sistema ARC

Il progetto di tesi si è svolto presso il dipartimento di ingegneria nucleare all'università di Berkeley, in California. Il lavoro, durato da Aprile a Settembre 2019, si è focalizzato sullo studio di un sistema di sicurezza passivo soggetto ad alcune modifiche. Questo sistema, chiamato Autonomous Reactivity Control (ARC), è stato ideato per reattori a neutroni veloci. Questi particolari reattori sono caratterizzati da un coefficiente di vuoto positivo [2]. Il sistema ARC è stato proposto come un ulteriore feedback negativo, che possa compensare le controreazioni postive durante i vari transitori accidentali. Il sistema è stato ideato come modifica di un fuel rod negli assemblies, come si può notare in Figura 1.

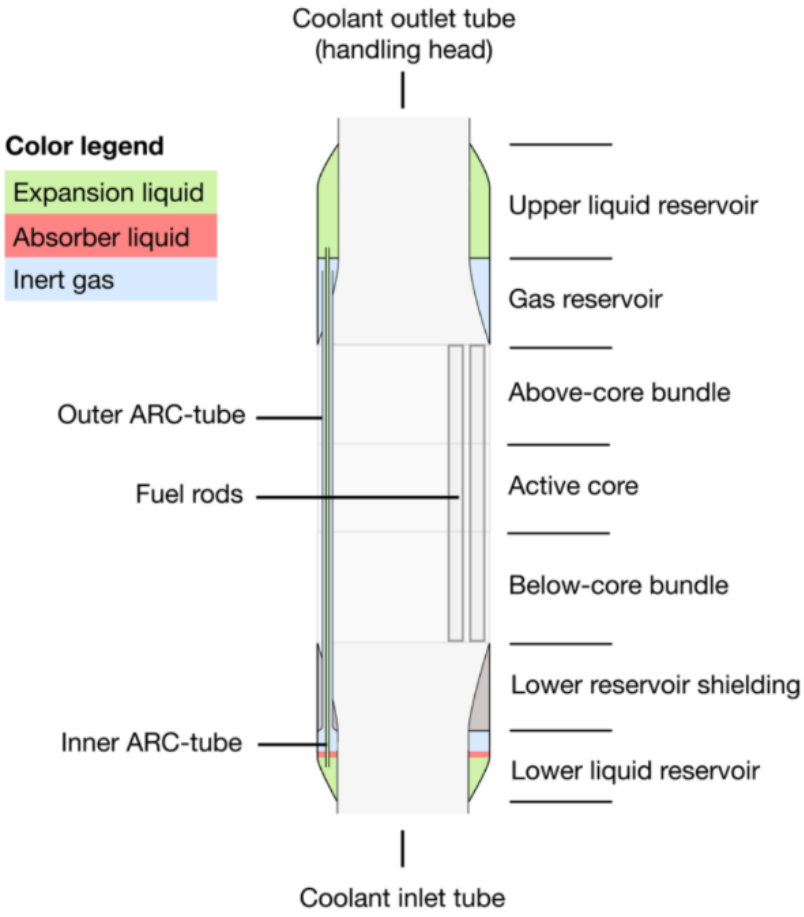

Figure 1: Fuel assembly con l'introduzione del sistema[5]

Dall'immagine si può notare che l'ARC è suddiviso in due parti, nella parte superiore troviamo due serbatoi, une riempito di liquido e uno di gas. Questi due serbatio sono

divisi da una lastra come si può notare in Figura 2. Invece, nel serbatoio inferiore i liquidi sono stratificati uno sopra l'altro senza nessuna divisione fisica. La parte inferiore e la parte superiore sono collegati tramite due tubi concentrici. Il sistema è costituito da tre fluidi. Il liquido d'espansione è presente nella parte superiore, nel tubo interno e anche nel serbatoio inferiore. Il liquido assorbente è presente nel serbatoio inferiore. Infine il gas inerte è presente nelle altre componenti.

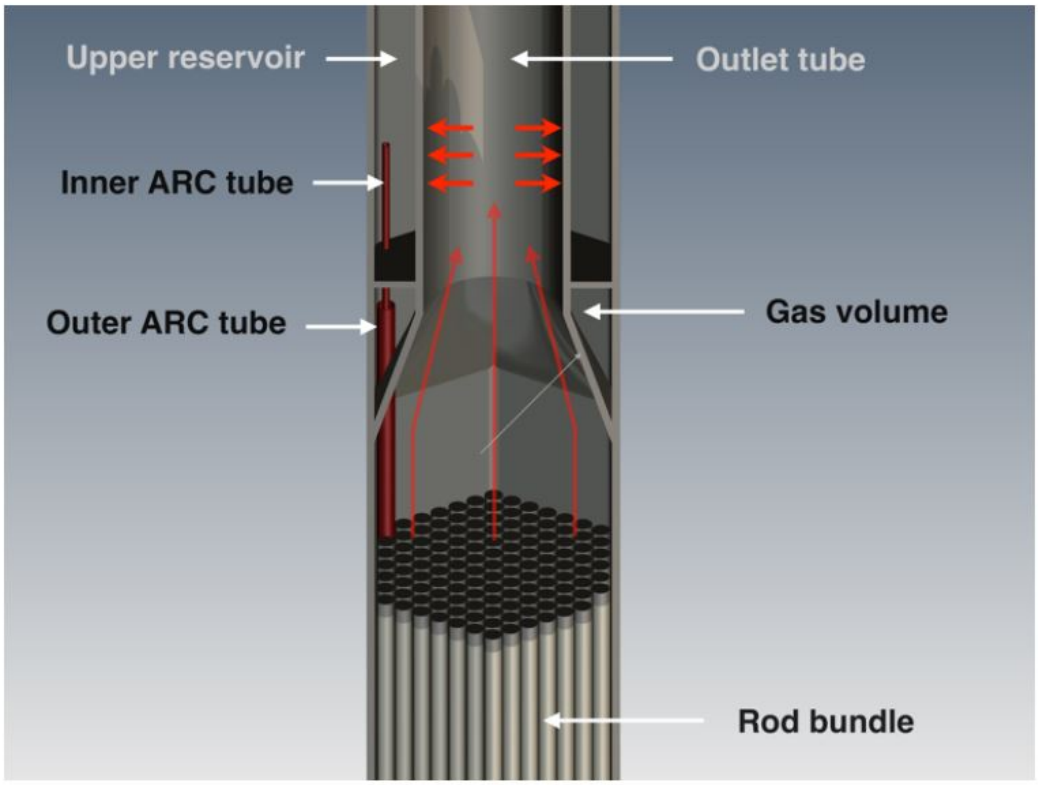

Figure 2: Fuel assembly modificato con il sistema ARC [5]

La scelta dei fluidi è essenziale. Prima di tutto i fluidi devono essere opportunamente stratificati. Ciò significa che il liquido assorbente deve rimanere sopra liquido di espansione e anche che i due liquidi devono essere in gran parte immiscibile. Poi, il liquido assorbente deve inserire una forte reattività negativa, mentre gli altri fluidi devono essere neutronicamente inerti. Infine, i liquidi devono rimanere nella fase corretta durante tutti i transitori. Tenendo conto di queste considerazioni [5], i fluidi adeguati sono: potassio come liquido di espansione, litio come liquido assorbente, elio come gas inerte. Durante uno transitorio accindetale, il sistema ARC si comporta nel seguente modo:

1. A causa dell'incidente la temperatura nel nucleo aumenta, e di conseguenza, il refrigerante si riscalda.

2. Il refrigerante riscaldato scambia calore con il serbatoio superiore, in particolare con il liquido di espansione.

3. Il liquido di espansione nel serbatoio superiore si espande termicamente, una parte del liquido di espansione, presente nel serbatoio superiore, entra nel serbatoio inferiore.

4. Il liquido di espansione spinge il liquido assorbente nel nucleo mentre il gas inerte di cui sopra viene compresso.

5. Il liquido assorbente assorbe neutroni nel nucleo, introducendo una reattività negativa che provoca una riduzione della temperatura e della potenza.

6. Quando il nucleo si raffredda, la temperatura del liquido di espansione inizia a scendere, si contrae e il livello del liquido assorbente inizia a diminuire. Questo effetto fornisce una reattività positiva. La potenza e la temperatura aumentano fino a quando il sistema raggiunge una configurazione stabile.

Quanto descritto finora rappresenta il design iniziale dell'ARC. Questo sistema è stato analizzato in precedenti lavori [5]. Questi studi hanno mostrato i benefici forniti da questo sistema analizzando le risposte a vari transitori accidentali in due reattori a neutroni veloci. Questi studi, hanno anche evidenziato il verificarsi di un fenomeno oscillatorio tra la temperatura e la reattività dovuto all'inserimento e all'estrazione del litio del sistema ARC . La ragione di questo comportamento è il forte legame tra l'ARC e le fluttuazioni della temperatura. Il sistema ARC è progettato per essere fortemente accoppiato ad un aumento della temperatura del nucleo al fine di fornire reattività negativa durante i transitori. Una volta che il nucleo diminuisce la sua temperatura, grazie al forte accoppiamento, il liquido assorbente viene disinserito, e questo fornisce una reattività postitiva e dunque un aumento delle temperature del nucleo. In certe condizioni, questo processo si ripete, portando ad un comportamento oscillatorio che conduce all'ebollizione del refrigerante. Pertanto, si desidera rimuovere tali oscillazioni utilizzando un metodo per distinguere l'inserzione e l'estrazione del liquido assorbente. Per raggiungere questo obiettivo, è stata proposta l'introduzione di una valvola unidirezionale nel tubo interno. Questo tipo di valvola consente un normale flusso in una direzione, ma lo ostacola nella direzione opposta, comportandosi come un diodo idraulico. Pertanto, l'inserimento del veleno neutronico è ancora veloce, ma il ritiro è ostacolato, lasciando il litio per più tempo all'interno del nucleo e potenzialmente eliminando le oscillazioni. Riassumendo, la valvola unidirezionale incide sulla velocità di attivazione del sistema ARC, ritardando l'estrazione del litio. Per garantire il corretto funzionamento della valvola unidirezionale, è necessario un volume di gas nella parte superiore, che era rimpita di liquido nel precedente design. Questo nuova componente gassosa si appoggia al di sopra del potassio, non vi è dunque nessusa separazione fisica.

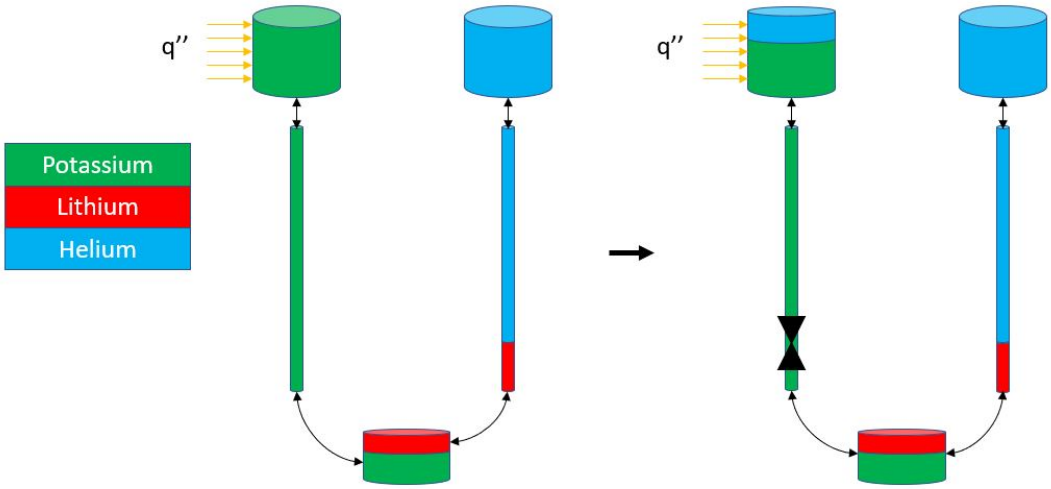

Figure 3: Sistema ARC modificato

In Figura 3 è presentato un diagramma approssimativo del sistema ARC. I due tubi concentrici sono separati e la parte superiore è separato nei due serbatoi. In questo diagramma approssimativo vengono mostrate le modifiche del sistema ARC. Come si può vedere nella parte superiore, è indcata una condizione limite di calore per mostrare l'accoppiamento tra l'ARC e il reattore. Nel sistema ARC vari parametri possono essere modificati, queste diverse scelte di progettazione si combinano nei seguenti parametri: (1) valore totale della reattività inserita dall'ARC (w [$]), (2) Volume di gas aggiunto nel serbatoio superiore (Cover-volume $[m^3]$), (3) Coefficienti di perdita di pressione per le diverse direzioni per la valvola unidirezionale ($K_{inse} - K_{estra}$)

Codici utilizzati

Nel corso di questo progetto sono state testate le prestazioni del sistema ARC modificato, simulando diversi incidenti per due reattori di riferimento. In questo lavoro si sono utilizzati due codici. Per valutare la risposta dinamica dei reattori è stato utilizzato il codice SAS4A/SASSYS-1 (chiamato SAS per semplicità), mentre per la fluidodinamica all'interno del sistema ARC è stato adottato il codice SAM. Una parte importante di questo progetto è stata l'accoppiamento dei due codici. Dopo aver varato varie possibilità, si è scelto di adottare un accoppiamento esterno realizzato mediante un script di Phyton. Questo script ha coordinato lo scambio di dati tramite un approcio ingresso/uscita su file specifici per ogni codice. Pertanto, lo script Python è stato utilizzato per lo scambio di dati tra SAS e SAM per ogni passo temporale ed è stata utilizzata la modalità RESTART dei due codici. Con questa modalità, i calcoli del codice partono da un file RESTART generato alla fine del passo temporale precedente. L'accoppiamento è delineato in Figura 4.

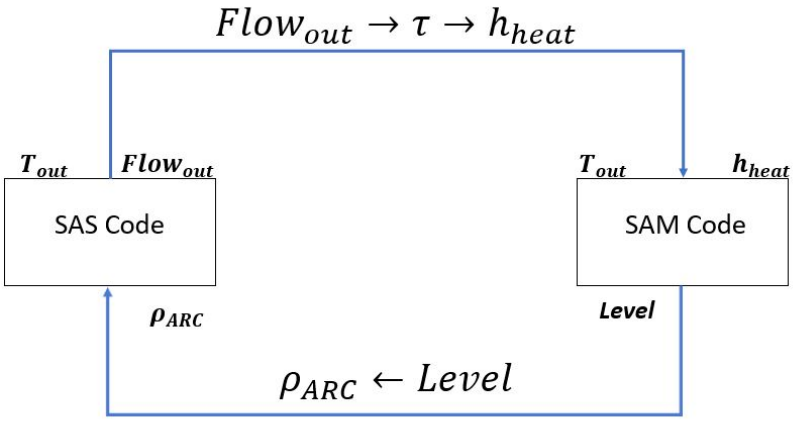

Figure 4: Accoppiamento dei codici

Da SAS, la temperatura e il flusso in uscita sono ottenuti. Il flusso è poi convertito nel coefficeinte di scambio termico tra il refrigerante e il serbatoio superiore. Questi due informazioni sono nesessarie come input per SAM. Da SAM, il livello del liquido assorbente è ottenuto e poi convertito nella reattività inserita dall'ARC. La reattività viene poi utilizzata come ingresso in SAS. Per essere certi della convergenza dei due codici, delle iterazione Picard sono state implementate nel script di Phyton. La Figura 5 rappresenta ciò che accade ad ogni passo tempoarle, il codice SAS viene eseguito almeno due volte. La prima volta con la reattività calcolata nel passo temporale precedente e la seconda con la reattività ottenuta nel passo temporale in questione. La convergenza è valutata comparando le temperature d'uscita del refrigerante ottenute dai codici SAS. Quando l'errore percentuale tra le due temperature è superiore a un certo limite ($err_{limit} = 10^{-4}$), la seconda temperatura viene utilizzata come nuovo input nel codice SAM e la convergenza viene nuovamente valutata.
Questo tipo di approcio è molto generale perchè non richiede l'accesso ai codici sorgente, dunque può essere effettuato su vari tipi di codici, non solamente su questi in questione. Il processo, però, risulta lento per l'inizializzazioni di ogni codice ad ogni passo temporale.

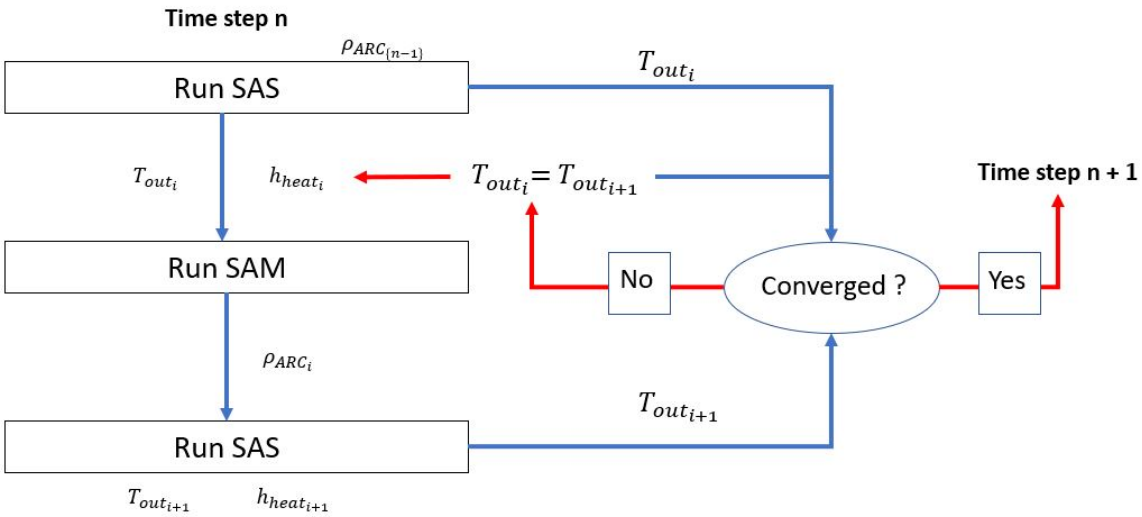

Figure 5: Iterazionei Picard utilizzate nel coupling esterno

Reattori e transitori di riferimento

Per valutare i benefici del sistema ARC sono stati scelti due reattori a neutroni rapidi rafferddati con sodio liquido. Il primo reattore di riferimento è un burner (ABR) di medie dimensioni progettato da Argonne National Laboratory e il secondo è reattore Breed and Burn (B&B) progettato da Argonne National Laboratory e dall'università di Berkeley. Il reattore B&B è caratterizzato da combustibile metallico e da un nucleo più grande. Il nucleo del reattore B&B non presenta la solita forma allargata dei reattori veloci. Questa scelta è voluta per limitare le perdite. Queste scelte di progettazione portano ad un coefficiente di vuoto fortemente positivo per il reattore B&B. Questa carattersitica può risultare problematica dal punto di vista della sicurezza passiva, quindi un ulteriore feedback negativo risulta necessario per questo reattore. Per valutare le prestazioni dei reattori tre diversi transitori sono stati esaminati: la non protetta perdita di scambiatore di calore (ULOHS), la non protetta perdita di flusso (ULOF) e la non protetta estrazione di barra di controllo (UTOP). Il termine "non protetto" implica che lo scarm del reattore non si verifica.

Risultati

Per il reattore ABR, senza l'introduzione del sistema ARC, l'ebollizione del refrigerante non si verificava in nessun transitorio testato. Con l'introduzione del sistema si sono guadagnati margini all'ebolizzione. Con il sistema modificato i margini sono aumentati. Per ottenere la configurazine con i margini più elevati diversi studi parametrici sono stati realizzati.
Per il reattore B&B, senza l'ARC l'ebollizione avviene per i tranistori UTOP e ULOF.

Con l'introduzione del sistame, l'ebollizione è stata evitata per il trasitorio UTOP, ma non per l'ULOF. Nel transitorio ULOF, si suppone che i motori delle pompe si arrestano immediatamente. Le giranti rallentano fino a raggiungere un valore dove improvvisamente vengono fermate, in quel momento si verifica il passaggio da circolazione forzata a la circolazione naturale. Quando avviene il passagio a circolazione naturale si verifica un improvviso calo del flusso, in questo transitorio il passaggio avviena a circa 1000 s come si nota dalla Figura 6. Senza la presenza dell'ARC, Figura 6, dopo il calo di flusso si verificano delle oscillazioni temperatura-reattività. Queste oscillazioni comportano l'ebollizione del refrigerante dopo circa 20 minuti.

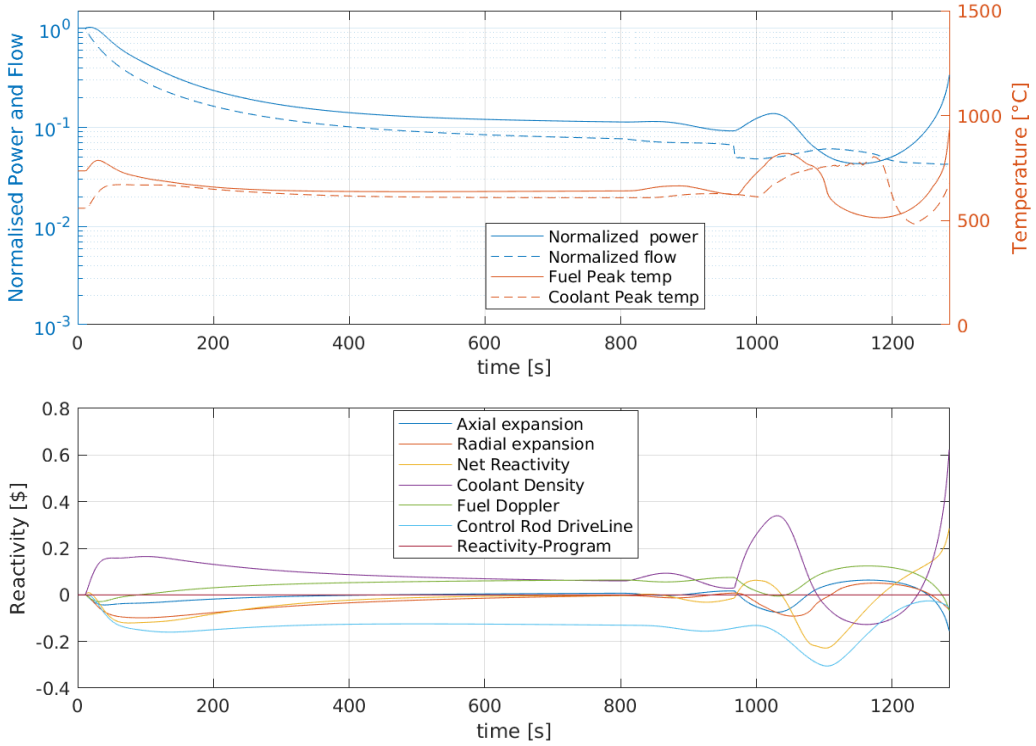

Figure 6: Risposta a un incidente ULOF nel reattore B&B senza sistema ARC.

L'introduzione del sistema ARC senza modifiche non comporta nessun beneficio, il comportamento oscillatorio risulta infatti peggiorato e l'ebollizione avviene dopo circa 9 minuti. In Figura 7 è mostrato il grafico delle controreazioni con l'introduzione del sistema ARC senza modifiche.

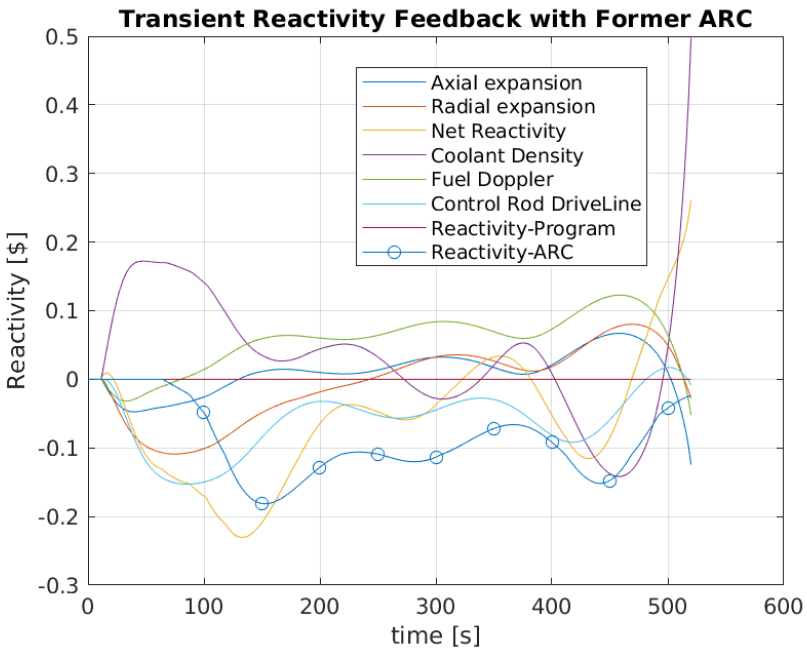

Figure 7: Risposta a un incidente ULOF nel reattore B&B con il sistema ARC senza modifiche.

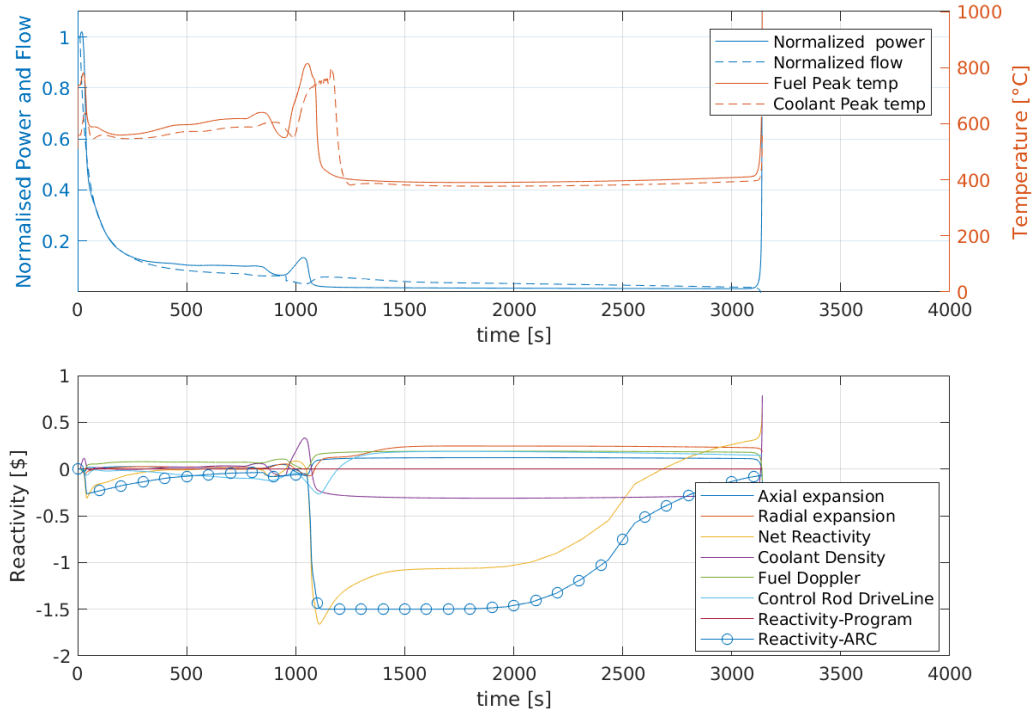

Figure 8: Risposta a un incidente ULOF nel reattore B&B con il sistema ARC modificato.

La Figure 8, mostra invece la risposta con l'introduzione del sistema ARC modificato. Si può notare l'aumento della temperatura causato dal passaggio alla circolazione naturale ($\sim$ 1000 s). Con questo aumento, l'ARC viene completamente attivato e si comporta come uno SCRAM prevalendo su tutti gli altri effetti di feedback. Così la reattività netta scende a $\sim$ \$ -1,6 , questo calo riduce fortemente la potenza e le temperature. Pertanto il sistema ARC sarebbe disinserito a causa della riduzione della temperatura del refrigerante. Tuttavia, si può facilmente notare una netta differenza tra l'inserimento e l'estrazione di anti reattività dell'ARC grazie alla valvola unidirezionale che ostacola l'estrazione. Si può infatti notare un ritardo di $\sim$ 1000 s tra il calo della temperatura e l'estrazione del liquido assorbente. A $\sim$ 2000 s il liquido assorbente inizia ad essere estratto e la reattività netta inizia ad aumentare, fino a raggiungere un valore positivo ($\sim$ 2700 s). Essendo la reattività netta positiva, la potenza di fissione aumenta. Tuttavia, questo aumento non è osservabile se si osserva la curva della potenza totale a causa della forte differenza ($\sim$ 6 ordine di grandezza) tra la potenza di decadimento e la potenza di fissione. Le diverse potenze sono mostrati in Figura 9.

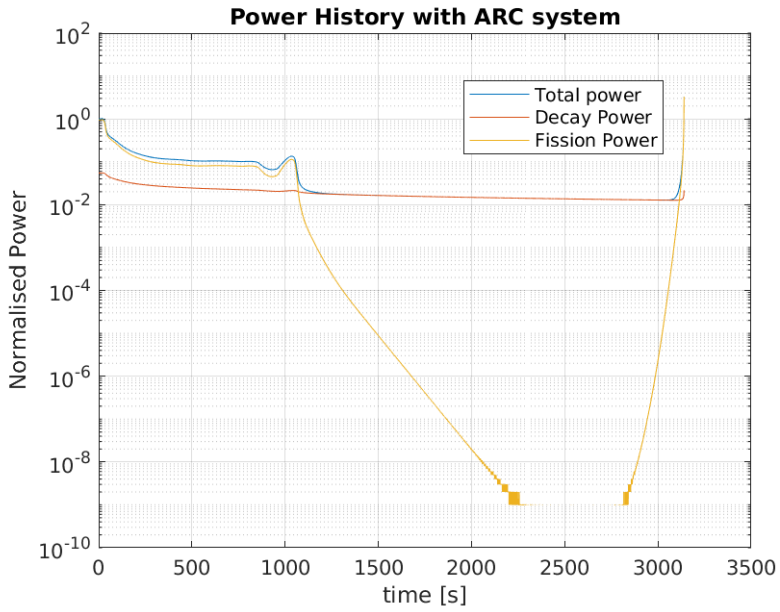

Figure 9: Potenza per il transitorio ULOF nel B&B reattore con l'aggiunta del sistema ARC modificato

Una volta che la potenza di fissione raggiunge la potenza di decadimento, anche la potenza totale inizia ad aumentare, ma con un'andamento così rapido che gli altri feedback non hanno il tempo di compensare la reattività netta positiva, la temperatura dunque aumenta comporantando l'ebollizione del refrigerante.
Per questo incidente è stato effettuato uno studio parametrico per valutare se si potesse evitare l'ebollizione. Ma in ogni configurazione testata l'ebollizione del refrigerante si

è sempre verificata.

Conclusioni

Questo lavoro mirava ad analazzare il sistema ARC modificato per ridurre il comportamento oscillatorio notato negli studi precedente. Come si è visto dai risultati, le modifiche del sistema fanno si che per fluttuazioni di temperatura del refrigerante, il liquido assorbente rimane costante allo stesso livello impedendo le conseguenti oscillazioni di reattività ARC. Questa modifiche riducono il comportamento di oscillazione e impediscono l'ebollizione generate da queste oscillazioni. Nel caso ABR, il sistema ARC modificato ha permesso di esplorare una configurazione più ampia dei parametri, rispetto al lavoro precedente [5], consentendo di ottenere margini ancora più elevati. Lavori futuri potrebbero estendere il dominio dei parametri per ottenere margini più elevati. Per il reattore B&B, il sistema ARC modificato ha evitato l'ebollizione per il transitorio UTOP, ha aumentato i margini nel transitorio ULOHS. Ha inoltre aumentato il tempo di ebollizione nell'ULOF, ma non è stata trovata alcuna configurazione per evitare l'ebollizione in questo transitorio. Tuttavia, contrariamente ai lavori precedenti, l'ebollizione non è causata dal fenomeno oscillatorio, ma è generata dal disinserimento del sistema ARC che impedisce il raggiungimento di una condizione stabile. Dunque questo lavoro sottolinea i possibili problemi causati dall'estrazione del liquido assorbente. Il sistema ARC è stato pensato per essere un sistema di sicurezza passiva che fornisca anti reattività, ma anche che la ritiri una volta che il reattore si raffredda. L'incidente ULOF nel reattore B&B è stato l'unico transitorio in cui è stato testato il disinserimento dell'ARC. Pertanto, i lavori futuri potrebbero incentrarsi sullo studio di questo fenomeno, ad esempio simulando incidenti che durano per un periodo di tempo limitato, per analizzare l'evoluzione dei transitori.
Possiamo infine concludere che in tutti i transitori testati durante questo lavoro le modifiche apportate al sistema hanno fornito notevoli benefici.

Acknowledgements

Before I get into my topic, I would like to express my gratitude to my tutor prof. Massimiliano FRATONI, Associate Professor of University of California, Berkeley, for the internship opportunity he offered me, for his advice, assistance and for facilitating my integration into his Section. I would also like to thank Christopher KECKLER, Ph.D. student at the University of California, Berkeley, for his advice and availability, allowing me to develop skills in the field of sodium-cooled fast reactors. I would also like to thank any members of the Department of Nuclear Engineering section for their welcome and availability. My gratitude goes to INSTN university, in particular to Mrs. Constance COSTON, director of training and education, for the financial assistance that allowed me to have this experience. My heartfelt thanks goes to my Italian university POLITECNICO DI MILANO, for the opportunity of the double degree and in particular to my tutors prof. Antonio CAMMI and prof. Francesca GIACOBBO, for their advice and their availability during my internship. Last but not list, I would like to thank my family for their support and their encouragement during all my years of stud, and also stefano FILIPPI et Federico PETRONIO for these two unforgettable years.

Contents

List of Figures

List of Tables

1 Introduction

This report summarizes the work and results of a 5 month internship, performed from April to September 2019 at the Department of Nuclear Engineering at UC Berkeley. The scope of this project is to contribute to the design of an engineered passive safety system, called the Autonomous Reactivity Control (ARC) system, into Sodium-cooled Fast Reactors (SFRs) aiming to provide negative reactivity feedbacks during transient scenarios. Previous works [5] have demonstrated performance improvements by reducing peak temperatures during a variety of transients, although challenges related to the potential to induce oscillatory behavior have been observed under certain situations. The reasoning for these oscillations is the strong coupling between the ARC system and core temperature fluctuations. This work proposed the use of a one-way valve to eliminate such issues and further enhance the performance of the ARC system.

2 Theory

The first part of this report represents an overview of the Fast Spectrum Reactor field.

2.1 Basic Physics of Fast Reactors

Fast reactors operate with a spectrum of neutrons not slowed down. They are therefore characterized by the absence of a moderator. Their primary advantage is the ability of "breeding", that means to produce new fuel compared to what has been consumed. The processing is held by the conversion of certain isotopes, called fertiles, to fissile isotopes through nuclear reactions. A well known fertile isotope is ^{238}U, it is the most common isotope of naturally occurring uranium, with a relative abundance of 99%. It could capture neutrons and convert into the fissile isotope ^{239}Pu with the following reaction.

$$^{238}U + n \rightarrow {}^{239}U \xrightarrow{\beta^-} {}^{239}Np \xrightarrow{\beta^-} {}^{239}Pu$$

Where β^- stands for the β minus decay [1].
This capture occurs at energies below 1 MeV, as we can see in Figure 10 where the microscopic cross section (σ) of neutronic radioactive capture [1] is showed.

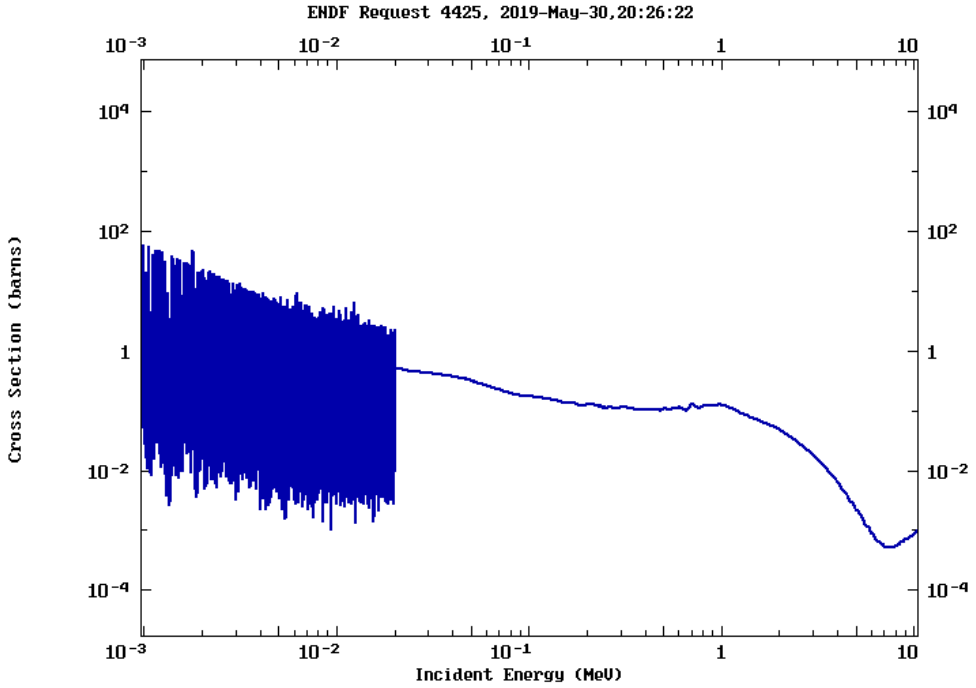

Figure 10: Radioactive capture microscopic cross-section of ^{238}U [3]

The key parameter of breeding technology is the conversion ratio defined as

$$C(t) = \frac{Fissile\ Material\ Produced(t)}{Fissile\ Material\ Destroyed(t)} = \frac{FP}{FD}$$

To obtain a breeding reactor this value has to be greater then 1. Another important value for these reactors is the Reproduction Factor (η), present in the four factors formula[2] and defined as

$$\eta(E) = \frac{\Sigma_F}{\Sigma_f + \Sigma_c}\nu$$

Where Σ is the macroscopic cross section [1], f stands for fission, c for capture and ν is the number on neutrons emitted in the fission reaction. The Reproduction Factor represents, for each isotope, the number of neutrons emitted in the fission reaction per neutron absorbed. To obtain a breeding reactor this value has to be greater than 2 because one neutron is used to breeding, one to sustain the chain reaction and a margin is needed for all the parasitic absorptions and leakages.

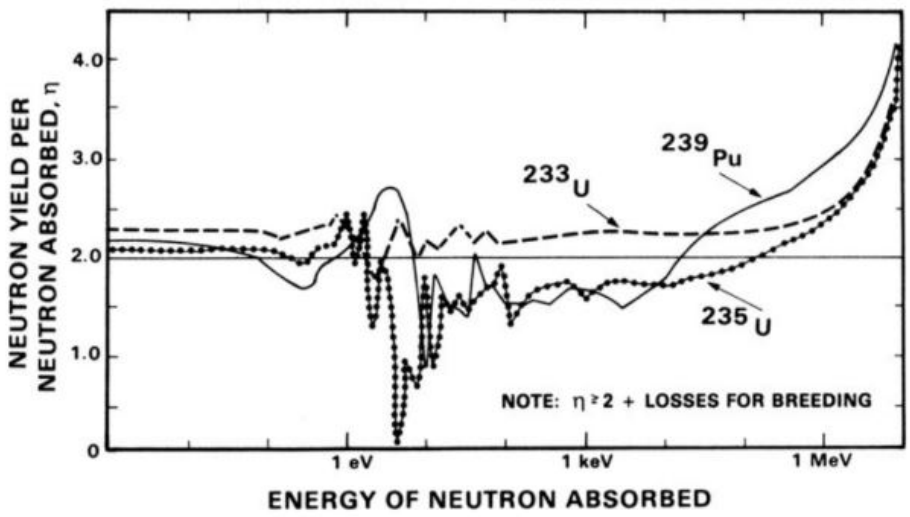

Figure 11: Neutrons produced per absorption vs. energy for fissile isotopes [2]

As we can see in Figure 11, the value of η for the fissile isotope ^{239}Pu is greater in the fast region. Therefore fast reactors, using the ^{238}U-^{239}Pu couple, could be breeder reactors. Moreover, this technology employed the same fuel cycle as the present commercial thermal reactors, for example this breeding couple is already used in MOX fuel technology in French reactors [11]. Plus, using this technology in fast reactors the energy potential of uranium increases significantly (by a factor of approximately 60) compared to light water reactors (LWRs) [2]. Another important characteristic of a fast reactor is the possibility of reducing the radiotoxicity of nuclear waste, through the fission of minor actinides and plutonium. Minor actinides represent only a small percent

($\sim 0.1\%$) of nuclear waste [11], but they have a long half-life and they decay mainly via α decay[1], that is the most radiotoxic decay if the isotope is ingested. For these reasons, they are considered High Level Waste (HLW), same as Haute Activité (HA) in French's classification [11]. As we can see in Figure 12, for the minor actinides and the plutonium the ratio fission over absorption is greater in SFR than in Pressurized Water Reactor (PWR). Thus, the fast spectrum reactor has the flexibility to operate either as a burner to fission long-lived isotopes, converting them into short-lived ones, or operate as a breeder to achieve the net creation of fissile fuel.

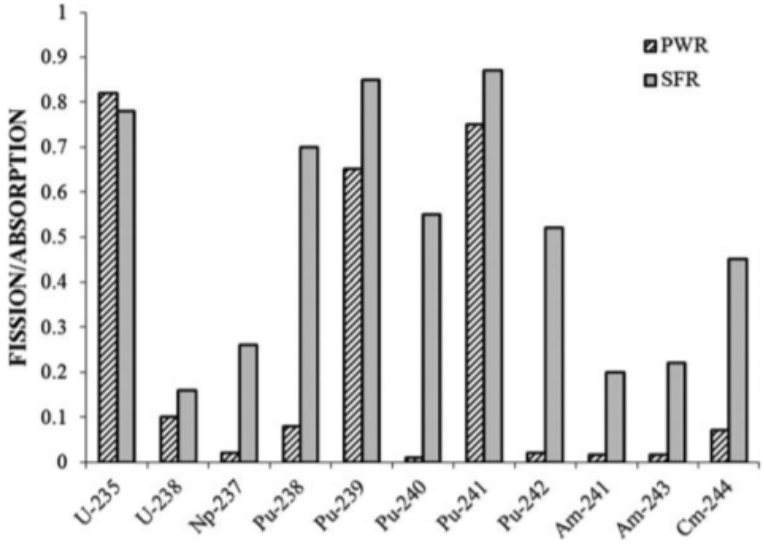

Figure 12: Fission to absorption ratio [2]

2.2 Reactivity Feedback

2.2.1 Doppler effect

The Doppler effect is a reactivity feedback driven by the fuel temperature. As mentioned in the section before, some isotope could capture neutrons having a high neutronic absorption cross-section. At low energy the absorption cross-section has a resonance shape, in Figure 10 we can notice the resonances region at energies below 5×10^{-2} MeV. With an increase of temperature, therefore with an increase of the thermal movements of the target nuclei, the resonance sections seen by the neutrons become wider. This is illustrated in Figure 13, where for three different temperatures the resonance of ^{238}U is shown. This broadening leads to a negative reactivity because more neutrons are absorbed by the resonance. This coefficient is also called the prompt temperature coefficient because it causes an immediate response to changes in fuel temperature.
This effect strongly depends on the temperature that the fuel can reach, the Doppler

effect in metallic fuel is less important than in oxide fuel. This effect depends also on the neutron spectrum of the reactor. The more important adsorption resonances are located at low energy, for example in Figure 13 the resonance absorption is located at 6.67 eV. Therefore the Doppler effect is less strong in fast spectrum reactors.

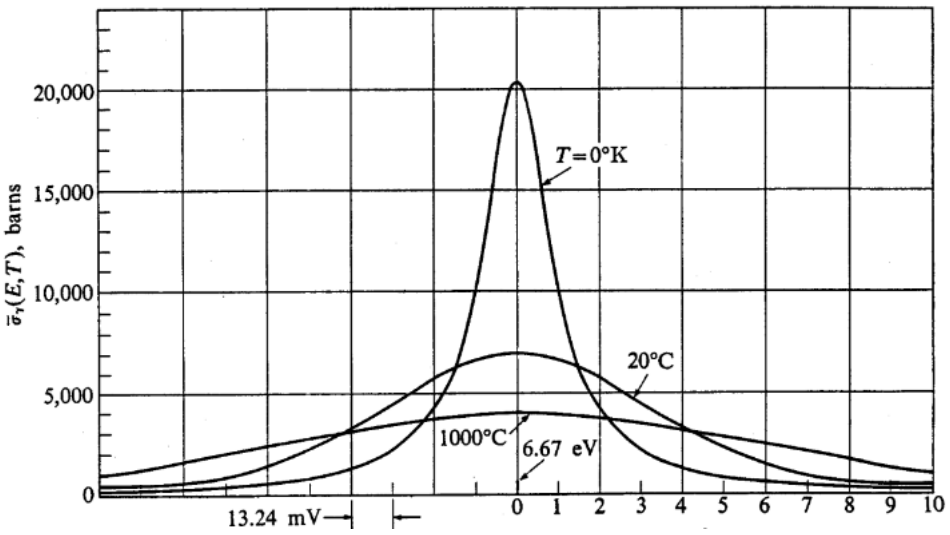

Figure 13: Doppler broadening of a capture cross section of ^{238}U of 6.67 eV [4]

2.2.2 Control rod DriveLine

One important effect in SFRs is the control rod drive line feedback. The sodium is chosen as a coolant because it has low neutron absorption and scattering cross-section. Moreover, being a liquid metal, it's characterised by a high thermal conductivity $\sim$ 65 W/mK at $\sim$ 600°C [16]. Therefore all the mechanical components in thermal contact with the sodium receive a significant heat flux for a change in sodium temperature. One component washed by the outlet coolant from the core is the control rod drive. Then, a rise of the outlet temperature implies an expansion of the control rod driveline that causes the control rod to be inserted further into the core, providing a negative reactivity. This effect is limited by the heating of the vessel walls that causes the whole core to move down or the control rod support to raise, leading a positive reactivity effect.

2.2.3 Core radial expansion

Another reactivity feedback related to the high thermal conductivity of sodium is the radial expansion of the core. Plus, fast reactors are more sensitive to change in core geometry because of the large neutron mean free path length. The radial expansion is mainly driven by the expansion of the lower grid support and by the expansion of the duct walls. The first expansion is proportional to the rise of the inlet temperature,

the second is proportional to the change in average structural temperatures. Radial expansion of the core will yield a more important leakage of neutrons and therefore a negative reactivity. On the other hand, a shrink of the core provides a positive reactivity.

2.2.4 Fuel Axial expansion

Contrarily to the radial expansion, the axial growth is driven by the fuel and cladding temperatures. Axial expansion can also depend on the cladding property if, during the transients, the fuel comes in contact with the cladding. Like the Doppler effect, the fuel axial expansion feedback provides a prompt effect. Fuel compaction leads to a positive reactivity effect, while fuel expansion results in a negative effect.

2.2.5 Coolant density

When the temperature of the coolant increases its density decreases. In LWRs the decrease of density involves two opposite effects. With less moderation, the neutrons will stay longer at resonance energy where the neutron absorption cross section is high [1]. This will provide a negative reactivity. On the other hand with the decrease of coolant density, the coolant parasitic captures will decrease as well, providing a positive reactivity. The LWRs are designed to be under moderated, that means that the negative effects are prevalent and so an increase of coolant temperature leads to a negative reactivity effect. For fast reactors, the decrease of moderation will harder the spectrum and, contrary to LWRs, will provide a positive reactivity. As we can see in Figure 11 the increase of reactivity is mainly due to the value of η. The other phenomena that contribute to the overall density effect are the variation of leakages, the change in parasitic absorption within the coolant and the change in self-shielding. The most important phenomenon that could ensure a negative effect, when the coolant heads up, is the increase of leakages. Having this strong bond with leakages, this feedback effect is extremely space-dependent.

3 Presentation of the ARC system

As we presented in Section 2.2.5, the coolant void feedback could be positive, this could lead to an overall positive net reactivity in the accident with a high loss of coolant. The situation gets worse as core size increases. With a bigger core, the coolant void reactivity feedback becomes more positive, because the leakage effect is reduced. For this reason, the ARC system has been proposed to provides another negative feedback mechanism to counter the positive feedback.

3.1 Former ARC system

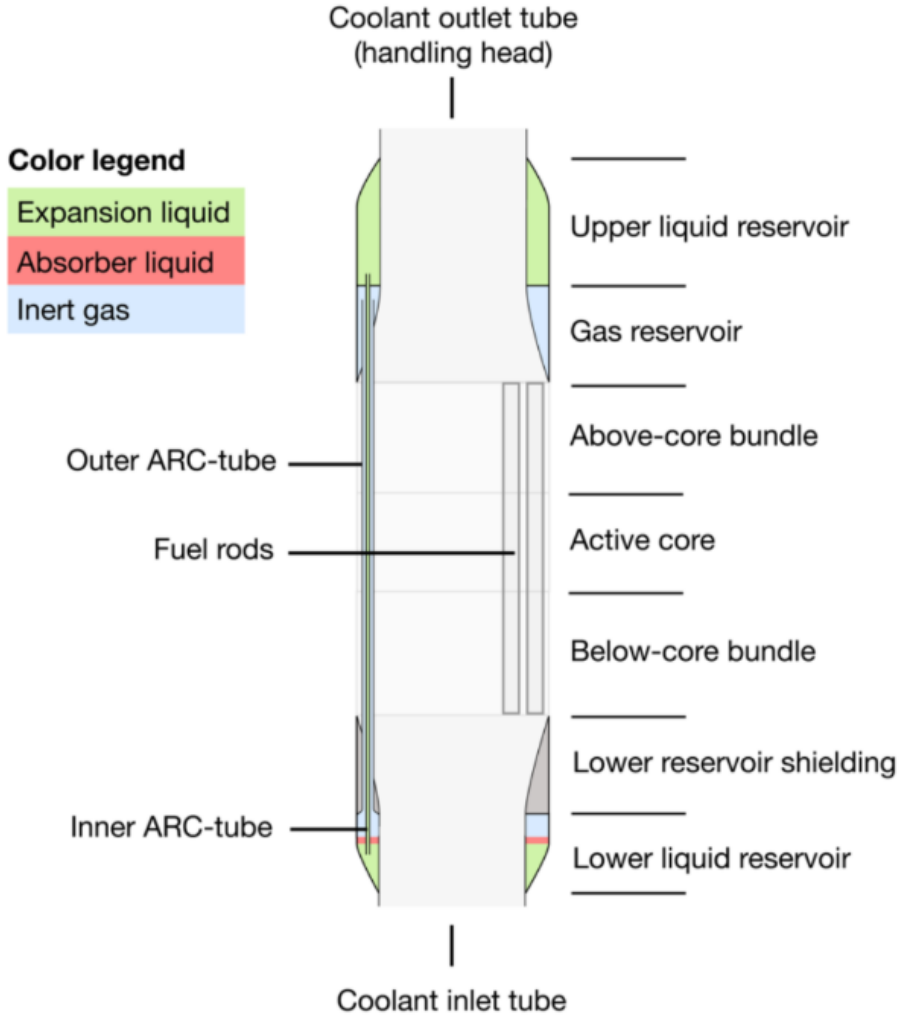

Figure 14: Fuel assembly modification with the ARC system[5]

In the ARC system, a neutron poison, an absorber fluid, is passively inserted and

retracted in response to changes in core temperature. The ARC system is installed as a modification to a conventional SFR fuel assembly design. We can see a fuel assembly modification in Figure 14. The system consists of two reservoirs, located at the bottom and top of the assembly. The lower reservoir contains only liquids while the upper one contains liquids and gas. The two reservoirs are link with two concentric tubes.

3.1.1 Materials Selection

The ARC system is composed of three fluids. The choice of fluids is really essential. First of all the fluids need to be properly stratified. That means that the absorber liquid has to sit on the expansion liquid and also they have to be largely immiscible. Then, the absorber fluid has to insert a strong negative reactivity while the other liquids have to be neutronically inert. Finally, the liquids have to remain in the proper phase during all transients situations Taking into account these considerations, the recommended material selections are [5].

- Expansion liquid: Potassium
- Inert Gas: Helium
- Absorber liquid: Lithium

As regards lithium, in nature it is composed of two isotopes: ^{6}Li and ^{7}Li. The absorber one is the ^{6}Li. Therefore the reactivity worth of the ARC system depends on the enrichment of lithium. The process of isotopic separation of lithium is called COLEX. This process uses the greater affinity of ^{6}Li than ^{7}Li for the element mercury to separate them. The ^{6}Li nuclear reaction is the following:

$$^{6}Li + n \rightarrow {}^{4}He + {}^{3}H + 4,78Mev$$

As we can notice, the nuclear reaction produces gas and tritium. Therefore, the addition of the ARC system increases the level of tritium in the reactor. Tritium is already present as a fission product and thought $^{10}B(n, 2\alpha)^{3}H$ reaction in control rod material. An accurate study of the neutronic impact of ARC system has previously been realized[5]. It investigates the neutronic impacts stemming from the inclusion of the ARC system that replaces a fuel rod. This study shows that, even with three fuel pins per assembly replaced by ARC tubes, a large design space exists to tune ARC systems without incurring significant neutronic penalties.
The microscopic cross section of the $^{6}Li(n, \alpha)^{3}H$ reaction is showed in Figure 15.
As we can see, the cross section's peak is located in the epithermal energy region. Same region where the neutron spectrum's peak of fast reactors is located. Different neutron spectrum can be found in previous works [12] [5].

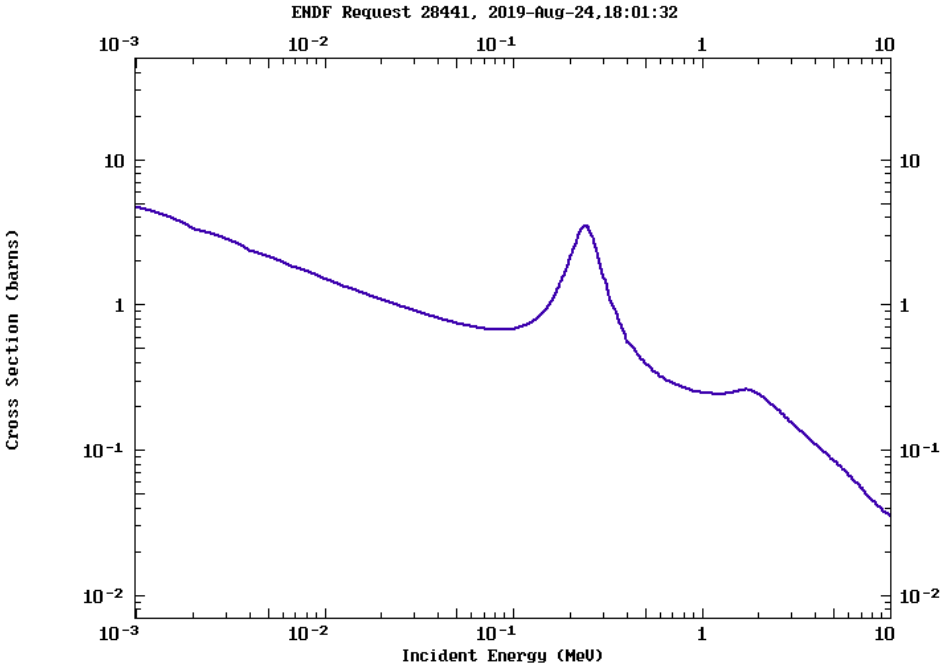

Figure 15: Microscopic cross-section of the reaction $^6Li(n,\alpha)^3H$ [3]

3.1.2 ARC's response

During a transient scenario in the reactor, an ideal ARC system behaves in the following way:

1. Due to the accident the temperature in the core rises, and consequently, the coolant heats up.
2. The heated coolant exchanges heat to the upper reservoir, to the expansion liquid.
3. The expansion liquid in the upper reservoir thermally expands a part of expansion liquid, present in the upper reservoir, will enter the lower reservoir.
4. The expansion liquid pushes the absorber liquid into the active core while compressing the inert gas above.
5. The absorber liquid absorbs neutrons in the core, this will introduce a negative reactivity that causes a reduction in temperature and power.
6. As the core cools down, the temperature of the expansion liquid starts to fall. The expantion liquid contracts and the level of the absorber liquid starts to decrease. This effect provides a positive reactivity. The power and temperature increases until the system reaches a stable critical configuration.

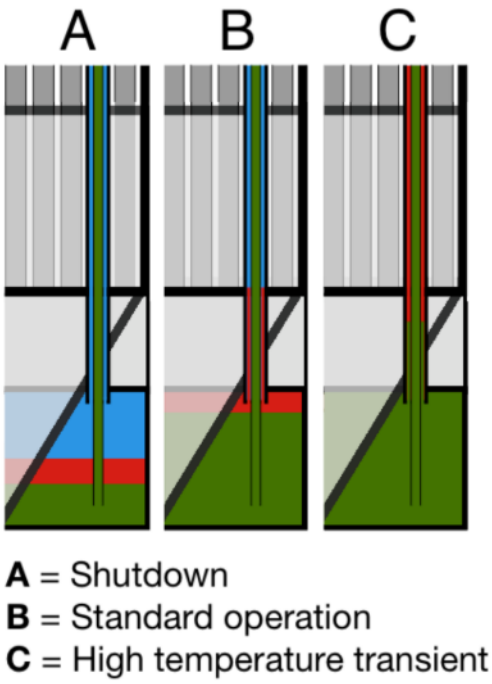

Figure 16: Lower reservoir in different states [5]

The behavior of the lower reservoir, in different states is shown in Figure 16. As we can easily understand, the behavior of the ARC strongly depends on the properties of the components liquids. The main references for the properties of lithium and potassium are: (1) Davison [13]. (2) Jeppson, Ballif, Yuan and Chou [14], and (3) Alcock, Chase and Itkin [15]. The properties of sodium derives from The Sodium-NaK Engineering Handbook [16]

3.2 Modified ARC system

Previous work [5] has shown the effectiveness of the ARC system, in gaining margins to boiling and melting for different accidents. However, it has also underlined an oscillatory behavior that leads to boiling in the B&B Core. The reason for this behavior is the strong coupling of the ARC to fluctuations in core temperature. The ARC system is designed to be strongly coupled to an increase of core's temperature in order to provide negative reactivity during transients. Once the core decreases its temperature, due to the strong coupling, the ARC system will be disengaged, and this provides a positive reactivity and an increase of core's temperatures. Under certain conditions, this process repeats, leading to oscillatory behavior. Therefore, it is desired to remove these oscillations using some method to distinguish the engagement and the disengagement of the ARC. In order to achieve this aim, it was proposed the introduction of a one-way valve in the inner tube. This type of valve would allow unimpeded flow in one direc-

tion but hinder it in the opposite direction, similar to a hydraulic diode. Therefore, the insertion of the neutronic poison is still fast but the withdrawal will be hindered, leaving the lithium for more time in the core region and potentially eliminating the oscillations. The one-way valve impacts the ARC system actuation speed, delaying the disengagement. To ensure the right behavior of the one-way valve, a cover gas is needed in the upper reservoir for the following reason. During a transient the heat received from the coolant expands the liquid present in the upper reservoir generating a flow in the inner tube. Therefore, with the upper reservoir filled with liquid, the flow depends only on the heat exchange. Then the presence of the valve doesn't influence on the flow. And because in the inner tube, the density could be considered constant because the compressibility of liquids is extremely small, the valve doesn't influence on the velocity. Consequently, the valve doesn't have the desired effect. Contrarily, the addition of a volume cover gas in the upper reservoir allows the expansion liquid to head in a different direction. It can expand in the inner tube or it can expand in the upper reservoir compressing the cover gas, with this additional path the flow in the inner tube will depend on the loss coefficient of the valve. Using an electrical analogy, the heat exchanged can be seen as a current generation and the ARC system with the addition of the cover gas volume as a hydraulic current divider in which the current in one branch, that is the flow in the inner tube, depends on resistance of that branch, the resistance is pressure loss of the valve. The simplified electric analogy is shown in Figure 17. It's simplified because the compression of the cover gas will contributes on the flow in the inner tube, therefore the two branches are not exactly in parallel.

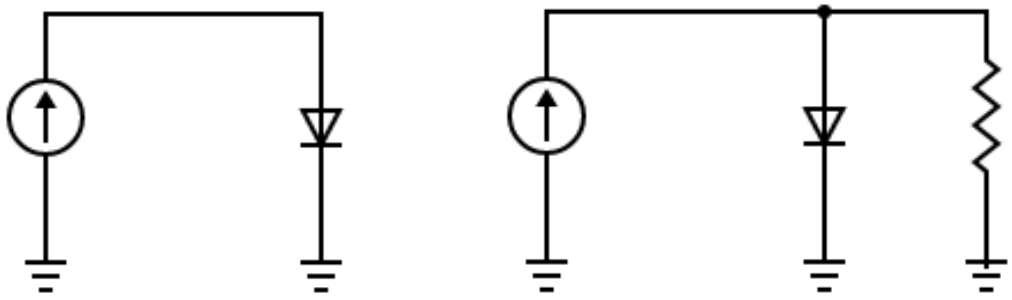

(a) One-way valve introduction (b) One-way valve and cover gas introduction

Figure 17: Simplified Electrical analogy of the modified ARC system

In Figure 18, an approximate diagram of the ARC system is presented. The two concentric tubes are separated and the upper reservoir is shown as two pieces. In this approximate diagram, the modifications of the ARC system design are shown. As we can see in the upper reservoir, a heat boundary condition is set to allow the coupling between the ARC and the coolant temperature.

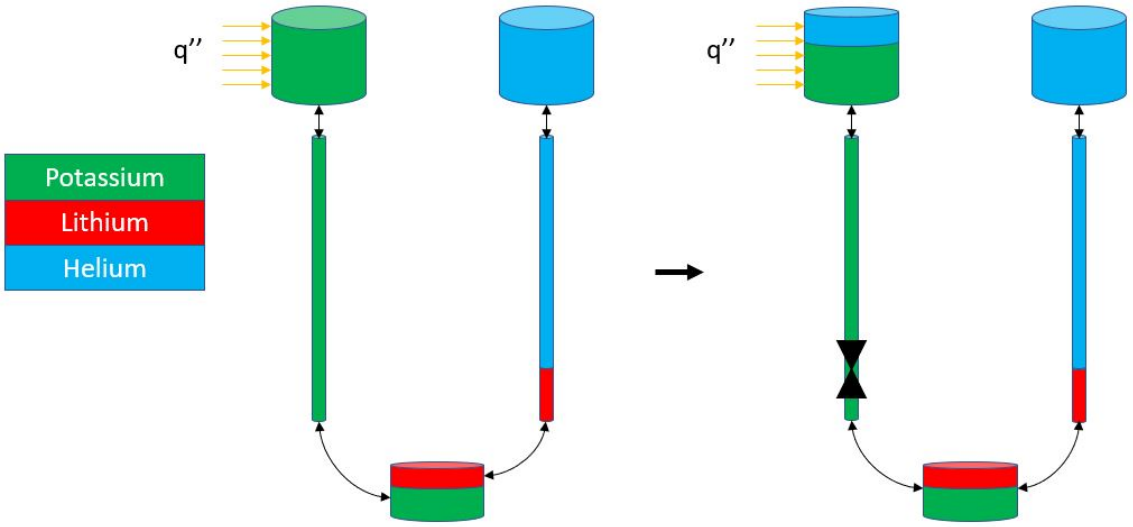

Figure 18: Modification of the ARC system

3.3 Modified ARC Parameters

In the ARC system a number of parameters may be modified including: lithium enrichment, ARC tube diameters, volumes of reservoirs, and loss coefficients of the one-way valve. These different design choices combine into parameters: (1) total system worth (w [$]), (2) Volume of the cover gas in the upper reservoir (Cover-volume [m^3]), (3) Time lag parameter (τ [s]), (4) Forward loss coefficients (K_{for}), (5) Backward loss coefficients (K_{back}). The first one is the total system worth (w). For simplicity in this rapport this value is referred always as positive even it's a negative reactivity. W depends on the enrichment of lithium, on the number of fuel assembly modified with the ARC system and on the volume of the tube. Some more detailed calculations are needed to know the exact value. The max value during this project was set equal to $ 1.5. This value is similar to the worth of two average-rods in the ABR core and similar to the worth of the max rod in the B&B core. The second parameter is the volume of the Cover Gas in the upper reservoir in the ARC system. The minimum of cover volume was set to 5×10^{-5} m^3. This value corresponds, considering an area of 10^{-2} m^2 for the upper reservoir, to a height of 5 mm. Another parameter is the value of τ, it's

a time parameter that characterises the response of the upper reservoir temperature to a change in the coolant temperature. More detail of this parameter could be found in Section 4.3. In previous work [5] this parameter was increased to delay the ARC system actuation and reduce some oscillations. However, increasing τ too much made the ARC system actuation too slow to be effective in arresting the transient. That's where the idea of a one-valve came from, to delay only the disengagement of the ARC, therefore in this work, τ was kept as little as possible ($\tau = 1.3\ s$ as will be explained in Section 4.3). The last parameters are the loss coefficients, the main references is I. E. Idelchik [18]. At the beginning of this work the one-way valve had not yet been chosen, its choice depends also on the values of the loss coefficients found running the simulations. One possible choice could be a Check valve, a simplified draw is shown in Figure 19. In the ARC system the spring inside the Check valve is not necessary, for example it could be replaced by a grate that holds the poppet inside the valve during forward direction. This valve was used to evaluate the loss coefficients.

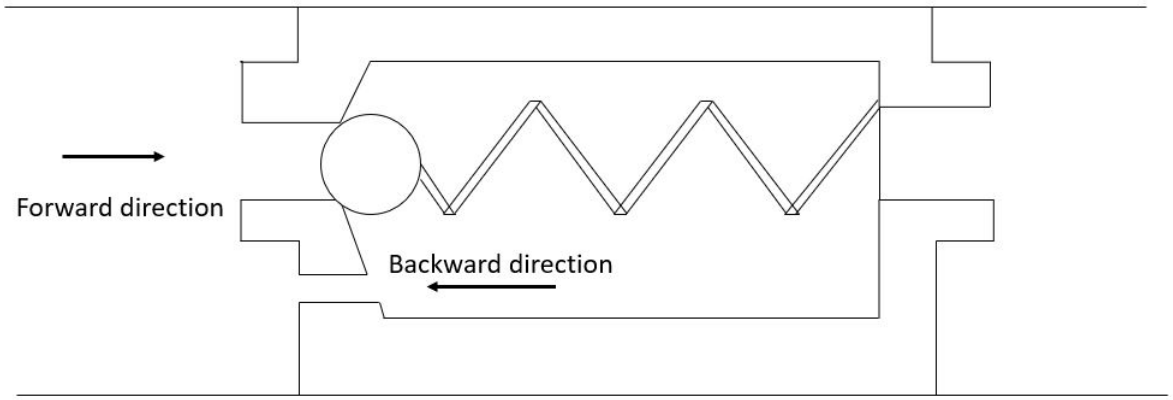

Figure 19: Check valve

To evaluate the K_{back}, an orifice with sudden change in velocity and in flow area was used as reference. In particular a thick edged orifice in a straight tube was chosen, as we can see in Figure 20. This choice was made because $l/D_h > 0.015$ [18], where D_h is the hydraulic diameter of the hole.

The resistance coefficient is given by the following formula:

$$K_{back} = \left[0.5\left(1 - \frac{F_0}{F_1}\right)^{0.75} + \tau\left(1 - \frac{F_0}{F_1}\right)^{1.375} + \left(1 - \frac{F_0}{F_1}\right)^2 + \lambda\frac{l}{D_h}\right]\left(\frac{F_1}{F_0}\right)^2$$

where $\tau = (2.4 - l)10^{-\psi}$ and $\psi = 0.25 + 0.535l^{-8}/(0.05 + l^{-8})$ and λ is the Fanning friction factor. The value of Reynolds number when the ARC is operating is $Re \sim 10^3 - 10^4$. Using the Moody diagram, see Figure 21, we can notice that these values correspond to a transition region, however $\lambda \sim 0.03 - 0.08$. Considering a little hole of radius 0.1 mm, a value of $K_{back\ Max} \sim 10^8$ was obtained. The calculation of K_{for}

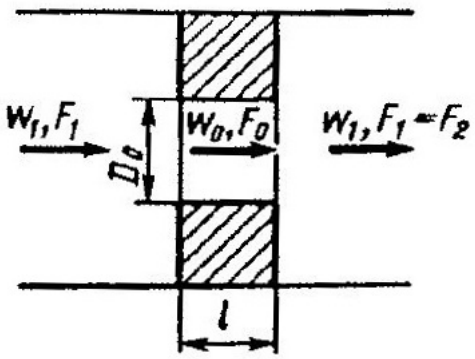

Figure 20: Orifice in a straight tube to evaluated the K_{back} [18]

is more complicated even for the Check Valve, therefore a difference of 4-3 order of magnitude between K_{back} and K_{for} was assumed.

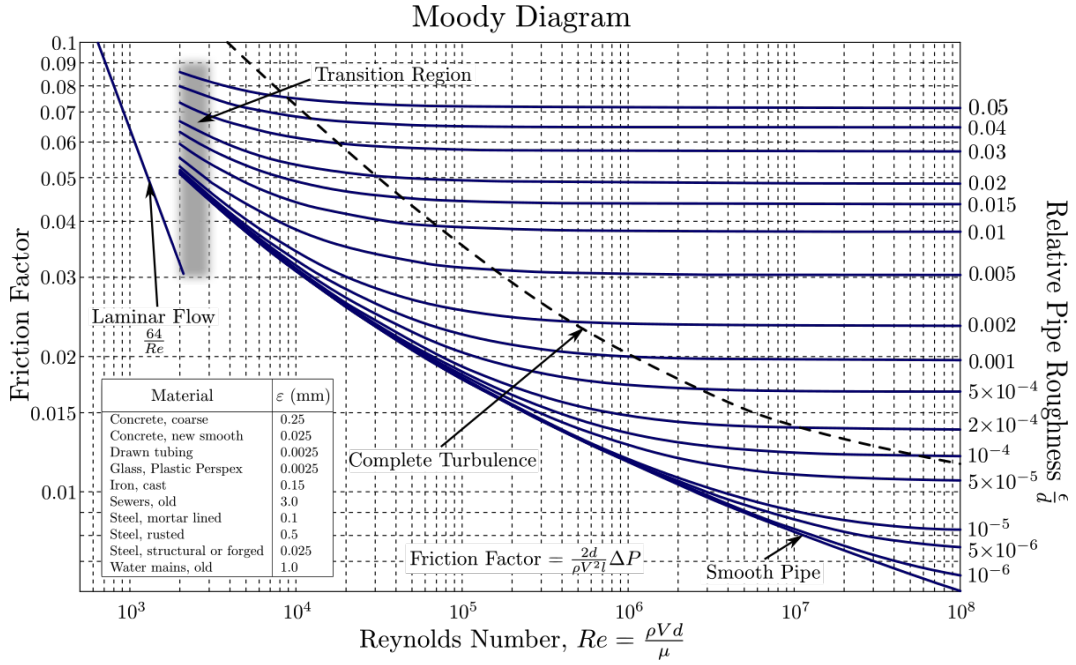

Figure 21: Moody diagram [20]

4 The code

In this section, the basis of codes used during this project are explained. More detail can be found in their manual guides [6] [9] [8]. During this project the performance of the modified ARC system was tested, simulating different accidents for two reference reactors. To evaluate the reactor and plant dynamic response the SAS4A/SASSYS-1 code was used, while for the internal ARC system fluid dynamics, the SAM code was adopted.

4.1 SAS4A/SASSYS-1

The SAS4A and SASSYS-1 codes were developed at Argonne National Laboratory in the Integral Fast Reactor (IFR) Program. The SAS4A code was developed to analyze severe core disruption accidents with coolant boiling and fuel melting. While the SASSYS-1 code was originally developed to address the loss of decay heat removal accidents. In the reactors modelling, all the primary and secondary sodium coolant circuits and the balance of plant circuit were simulated using SASSYS-1. Argonne merged both codes into a single code referred to as SAS4A/SASSYS-1. In the following for simplicity, the SAS4A/SASSYS-1 code will be mentioned as SAS code.

4.1.1 Geometry and mesh

SAS provides a multiple-channel treatment of the reactor core. Each channel represents a fuel pin, the associated coolant, its cladding, the associated reflector, and a fraction of the sub assembly duct wall. Figure 22a shows the axial mesh structure used for a channel. The geometry used for fuel, gas and coolant parts is cylindrical while a slab geometry is used for structure and reflector ones. The reflector zone represents any material outside the pin section, included orifice blocks and instrumentation. Any simple geometrical treatment will be an approximation because there is no fixed geometry for these components, for a simple heat transfer calculation a slab geometry has been chosen. As we can see from Figure 22a the channel is axially divided into different regions. Usually, a channel represents an average fuel element in a subassembly or a group of subassemblies. In the Advanced Burner Reactor (ABR cf Section 5.1) core assemblies were grouped into 4 channels. The first two representing the driver assemblies: Channel 1 the inner core and Channel 2 the outlet core.

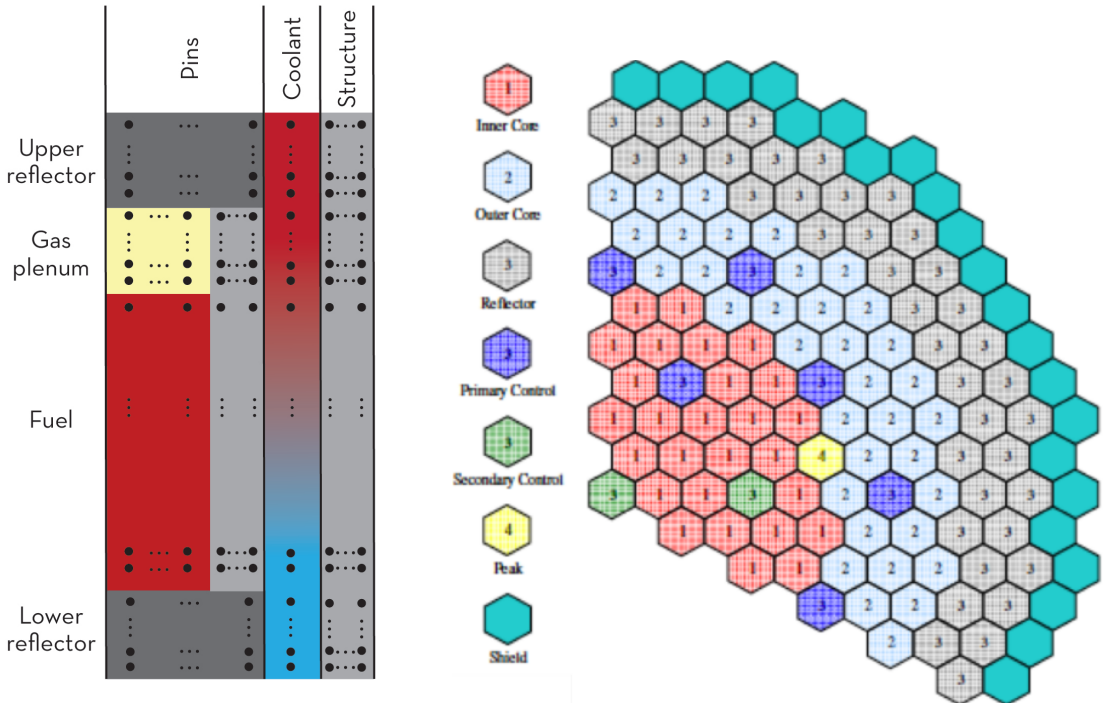

(a) Channel model used in SAS code [5]

(b) Grouping of assemblies into channels for the ABR core [5].

Figure 22: Some details about the modelling of the reactors using SAS

Channel 3 represents the control and shield assemblies and Channel 4 the peak power-to-flow assembly. A diagram of the channel allocation in ABR core is provided in Figure 22b. For his the greater complexity, see Figure 32, the Breed and Burner (B&B cf Section 5.1) core assemblies were grouped into 7 channels. Fuel assemblies are grouped in 4 channels, 2 addition channels are devoted to peak power and peak power over flow assembly ad the last channel concern the reflectors and controls assemblies. A diagram of the channel allocation in B&B core is provided in Figure 23.

4.1.2 Steady State and Transient Calculation

Using SAS code, it is possible to evaluate the reactors' responses when the coolant boiling and the fuel melting occurs. Nevertheless this project focused on the introduction of a modified ARC system in the reactors to prevent the oscillation behavior that, in some cases, leaded to coolant boiling. Therefore the parts of the code that model the Two/Phase Coolant, the molten of cladding/fuel were unnecessary. In fact, during this project, a simplified version of SAS was used during this project. This version stopped the calculation when the boiling occurs, more precisely when the cladding temperature reaches the saturation temperature of the coolant.

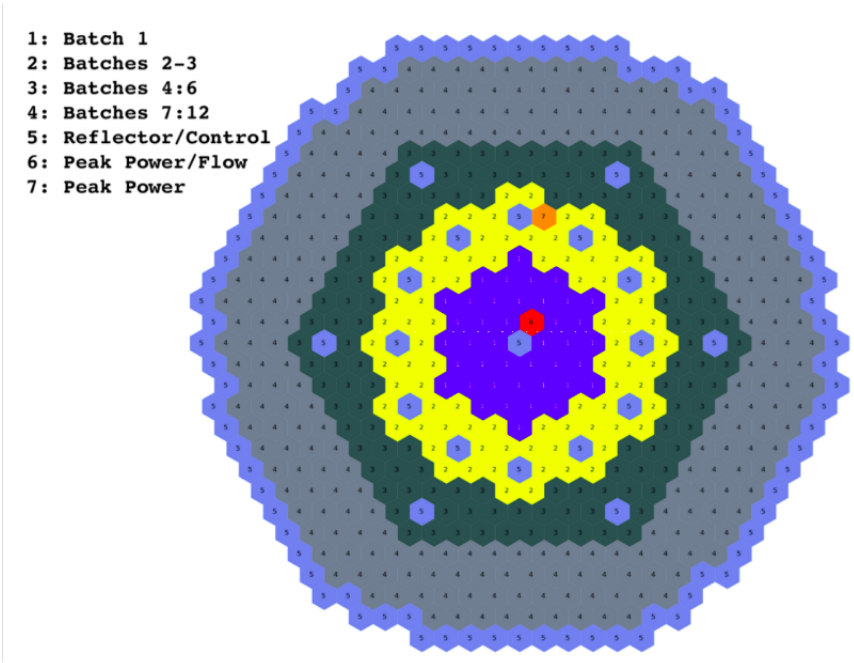

Figure 23: Grouping of assemblies into channels for the B&B core [5].

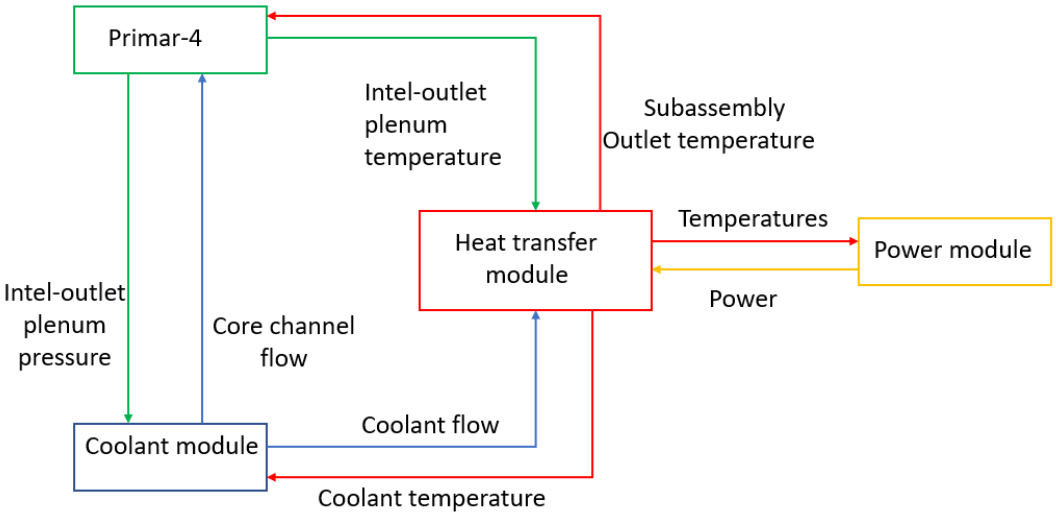

Figure 24: Interaction of Models in SAS code

In SAM the thermal hydraulic calculations are performed by separates module that interacts each other exchanging data, as shown in Figure 24. In Section 7 many reactivity and power graphs will be shown. The module that calculates the power, called Power module in Figure 24, uses a point reactor kinetics approach. Point kinetics approximations can be used effectively for fast reactors because the fast neutron flux is more nearly separable in space and time. This characteristic is the necessary condition for point kinetics approximation [2]. In the reactivity calculations, the net reactivity is assumed to be the sum of the following reactivity feedbacks: fuel Doppler, fuel and cladding axial expansion, coolant density or voiding, core radial expansion, control rod drive expansion. Many of these were addressed in Section 2.2.

4.1.3 Validation and verification of the code

The code has been validated with data from the Experimental Breeder Reactor II (EBR-II) tests conducted in the 1980s [7]. EBR-II was a metal-fueled, sodium-cooled fast reactor that was shut down in 1994. It designed to operate at a thermal power level of about 60 MW and a net electrical power output of about 20 MW. The testing program has realized protected and unprotected transients including reactivity feedback verification tests, unprotected loss of flow tests (ULOF), and unprotected loss-of-heat-sink (LOHS) tests. In these categories, "unprotected" accidents mean that the reactor system fails to scram. Other sensibility studies have been carried out [17]. They underline the importance of the control rod driveline effect for the Unprotected OverPower (UTOP) Transient and the importance of the pumps' loss for the ULOF transients.

4.2 SAM

The System Analysis Module (SAM) is code developed at Argonne National Laboratory. SAM focuses on modeling advanced reactor concepts including SFRs (sodium fast reactors). SAM performs thermo-hydraulic calculation using a hydraulic model for single-phase incompressible but thermally expandable flow and a heat transfer model to evaluated heat transfer. The hydraulic and thermal model are coupled through convective heat transfer at the solid surfaces.

4.2.1 ARC modeling

During this project, SAM was used to model the modified ARC system and to simulate its fluid dynamic transients. As we saw in previous Figure 18, the two modifications in the ARC's design are the one-way valve and the addition of a cover volume in the upper reservoir that allows the valve to operate. One benefit of SAM is the possibility to model liquid volumes with cover gas on top it. Plus during the transients, the liquid level in the volumes can be tracked. These types of components were used to model the upper reservoir and the outlet tube. Therefore, using SAM, the outlet liquid level can be obtained during the transients. This level is strongly related to the insertion of the negative reactivity by the ARC, the conversion will be explained in Section 4.3. Regarding the one-way valve, in SAM it is possible to model minor flow loss $\Delta P = K\rho u^2/2$, with a different value of K for different directions. Therefore, using SAM the modified ARC system could be modeled. However, SAM was not able to model the interface liquid-liquid between lithium and potassium. Interfaces liquid-liquid between these fluids at high temperatures are complicated to model even for Computational Fluid Dynamics (CFD) codes more sophisticated than SAM; not only for the complexity of the physical phenomena but also for the lack of experimental data. Therefore, for simplicity, it was assumed that all of the liquid presents in the ARC system was potassium. This approximation was entitled by similar characteristics of the two liquids, as shown by Table 1. The properties of the fluids were taken from the references as explained in Section 3. Plus, this choice was made because, in the ARC system fluids, potassium was chosen for his expansion characteristics while lithium for his neutronic features. Since SAM evaluated only the fluid dynamic aspects, while the neutronic ones were considered in a following step, it is a reasonable approximation to consider all the fluids as potassium. Certainly, the outlet liquid level value will not be precise, but its trend will be the same, therefore for the aim of this work, the approximation is valid.

Table 1: Characteristics of Potassium and Lithium

	Potassium	Lithium
Density $[kg/m^3]$	723	512
Viscosity$[Pa\,s]$	1.64E-4	6.45E-4

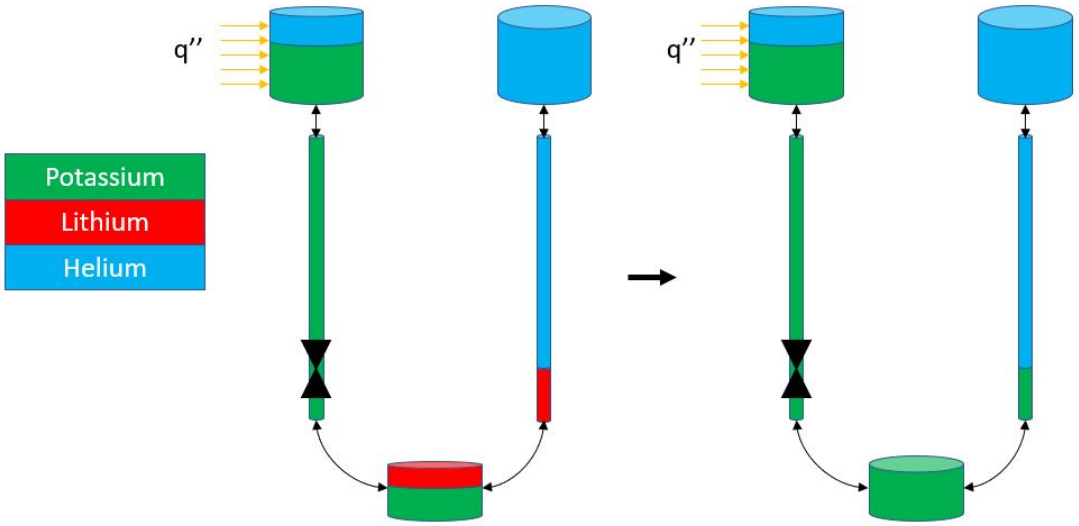

Figure 25: Modelling of modified ARC system in SAM code

Figure 25 shows a diagram of the ARC system modelling used in SAM code. In this project one single ARC system was modeled with SAM. This ARC system was supposed to be the representative of all the ARC systems in all the assemblies. In previous works [5], the former ARC system was directly modeled in SAS using a lag-compensator from the control system module present in the code. In brief, using a time lag parameter, the upper reservoir temperature was calculated knowing the coolant outlet temperature and flow. Then the level of the outlet liquid was evaluated using only the conservation of mass in the ARC system. More details can be found in the rapport [5]. In the modified ARC system the conservation of momentum has to be taken into account to evaluate the outlet liquid level. This requires more detailed calculations for the internal ARC system fluid dynamics that are performed by SAM.

4.2.2 Validation and verification of the code

SAM has been verified with analytical benchmark and with Code-to-Code comparison[10]. SAS is typically used for verification of SFR safety analysis. The results provide confidence that the physical models are correctly implemented and the numerical algorithms are representing the physics correctly. The validation of the code is based on the DOE Advanced Reactor Technology Fast Reactor Program's (ART-FR) Fast Reactor Knowledge Preservation Task in which the EBR-II and Fast Flux Test Facility (FFTF) data have being collected and organized in respective databases.

4.3 Coupling of the codes

One important part of this project was the coupling between the two codes. To couple the codes I utilized an external coupling paradigm, where the flow of execution was controlled with a specially developed script. This script coordinated data exchange by performing input/output on files specific to each code. Therefore, Python script was used to exchange data between SAS and SAM for each time step and the RESTART mode of the two codes was used. With this mode, the calculations of the code start from a RESTART file generated at the end of the previous time step. The coupling is outlined in Figure 26.

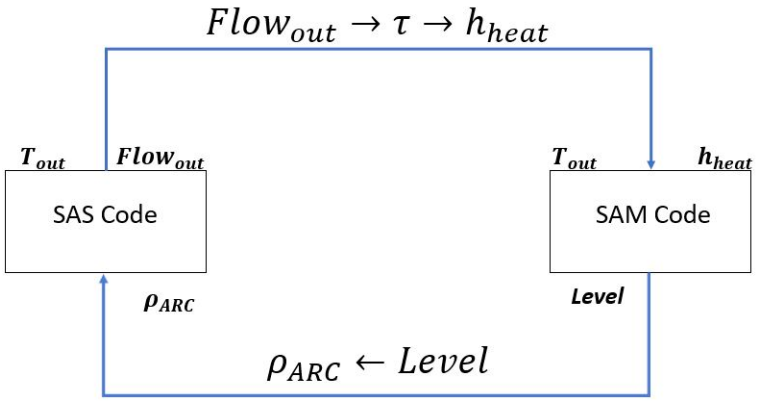

Figure 26: Coupling of codes

From SAS calculation, the outlet temperature and the outlet flow values were obtained. They are indicated as T_{out} and $Flow_{out}$ in Figure 26. The outlet temperature became directly input to SAM, while the flow was used to determine the heat transfer coefficient between the flowing coolant and the expander fluid contained in the upper reservoir. This coefficient is indicated as h_{heat} in Figure 26. Previous work [5] have studied the relationship $Flow_{out}$-h_{heat} using high-fidelity Computational Fluid Dynamics (CFD) calculations, performed using the COMSOL Multiphysics finite element software. In these studies, a time lag parameter (τ) was fit to the time that it takes for the upper reservoir to heat up in response to a change in coolant temperature. This parameter is defined as by the following formula:

$$T_{UR}(t) = T_{coolant} + (T_{UR}(0) - T_{coolant})exp(-t/\tau) \quad (1)$$

Where UR stands for the upper reservoir. So the response of the ARC will be faster with smaller value of τ. Through the detailed COMSOL analysis, the relationship between the flow and τ was quantified. The results were fit to a curve as given in Equation 2

$$\tau(F) = \tau(F)(4.24exp(-26.44F) + 2.074exp(-0.729F)) \quad (2)$$

Where F was the normalized mass flow and $\tau(F = 1)$ was set to 1.3 s that was the smallest value obtained through COMSOL simulation [5]. Therefore having the $Flow_{out}$, the value of τ could be obtained using the formula 2. The last passage consisted of converting the value of τ in h_{heat}. To accomplish this relationship several SAM jobs were run with fixed values of heat transfer ($h_{heat-fix}$) and with a step temperature in the UR's boundary condition as we can see in Figure 27a. This temperature represents the $T_{coolant}$ in Equation 1 . Then, with the solutions from SAM (so with the values of $T_{UR-code}$), the corresponding value of τ_{fix} was calculated for each job.

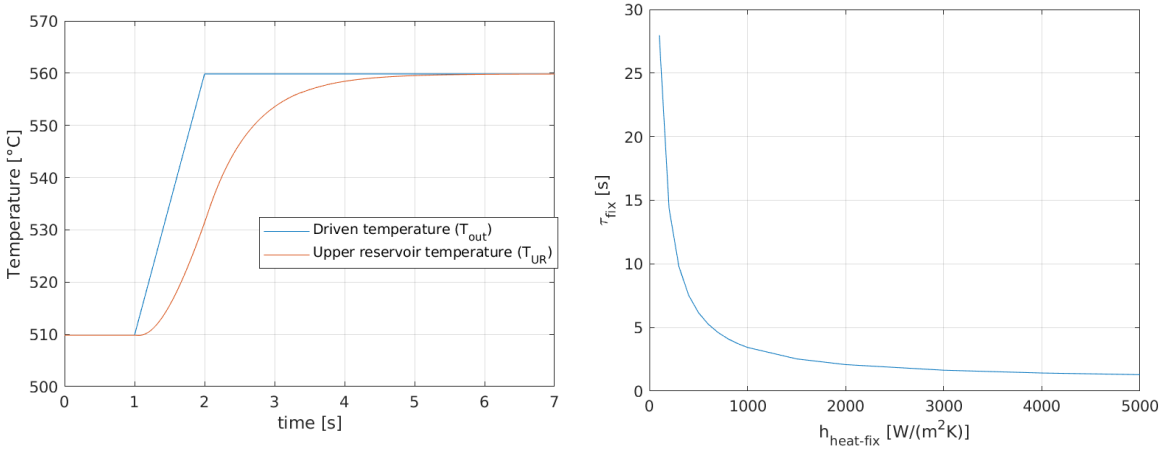

(a) Temperature history

(b) Relationship between τ_{fix} and $h_{heat-fix}$

Figure 27: Details for the external coupling of SAS and SAM

To do that, first of all of $T_{UR-formula}$ for t = τ was calculated that, using Equation 1, corresponds to:

$$T_{UR-formula}(\tau) = T_{coolant} + (T_{UR}(0) - T_{coolant})exp(-1)$$

Then it was compared with the results $[T_{UR-code}(t)]$ obtained by the code to find out at what time $T_{UR-code} = T_{UR-formula}(\tau)$. By doing so, the values of τ_{fix} correspond to $h_{heat-fix}$ were obtained. The relationship between these two values is shown in Figure 27b. Therefore during normal calculations,the value τ, calculated in Equation 2, was interpolated, and the corresponding value of h_{heat} was obtained. This value was used as an input to SAM. All these steps were made by the python script that initialized the SAM code. Then the SAM code was run and the level of the absorber liquid in the outer tube was obtained. This level was then converted to a normalized reactivity value using a worth table used in previous works [5]. The table uses a correlation similar to an integral control rod worth of the reactor, as shown in Figure 28

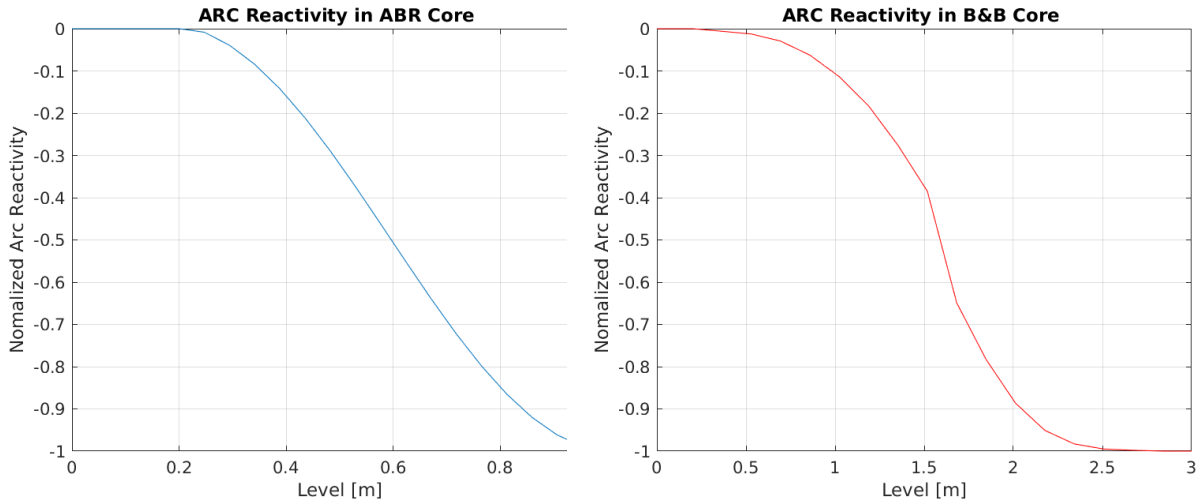

Figure 28: ARC reactivity for different Core

In Figure 28 the level over which the ARC system is fully actuated is 1 m. It represents the height of the ABR core, while the initial value, that is 0.2 m, is the initial level of the absorber liquid. For the B&B the height is 3 m. As mentioned before, SAM modeled only one ARC system, so the normalized reactivity obtained is multiplied by the reactivity worth of all the ARC systems in the reactor. Finally, the reactivity inserted by the ARC system is obtained, in Figure 26 it is indicated as ρ_{ARC}. This value was used as input to SAS code. This process was repeated for each time step.

4.3.1 External coupling with Picard's iterations

In the coupling described so far the codes communicate only at the begging and at the end of the time step. Therefore this implies that during the time step the reactor and the ARC system don't communicate. This hypothesis could be valid when the time step is little, once the delta time is larger a step is needed to be sure that the two codes are converged. In the project, this check was realised with Picard iteration as shown in Figure 29.

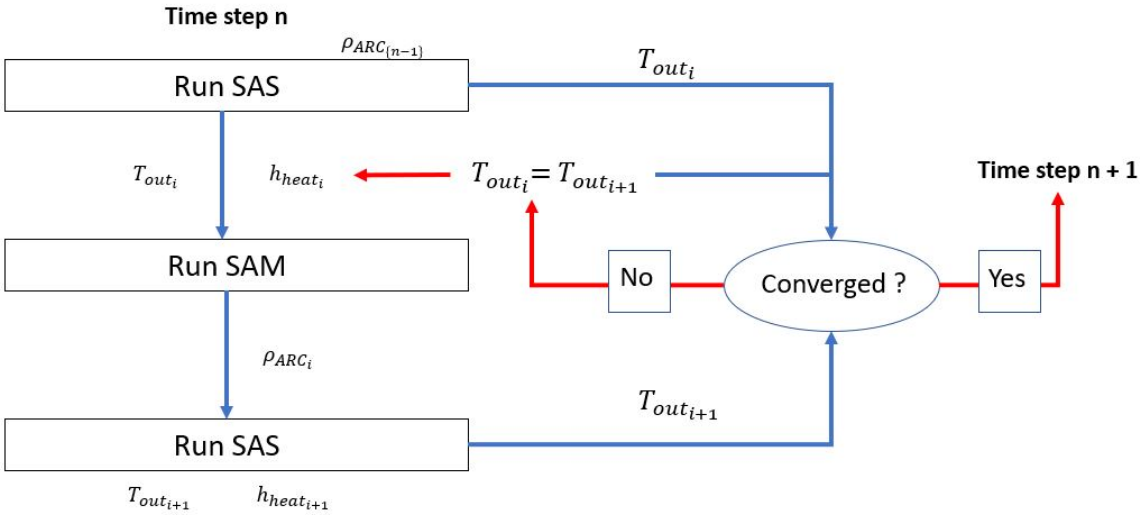

Figure 29: Picard iteration used in the external coupling

In each time step the SAS code ran at least two times. The first time with the reactivity of the previous (n-1) time step and the second time with the reactivity calculated in the current time step. The convergence was checked on the value T_{out} obtained by SAS codes. When $err = (|T_{out_i} - T_{out_{i+1}}|)/T_{out}$ was bigger than a certain limit ($err_{limit} = 10^{-4}$), $T_{out_{i+1}}$ was used as new input in the SAM code and the convergence was checked again using $T_{out_{i+1}}$ and $T_{out_{i+2}}$. The external coupling is a slow process because of the initialization of the codes in each time step. In this work, the time step was increased and the Picard iteration were implemented in the Python file. The reactivity inserted by the ARC system and the total power were compared to evaluate the accuracy of the results with different delta time.The reference case will be the transient with a delta time = 0.01 (black curve in Figure 30 and 31). In this analysis we focus on the difference between the different curves without concentrate on the physic of the transients or on the characteristics of the ARC system. These topics will be fully discussed in Results Section For the first analysis (Figure 30), an Unprotected Loss of Flow accident (ULOF) was chosen as the transient initiators with the introduction of an ARC system without the presence of the one-way valve was, that is the reason why we can see some oscillations in the results. As first, we can analysis the results with a delta time of 0.5 s, with the Picard's iteration and without it (respectively blue and

red curve in Figure 30). Comparing the red curve and the blue one to the black one we can witness that the implementation of the Picard's iteration has canceled the time shift. Therefore with a time step of 0.5 s with the Picard iteration we can follow the behavior of the reactor with an error in the results lower than 5% Then, we can analyse the results with a delta time of 2 s (green curve in Figure 30). In this case we can still follow the behavior of the reactor, but with an error max of 20%. This high error is located during the oscillations, for example in Figure 30a between 130-150s. These oscillations are the ones that the one-way valve aims to avoid.

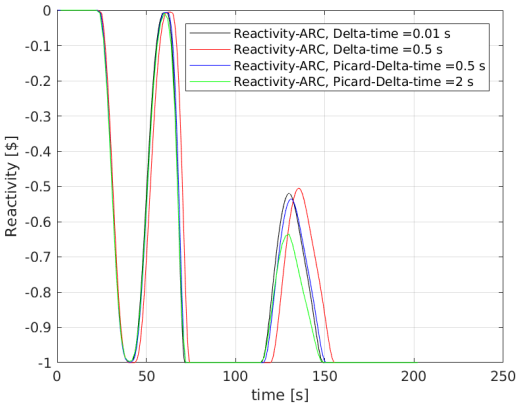

(a) ARC reactivity Comparison

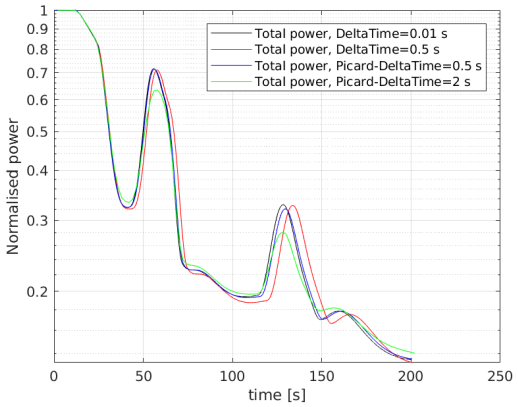

(b) Total power Comparison

Figure 30: Comparison Results without Tesla Valve

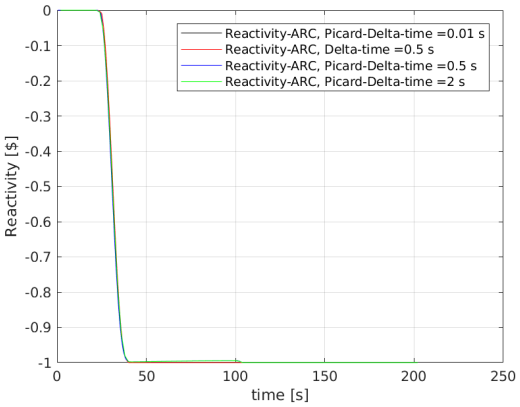

(a) ARC reactivity Comparison

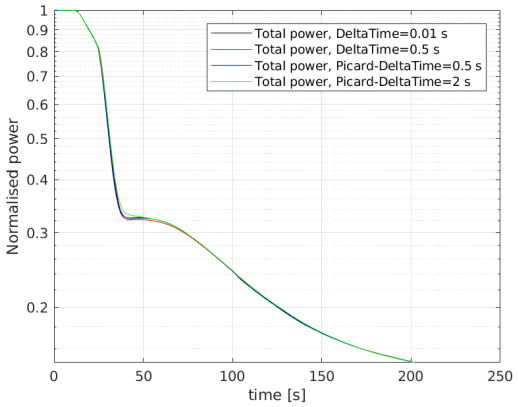

(b) Total power Comparison

Figure 31: Comparison Results with Tesla Valve

The same transient but with the introduction of the vale was run. As we can see in Figure 31 the difference with different delta Time are negligible. Therefor, the

simulations were run with a Timestep of 2 seconds for the analysis of different ARC system's parameters and then a smaller delta time (0.5 s) was used to analyze the final configuration and to evaluate the margins. The 2 seconds was chosen because only 6 hours were required to complete a transient of 4000 seconds. The 0.5 s was chosen because with, comparing the simulation, an error lower than 5% was found between the 0.5 s and the reference case.

4.3.2 Internal Coupling

The external coupling was the first idea to couple the codes because it doesn't require direct access to the source code of SAM and SAS and it is also easy to develop. Another possibility was to develop a different coupling. Codes can be coupled at a source code level via the internal coupling paradigm by making the changes needed to pass information in memory, rather than through the filesystem. In this case an internal coupling between SAS and SAM could be achieved using the MOOSE framework as the driver, instead of Python as in previous coupling. This would mean that the codes don't need to be restarted on every timestep. This solution involve making changes to the MOOSE source code. This idea was abandoned after the results with the external coupling.

5 Reference Reactors

5.1 Reference Core

Previous work [5] has analyzed the benefits of the ARC system studying the response of two different cores. The first reference core is a medium-sized oxide-fueled Advanced Burner Reactor (ABR) designed by Argonne National Laboratory and the second one is a large, low-leakage Breed and Burner ($B\&B$) SFR. Their layouts are provided in Figure 32. A summary of the characteristics of each core is given in Table 2.

Table 2: Characteristics of the cores [5]

	ABR	**B&B**	**units**
Thermal Power	1000	3500	MW
Cycle Length	365	916	days
Number of Batches	6	12	-
Reactivity Swing	-2.3	3.05	%
Active Fuel Height	114.3	300.0	cm
Core Diameter	321.1	453.0	cm
Gas Plenum Height	160.0	-	cm
Clad Thickness	0.056	0.061	cm
Pin Diameter	0.626	1.222	cm
Fuel Type	UO_2-TROUO_2	DU-10Zr	-
Fuel Thermal conductivity	4.0	30	W/m-K
Fuel Specific Heat Capacity	0.26	0.12	kJ/kg-K
Coolant Void Worth [1]	1.253E-02	4.597E-01	δ k/k
Doppler coefficient [2]	-3.33E-03	-4.79E-04	δ k/k
Control Rod Driveline α_{cr}	-43.86	-12.49	\$/m
Control Rod Driveline β_{cr}	-42.84	0.00	\$/m^2
Delayed Neutron Fraction	316	359	pcm
Prompt Neutron Lifetime	0.48	0.19	μs
Pump Coast Down Time	20	20	s

[1] At Beginning of Equilibrium Cycle (BOEC) and End of Equilibrium Cycle (EOEC) for the ABR and B&B cores, respectively.
[2] Values are for flooded core.

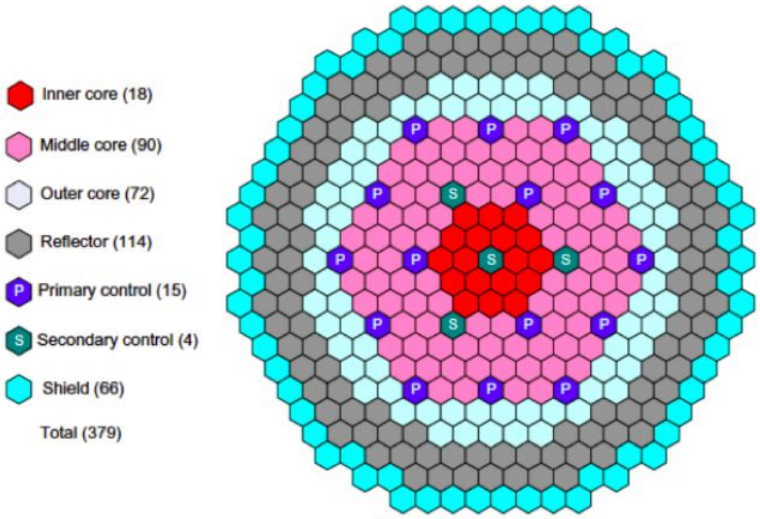

(a) Layout of ABR Core [5]

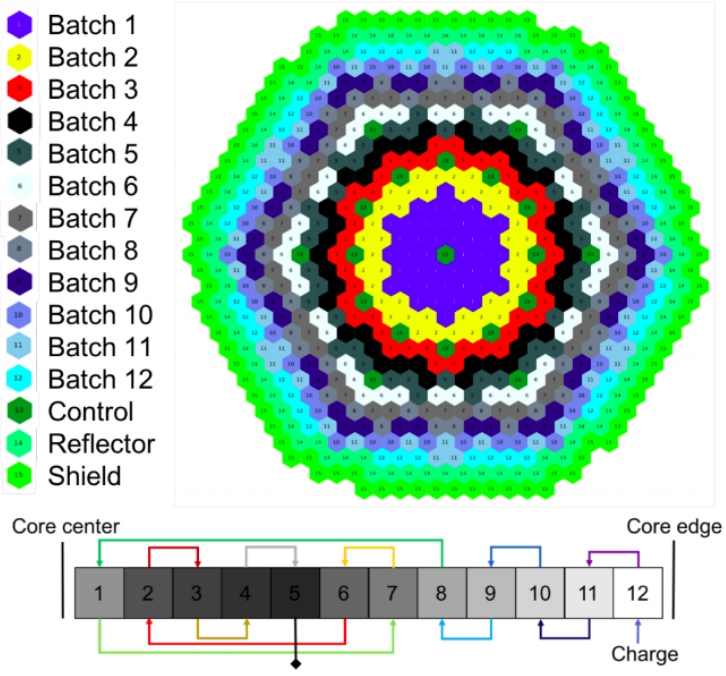

(b) Layout and shuffling scheme of BB Core [5]

Figure 32: Layout of references cores

5.2 Comparison of References Cores

As explained in Section 2.1 to obtain a breeding operation η must be greater than 2. Using ^{238}U-^{239}Pu cycle breeding could be achieved in the fast region, so B&B core needs a high neutron energy spectrum and a very low neutron leakage. Therefore, the core is large to reduce the leakages, the pitch must be small to reduce moderation and absorption in the coolant. To allow for a tight lattice pitch, the fission gas plenum is removed, the fission gas is vented. Moreover, the fuel is metallic the neutron spectrum of a metallic core is harder than that of an oxide-fuel due to moderation by the oxygen. Talking about the fuel, the ABR is provided with fuel natural oxide uranium enriched with recycled TRU, with a core-average enrichment of 28%. The equilibrium TRU vector is provided in Table 3, where we can notice the presence of the minor actinides supposed to be burned.

Table 3: TRU vector [5]

Isotopes	**Percent**
Np-237	1.5
Pu-238	3.1
Pu-239	41.1
Pu-240	31.3
Pu-241	5.7
Pu-242	8.1
Am-241	3.6
Am-242m	0.2
Am-243	2.6
Cm-244	1.8
Cm-245	0.5
Cm-246	0.3

In the B&B each new fresh fuel is composed by depleted uranium (DU), which becomes fissile following the shuffling scheme, shown in Figure 32b. Therefore, the core becomes more fissile during the cycle, this is the reason why the reactivity swings is opposite in sign. As explained in Section 2.2.5, these design choices lead to a strongly positive coolant void reactivity feedback as we can see in Table 2. This can be challenging from the perspective of passive safety, therefore it's in these reactors where a passive safety, as the ARC system, is required. More details on the fundamental design choices and their justifications for the B&B core can be found in previous work [5]. As we can see in Table 2 the Doppler coefficients is different, it is influenced by the spectrum of the reactor and the choice of fuel. A brief explanation of Doppler effect is presented in Section 2.2.1. Another difference is the values α_{cr} and β_{cr}, they are coefficients used to calculate the control rod driveline feedback. In SAS the control rod

drive line reactivity is modeled as follows:

$$\delta k_{cr} = a_{cr}\Delta Z_n + b_{cr}\Delta Z_n^2$$

Where $\Delta Z_n = \Delta Z_{cr} - \Delta Z_v$, cr stands for control rod and v stands for vessel. The control rod driveline feedback in the ABR core is more strong than that in the B&B core because of the shorter height of the ABR, although the feedback in the B&B core is well approximated by a linear relation, whereas the ABR control rod driveline is not.

5.3 Plant system

Both reactors utilize the same heat transport and balance-of-plant systems, with that for the $B\&B$ core simply a scaled-up version of the ABR's to match the higher thermal output. An overview of the plant systems is presented in Figure 33 [5]. The primary loop consists of four loops equipped with one pump each. It provides the primary heat removal capability. In the primary loop core flow pass through the core, it increases his temperature and then flows through the Intermediate Heat Exchangers (IHXs) to transfer heat to the intermediate loop. The intermediate flow is then pumped up and out of the pool to the steam generators (SG), where it gives up its heat to produce steam, that will be sent to the turbines to produce power.

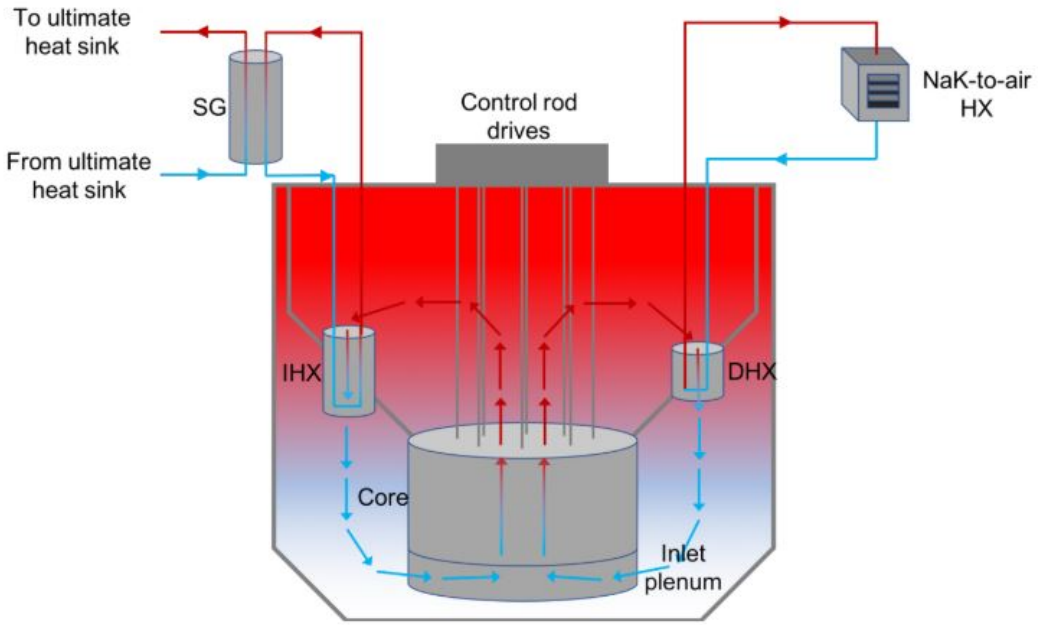

Figure 33: General plant layout for both reference cores [5].

The other possible path to cool the reactor is through the emergency Direct Reactor auxiliary cooling system (DRACS). The DRACS loops working fluid is NaK and it flows by natural circulation. Similarly to the intermediate loop, the DRAC loops remove

heat from the core flow through some heat exchanger (DHX) and it transfers heat through air dump heat exchangers located outside containment. In normal condition, the DRACS system operates but with heat losses limited by dampers on the NaK-to-air heat exchangers. In the case of an accident scenario, these dampers may be opened to allow the DRACS loops to operate at full capacity. Each DRACS loop is designed to remove 0.5% of full power during an accident scenario. In the reactor, there are two independent DRACS loops.

6 Transients and assumptions

To evaluate the performance of the reactors three different transients were examined – the Unprotected Loss of Heat Sink (ULOHS), Unprotected Loss of Flow (ULOF), and Unprotected Transient Overpower (UTOP). As mentioned before, the term "unprotected" means that the reactor system fails to scram. These accidents were chosen because SAS code was verified with a reactor that was tested with these transients, as explained in Section 4.1.3. Moreover, choosing these transients, the ARC system behavior has been tested on wide different situations concerning reactivity introduction, coolant temperature increases and loss of flow. At the beginning of the transients, the core was at its initial steady-state conditions. Moreover, it was assumed that one of the DRACS loops fails too, so a single DRACS loop was engaged by opening the dampers on the NaK-to-air heat exchanger. Further assumptions were taken from different transients. They are reviewed in Table 4.

Table 4: Assumptions specific to each of the three transients examined

	UTOP	**ULOF**	**ULOHS**
Primary Loop Heat Rejection	Nominal	Nominal	Zero
Pump Speed	Nominal	20s halving time	Nominal
Control System (ABR)	\$0.75 inserted at 0.005 \$/s	No scram	No scram
Control System (B&B)	\$1.66 inserted at 0.005 \$/s	No scram	No scram

In UTOP, a reactivity insertion equivalent to the worth of a control rod was withdrawn. This was the only transient that differed for the two cores. For the ABR its average rod was considered due to lack of information on peak rod worths, therefore the full insertion was \$ 0.75. For the B&B, its maximum worth rod was withdrawn, so the full reactivity insertion was \$ 1.66. The value \$ 1.66 stems from a study on the control assembly in B&B core [19]. The pumps were supposed to operate at nominal speed during the transient. Contrarily in ULOF, the pump motors were assumed to stop immediately. The impellers coasted down till reaching a value where they suddenly stopped, at that moment natural circulation occurred. The slowing down of the impellers causes a decrease in the flow. The same flow halving time was assumed for all pumps, both primary and intermediate. Unlike ULOF and UTOP, in ULOHS the

cooling from the SG was assumed to immediately stop, while the pumps still operated during the transient.
As mentioned in Section 4.3, the driven forces of the ARC system are the outlet temperature and the outlet flow obtained from SAS calculation. However, as briefly explained in Section 4.1.1, the core modeled in SAS was grouped in different Channels. In previous work [5], Channel 1 was assumed to be representative of all the core and so its outlet values were used as driven forces for the ARC system. In this project this hypothesis was verified., more details about it can be found is Section 7.2.4

7 Results

In this section, the response of the ABR and B&B Core will be analyzed

7.1 ABR-Nominal performance

The ABR response for the three transients is shown in Figure 34, 35, 37. For all these scenarios coolant boiling and fuel melting don't occur.

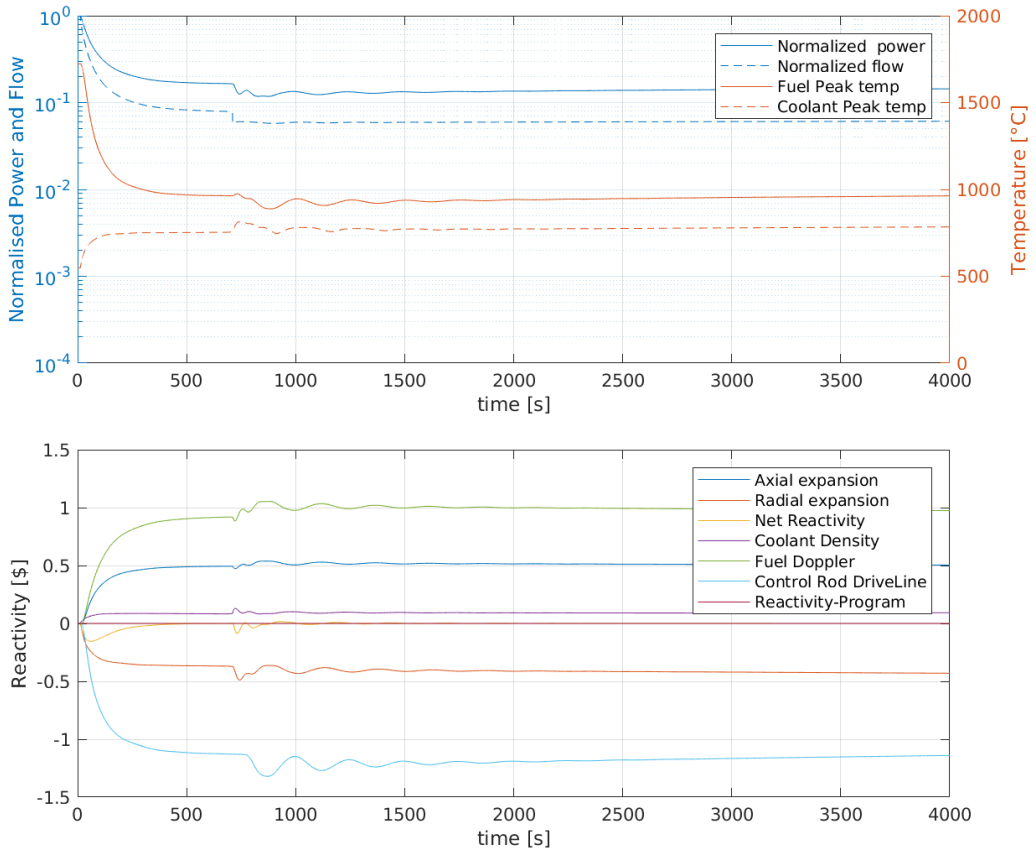

Figure 34: Response to a ULOF accident in the nominal oxide ABR core.

In the ULOF scenario, Figure 34, the flow decreases for the slowing down of the pumps, this involves an immediate increase of the coolant temperature. Consequently, the net reactivity turns negative, mainly because of the rod driveline feedbacks. This leads to a strong power decrease and therefore a strong temperature fuel decrease. Then, the net reactivity increases, because of the Doppler and the axial expansion feedback, till reaching a value close to zero where we notice a balance situation. We can notice small oscillations when the pumps lock ($\sim 650s$), these oscillations are generated by the transition from forced flow to natural circulation, which causes a sudden drop

in flow rate and resulting temperature-reactivity oscillations. These oscillations are damped, however, and no negative impacts result from these.

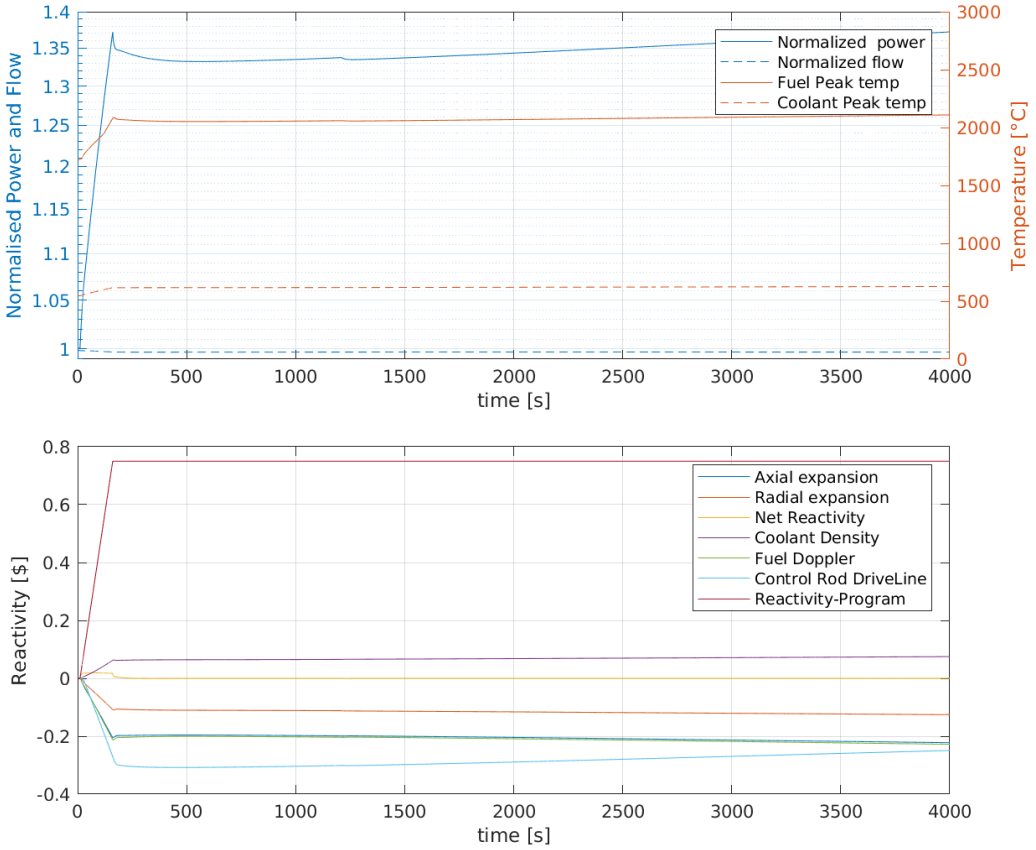

Figure 35: Response to a UTOP accident in the nominal oxide ABR core.

The UTOP scenario, Figure 35, is initiated by a sudden constant withdrawal of an average-worth rod, which ends at approximately 160 s. This leads to an increase in the power and the fuel temperature with Doppler and axial expansion feedbacks providing the main negative reactivity and coolant feedback providing the only positive reactivity apart from the control rod withdrawal. The UTOP scenario is driven by fuel temperatures, so the reactivity feedbacks related to the coolant temperature, such as the control rod driveline, occurs with some delay, related to the low conductivity of the oxide fuel. We can see the delay in the Figure 36, where the reactivity feedbacks in the first 70 s are shown. However, when the rod withdrawal sequence is complete, the other feedbacks can catch up and provide enough negative reactivity to stabilize the situation.

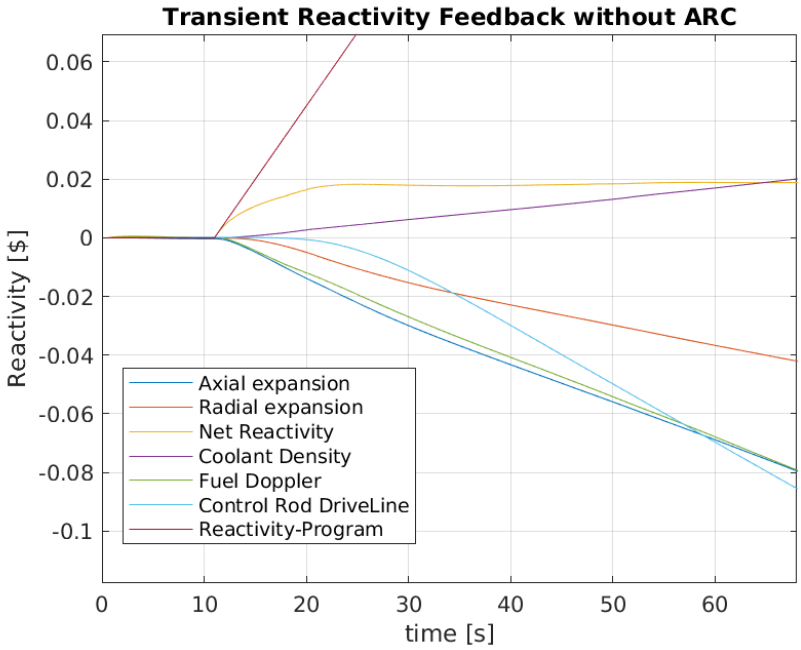

Figure 36: Transient reactivity for UTOP scenario for ABR Core.

In the ULOHS scenario, Figure 37, as the SGs stop the coolant temperature increases. This would lead to a negative net reactivity mainly because of the rod driveline feedbacks. Therefore the power decreases and consequently also the fuel temperature decreases. Later on, the net reactivity reaches a value close to zero because of the Doppler effect, the axial expansion, and the coolant feedback. In all the transients the net reactivity returns to zero after a while, so we reach a different steady-state than the initial one. We witness also the importance of the Doppler effect and the control rod drivelines for all the transients.

Table 5: Peak temperatures in the nominal transients of the ABR core.

	Peak coolant temperature[$°C$]	Peak fuel temperature[$°C$]	Margin to boiling[$°C$]	Margin to fuel melting[$°C$]
ULOHS	722	1724	311	1026
UTOP	623	2089	389	661
ULOF	813	1724	144	1026

A summary of peak temperatures for all three scenarios is given in Table 5. As said before, no coolant boiling is seen to occur. However, in the ULOF accident, the margin is 144 $°C$. Therefore, this margin should be increased with the introduction of the ARC system. Regarding the fuel melting, the smallest margin is obtained in the UTOP accident, but it's a large margin of 661 $°C$.

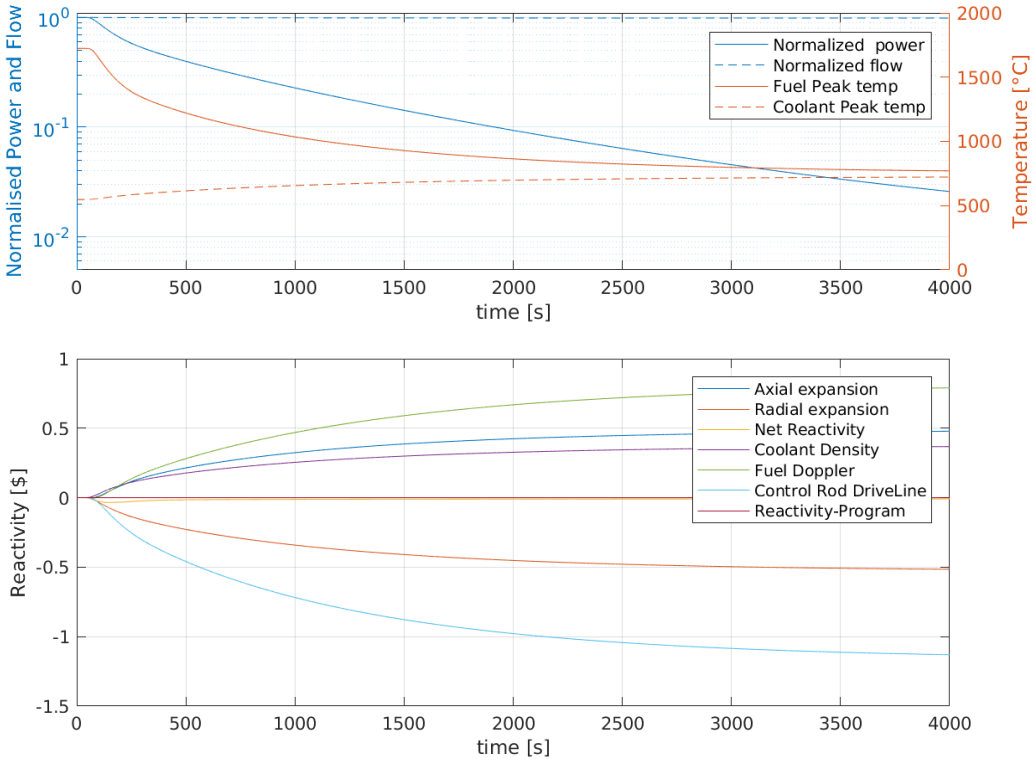

Figure 37: Response to a ULOHS accident in the nominal oxide ABR core.

7.2 ABR-performance with ARC inclusion

7.2.1 ABR-performance with former ARC inclusion

In previous work, the introduction of the ACR system in ABR Core provided remarkable benefits. As briefly mentioned in Section 4.2.1, in previous work, it was possible to evaluate the reactivity insertion of the ARC system knowing the temperature of the upper reservoir. The parameters that characterized the former ARC configuration were, (1) Total system worth (w [\$]), (3) Time lag parameter (τ [s]), (3) Coolant temperature difference at which the ARC system begins to activate (ΔT_{act}), and (4) Coolant temperature span over which the ARC system is fully activated (S). We can notice a strong link with the coolant temperature, consequently with the upper reservoir temperature. The modifications of S and ΔT_{act} have a similar effect to the modification of cover volume of the gas since they all act on the activation speed of the ARC system. In previous work, the introduction of the ARC system in the ABR core allowed for significant safety margin to be gained, although an oscillation behavior was observed in the ULOF transients, as we can see in Figure 38.

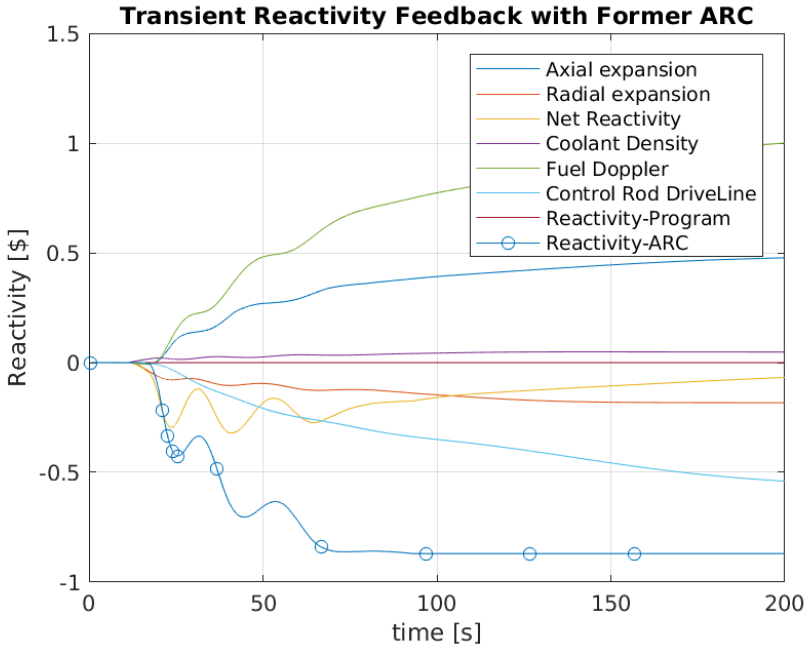

Figure 38: Response to a ULOF accident in ABR core with former ARC inclusion.

One method to reduce these oscillations was the increasing of the value of τ till 10 s [5]. As we can see from Figure 38, w = \$ 0.87. That was the maximum value of the worth reactivity before that boiling occurred. A parametric study was conducted to analyze the transients varying the ARC parameters. It was observed that at high w the ARC response was so strong that oscillations led to coolant boiling in the ULOF and UTOP accident. More details can be found in previous work [5].

7.2.2 Parametric study of the modified ARC's parameters in ABR core

As mention before, see Section 3.3, in this project τ was kept as little as possible ($\tau = 1.3\ s$ as explained in Section 4.3). In summary, if τ is kept constant the parameters that identify one ARC's modified configuration are:

1. The total system worth (w [\$]).
2. The volume of the cover gas in the upper reservoir (cover volume [m^3]).
3. The forward loss coefficients (K_{for}).
4. The backward loss coefficients (K_{back}).

In this first analysis, the UTOP accident was considered because, as explained in Section 7.1, the accident is driven by fuel temperature, therefore, coolant temperature doesn't immediately increase, so also the ARC actuates slow. It's then easier to analyze the transient. The first parameter that was analyzed is K_{for}. Some fixed reasonable values were chosen for the other parameters, w = \$1, Cover Volume = $10^{-4}\ m^3$, $K_{back} = 10^7$, and K_{for} was modified. As we can see in Figure 39a, we notice some oscillations of the level of the liquid even if the driven temperature is increasing. These oscillations are due to the compression and the expansion of the inert gas present in the upper reservoir and the outer tube. We can see that with $K_{for} = 10^4$ this phenomenon is avoided, therefore this value was kept for the next analysis. Later on, the value of K_{back} was modified. In Figure 39c-39d we notice some oscillations that will be explained in Section 7.2.3, but if we focus on the time interval where the temperature is decreasing we can see that for $K_{back} = 10^7 - 10^8 - 10^9$ the liquid stays almost constant because of the one-way valve that hinders the decrease of liquid absorber height. As we can notice, K_{back} was modified until 10^9, even if the max value found in Section 3.3 was 10^8. That was done to determine if a saturation effect occurred increasing the value. As we can notice in Figure 39c the level of liquids stays more constant with a value of K_{back} as 10^9. However, in the others transients the maximum value of K_{back} was set to 10^8 according to the limit found before. Then the Cover volume was modified, as we can see in Figure 39e with a smaller cover volume for the same ΔT, see Figure 39f, the level is higher. That is because decreasing the cover gas volume, the upper reservoir is filled with more expansion liquid. Consequently, the ARC is more reactive to change in temperature because more expansion liquid is in thermal contact with the coolant temperatures changes. Moreover, with a smaller volume, the pressure of the gas is higher and so the push of the cover gas on the expansion liquid during the transient is greater, allowing a higher level.

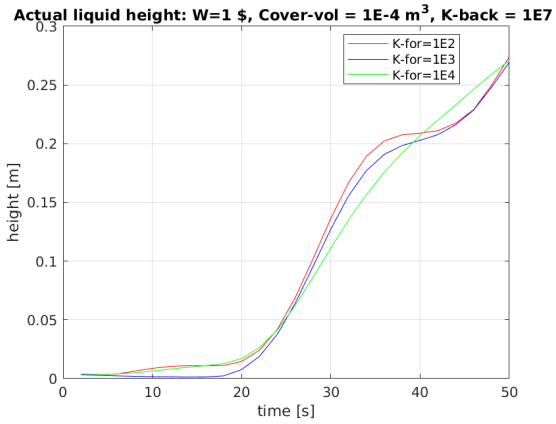

(a) Liquid Height

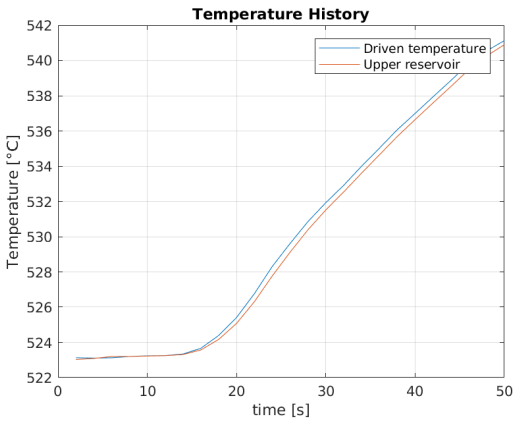

(b) Driven Temperatures of the ARC

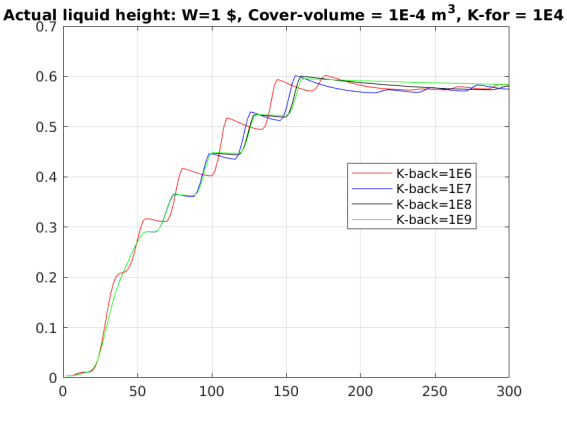

(c) Liquid Height

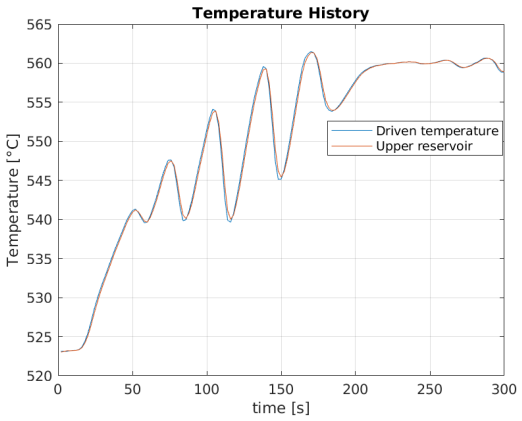

(d) Driven Temperatures of the ARC

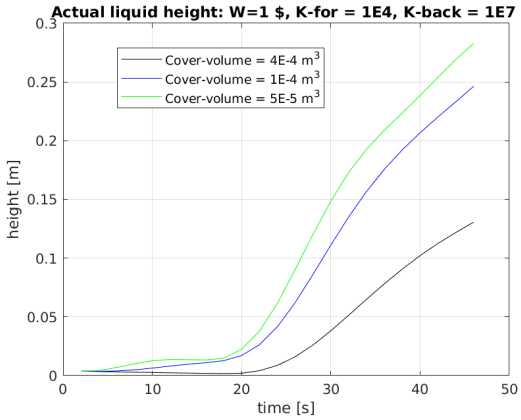

(e) Liquid Height

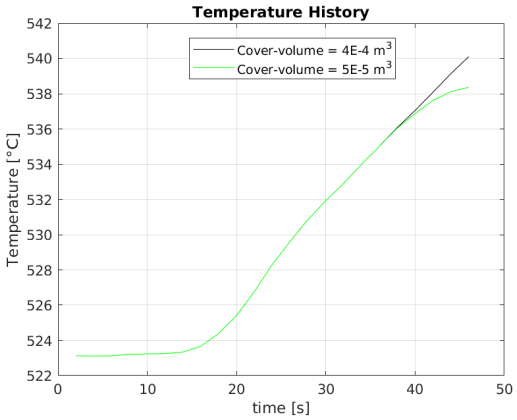

(f) Driven Temperatures of the ARC

Figure 39: Parametric Analysis in ABR core with modified ARC inclusion.

7.2.3 ABR-transients with modified ARC inclusion

During this project, many ARC's configurations have been analyzed. In this report I chose to show the transient with the following configuration $w = \$1.25$, cover volume $= 10^{-4}\ m^3$, $K_{for} = 10^4$ and $K_{back} = 10^8$. I chose this one because some phenomena, for example the oscillation trend, are more evident. It's then easier to analyze them.

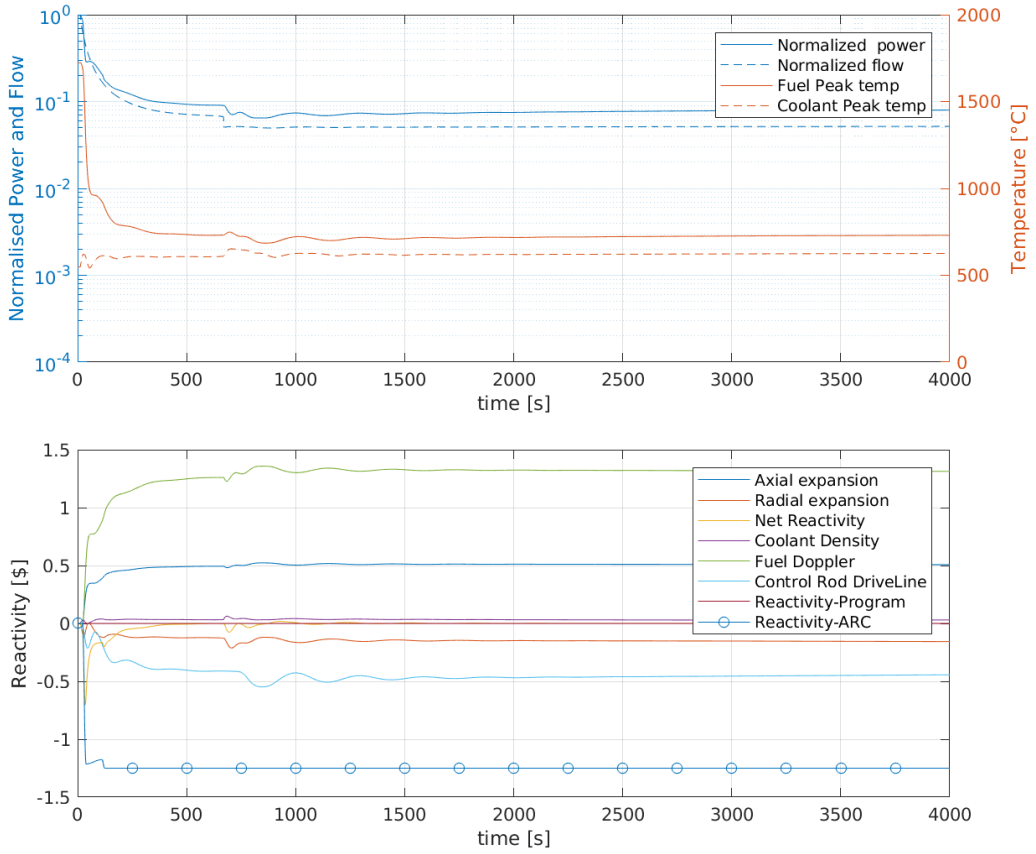

Figure 40: Response to a ULOF accident in ABR core with modified ARC inclusion.

In the ULOF case, Figure 40, we can notice a faster drop in the power and temperature caused by the full activation of the ARC system. The reactivity becomes negative for the ARC and then it reaches zero for the Doppler effect and the axial expansion. Comparing Figure 34 with 40 we can witness a reduction in the fuel and coolant temperature. We still notice the oscillations caused by the transition to the natural circulation and it seems that these oscillations are damped faster than the case without ARC. To prove it, a worse ULOF transient with a faster drop of flow was run. As we can see from Figure 41, in this worst scenario the lock of the pumps occurs earlier ($\sim 175s$). Moreover, in the case without the ARC system, we notice some oscillations even in the period of forced convection because of the strong drop of flow. As we can see in Figure 41, the addition of ARC reduces the oscillations noticed in the case with-

out ARC. In figure 40, we can notice that in the first $\sim 100s$ the reactivity inserted by the ARC doesn't oscillate even if the temperatures of the coolant does. That is the effect of the one-way valve that hinders the decrease of liquid absorber height. This behavior can be easily seen in Figure 42.

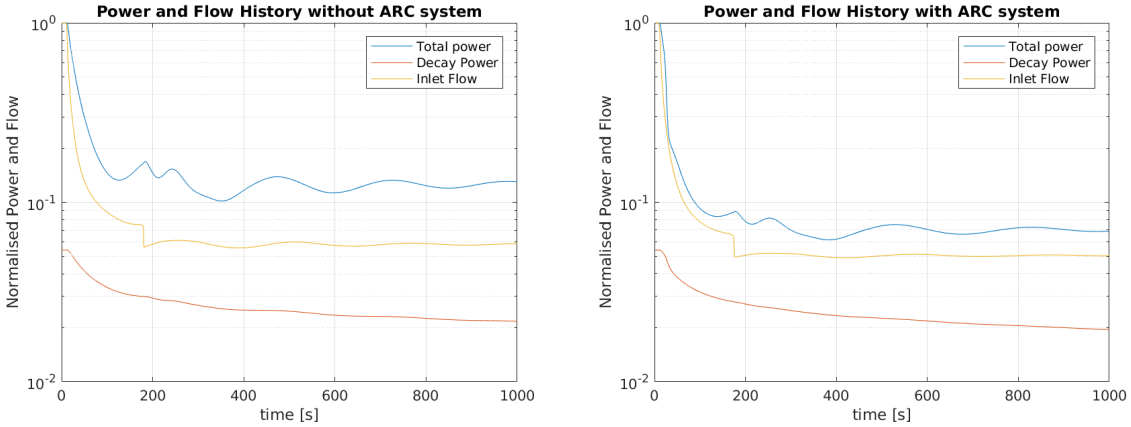

Figure 41: Comparison Power for Worst ULOF Transient

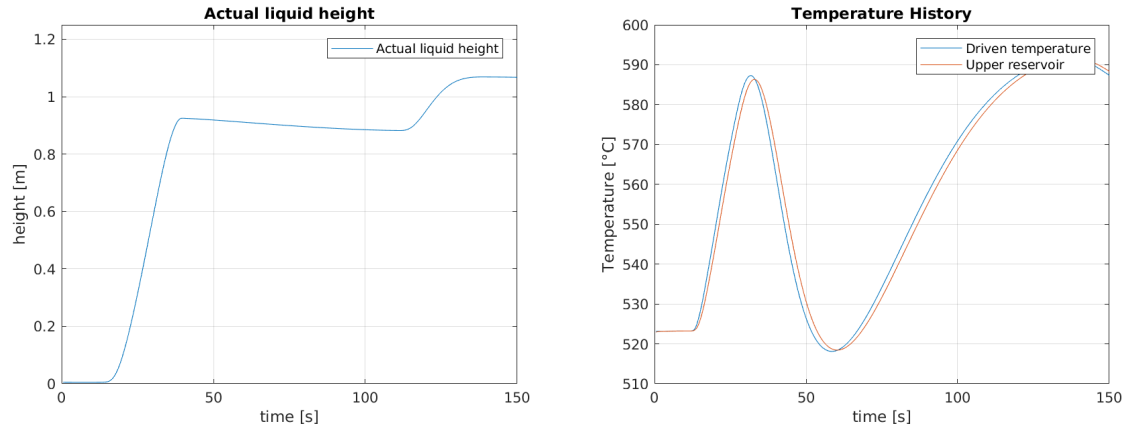

Figure 42: ARC characteristic during the ULOF transient

In the UTOP case, Figure 43, we witness some oscillations in the period in which the rod is withdrawn [10-160 s]. In the plot of power and temperature in Figure 43 the final time has been set to 2000s to emphasize these oscillations.

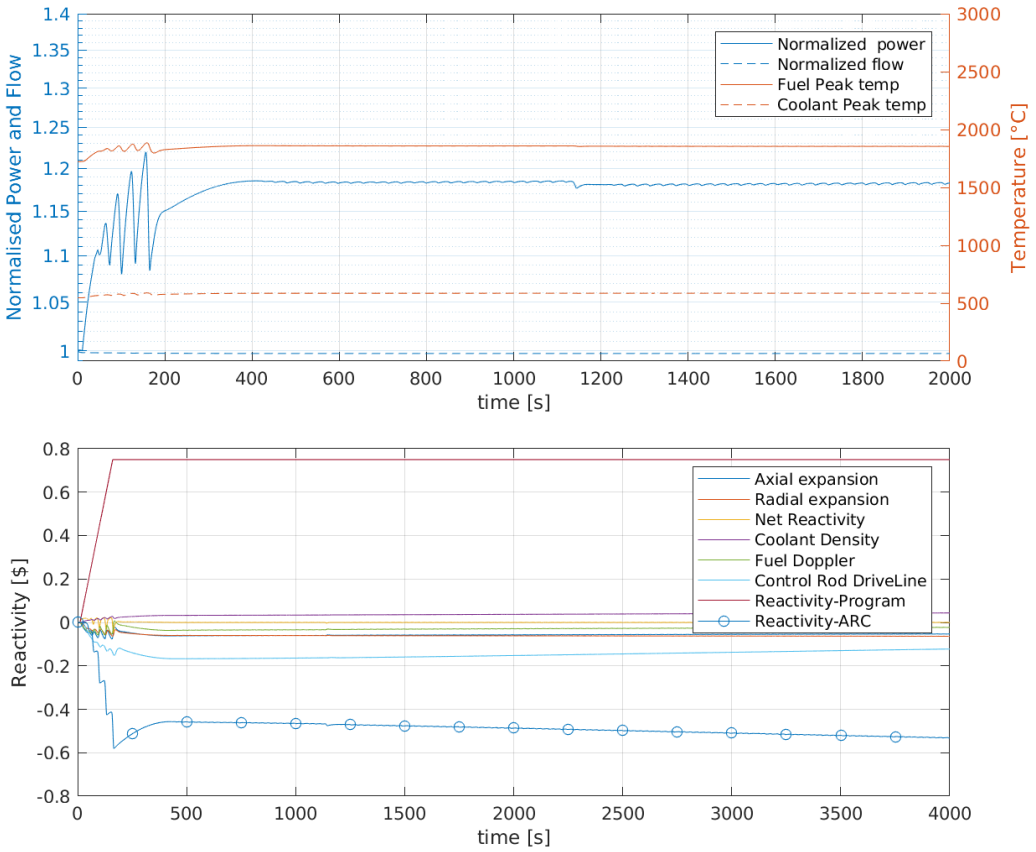

Figure 43: Response to a UTOP accident in ABR core with modified ARC inclusion.

In this case, the power increases for the withdraw of the rod, while it decreases by Reactivity-ARC. These oscillations stop as the rod is completely extracted and the final steady-state power is lower than the case without the ARC system. From these results, it seems that the ARC stabilize the situation at every step but the withdrawing of the rod destabilizes the situation causing a step behavior of the ARC. In Figure 44, at $\sim 90s$ we notice a reduction of the power that is caused by Reactivity-ARC. In fact the power stops to decrease when the insertion of reactivity stops. While the positive increase of power (at $\sim 100s$) occurs when the insertion of reactivity is stable but the rod is still withdrawing so the power is increasing.

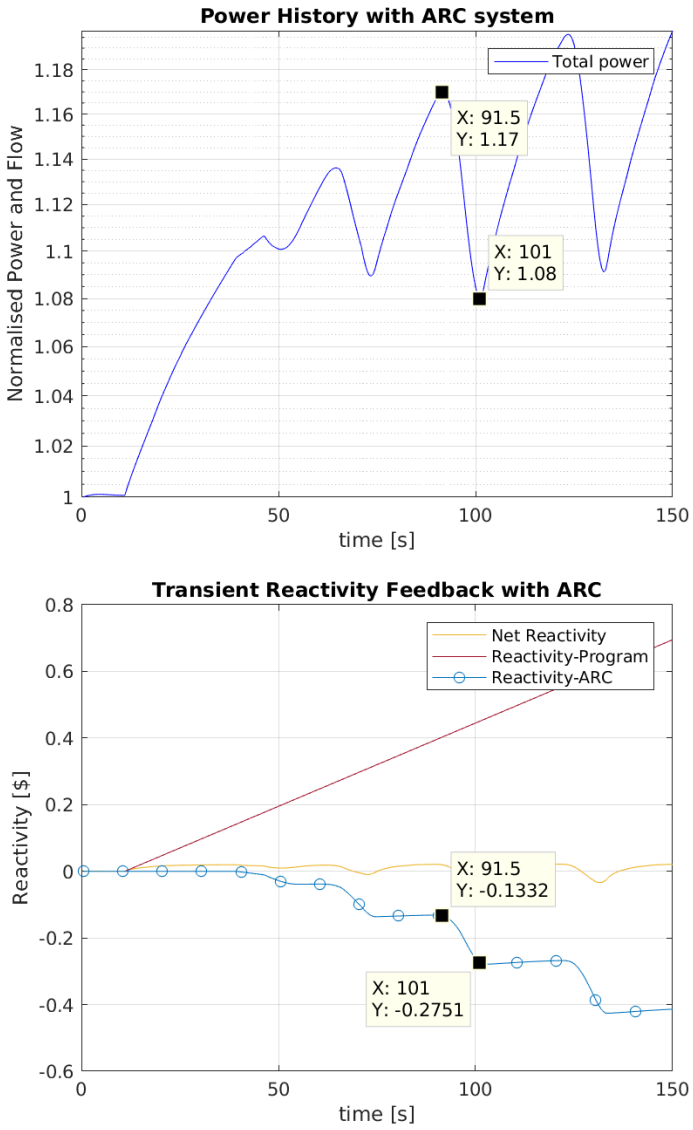

Figure 44: Comparison Reactivity-Power UTOP Transient with modified ARC inclusion

We can notice a similar step behavior also in the ULOF, see Reactivity plot in Figure 40 and Level height in Figure 42. However, in the ULOF case, with the second step, the ARC becomes fully inserted, so the step behavior is less evident than in the UTOP scenario. In both cases, the oscillations are not directly produced by the ARC. The system behaves as we would like: it inserts reactivity and then the reactivity inserted doesn't oscillate for a temperature oscillation. On the other hand, as long as the transients continue (reduce of flow or insertion of positive reactivity) there will be a competition between the ARC and this swing generates oscillation. The transient destabilizes the situation while the ARC tries to stabilize it.

In the ULOHS scenario, see Figure 45, the presence of the ARC lead to a stronger negative net reactivity that causes a faster decrease of the power and the temperatures. As in the ULOF accident, the reactivity reaches to zero for the Doppler and the axial expansion. However, for the slow increase of coolant temperature, therefore slow actuation of ARC.

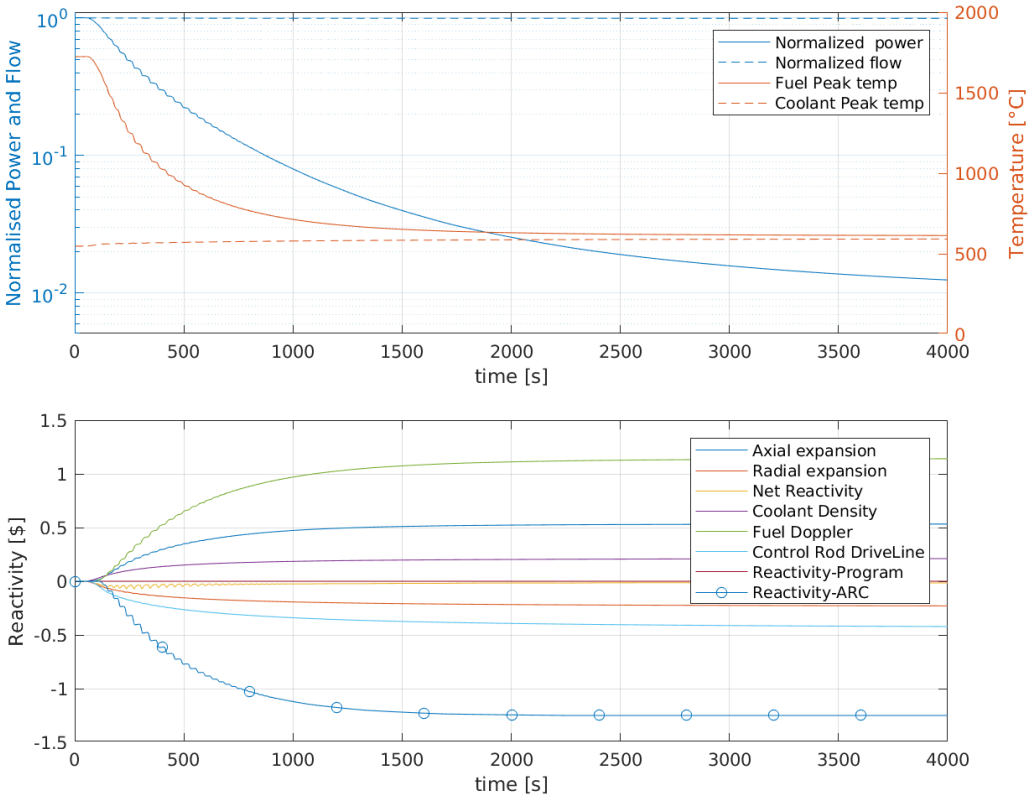

Figure 45: Response to a ULOHS accident in ABR core with modified ARC inclusion.

Looking carefully at the transients, we can notice the step oscillations of the ARC-reactivity in the first $\sim 700s$, which generates oscillations in the power. The reason for this behavior is not numerical, in fact, we can still witness these oscillations even decreasing the time step as shown in Figure 47.

7.2.4 ABR Margin calculation

A parametric study was performed to evaluate the configuration with the highest margin and to be sure that the oscillations don't diverge with different configurations. The value of $K_{for} = 10^4$ and $K_{back} = 10^8$ were kept constants, w was varied from \$ 1 to 1.5 and the cover volume from 5×10^{-5} to $4 \times 10^{-4} m^3$. The yardstick for this parametric study was the peak coolant temperature whose margin, as shown in Table 5, was the smallest.

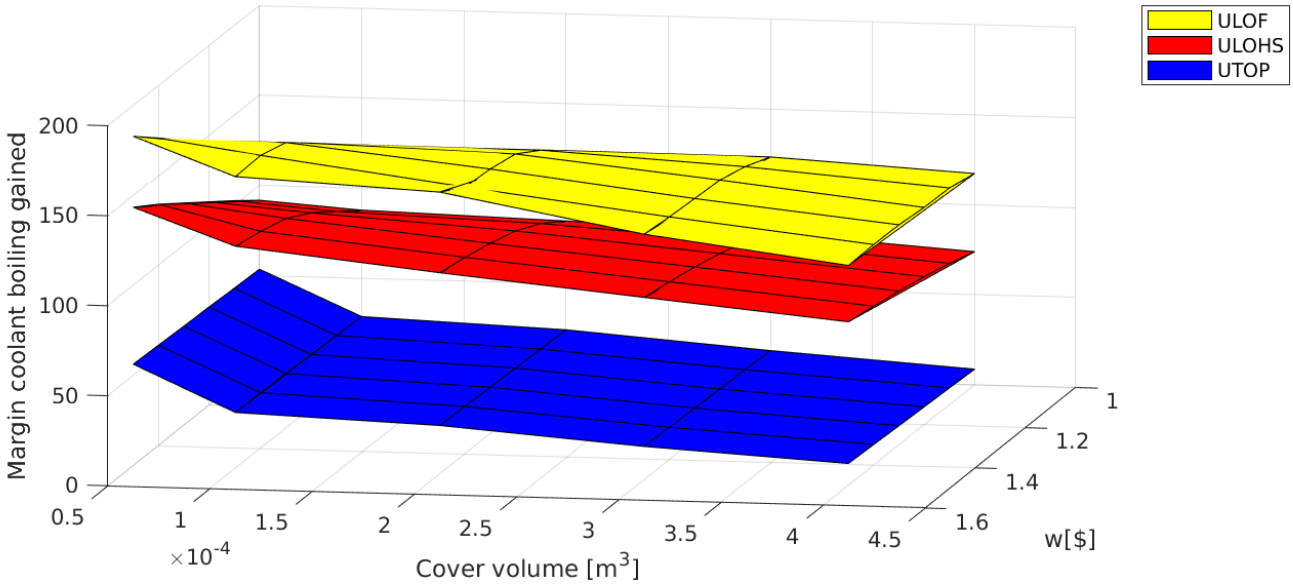

Figure 46: Coolant margin in ABR core with modified ARC inclusion

As we can see in Figure 46 the coolant boiling doesn't occur and the highest margin is found with the smaller cover gas ($5 \times 10^{-5}\ m^3$) and the higher reactivity (\$1.5). This result suggests that it could be possible to obtain higher margins extending the domain of the parameters, for example increasing the value of w. The peak temperatures obtained, using this configuration, are shown in Table 6.

Table 6: Peak temperatures in ABR core with modified ARC inclusion.

	Peak coolant temp[$^\circ C$]	Peak fuel temp[$^\circ C$]	Margin to boiling gained [$^\circ C$]	Margin to melting gained[$^\circ C$]
ULOHS	561	1724	143	-
UTOP	566	1729	51	360
ULOF	621	1724	183	-

In Table 7, the highest margins obtained with the former ARC design [5] are reported. As we can see, the modification of the ARC system leads to higher margins.

Table 7: Peak temperatures in ABR core with former ARC inclusion

	Peak coolant temp[$^\circ C$]	Peak fuel temp[$^\circ C$]	Margin to boiling gained[$^\circ C$]	Margin to melting gained[$^\circ C$]
ULOHS	635	1724	73	-
UTOP	590	1900	31	189
ULOF	705	1724	103	-

Then, I also simulated the transients with the same configuration but with $K_{back} = 10^7$. Even with this value, boiling doesn't occur and the coolant margins are almost the same (there is a difference $< 1\%$). So for the ABR's transients a value of $K_{back} = 10^7$ is acceptable.
All the results shown so far were obtained using Channel 1 outputs, as briefly explained in Section 6. Therefore, as the last analysis of the ABR core, the ARC system was coupled to Channel 2 outputs and the percentage error defined as:

$$Error = \frac{|Peak\ coolant_{Channel1} - Peak\ coolant_{Channel2}|}{\overline{Peak\ coolant}}$$

was calculated. In the previous equation, $\overline{Peak\ coolant}$ stands for the average value of Peak coolants. The results are shown in Table 8, as we can see the error is $< 5\%$, therefore it is a good approximation to consider the Channel 1 as representative of the core.

Table 8: Percentage Error of the peak coolant temperature in ABR Core

	UTOP	**ULOF**	**ULOHS**
Percentage error [%]	3.7	2.1	0.16

7.2.5 ABR Numerical accuracy

Regarding the time step used in the coupling, the UTOP case was the only one that required a smaller time step, as we can see in Figure 47. More over, in the UTOP with time step = 2 s we can also notice some numerical oscillations.

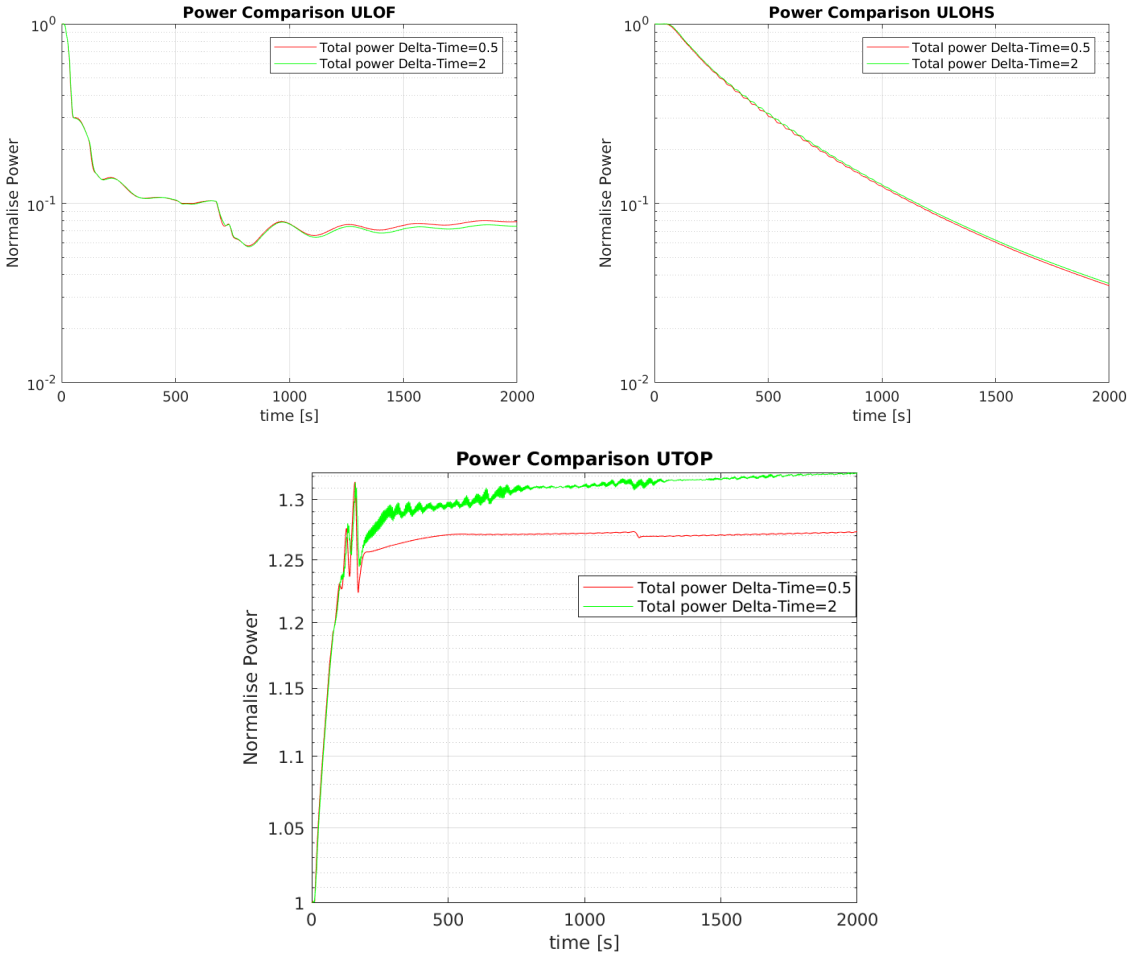

Figure 47: Comparison Delta Time in ABR transients with modified ARC inclusion.

7.3 B&B-Nominal performance

The B&B responses for the three transients without ARC system inclusion are shown in Figure 48, 50, 51. Unlike in the ABR case, the coolant boils in UTOP and ULOF accidents. The main differences in this core are the high conductivity of the metal fuel that allows substantial heat transfer between the fuel and the coolant and the strong positive coolant void reactivity feedback. Moreover, this reactor is characterized by a lower Doppler coefficient, see Table 2, caused by the harder spectrum. Plus, during the transients, the strength of the Doppler feedback is also impacted by fuel temperatures, which reaches lower values than in the ABR core. So its effect is limited.

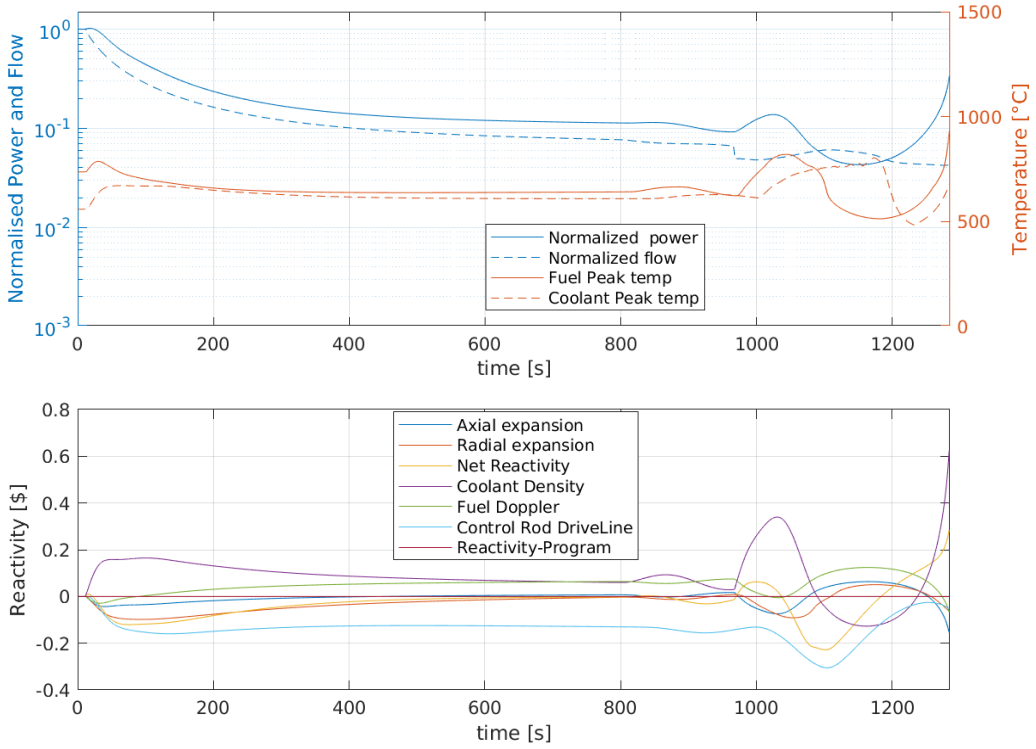

Figure 48: Response to a ULOF accident in the nominal B&B core.

The start of the ULOF scenario for the B&B, see Figure 48 is similar to the ABR, shown in Figure 34. Therefore the flow decreases and the coolant temperature increases. However, for the strong void coefficient, the net reactivity becomes positive for a short period (between $\sim 10 - 20s$), see Figure 49. Consequently, the fuel temperature increases, this increase will lead to a negative net reactivity because of Doppler and the axial expansion feedback. This explains the first spike in the fuel temperature. Once the net reactivity is negative, the fuel temperature decreases and for the high conductivity of the fuel, this decrease stops the increase of the coolant temperature

generated by the reduction of flow. The two phenomena could be summarized as

$$\begin{aligned} &\bullet\ \rho_{net} < 0 \ \Rightarrow P_{core} \downarrow \Rightarrow T_{Fuel} \downarrow \Rightarrow T_{Coolant} \downarrow \\ &\bullet\ Flow \downarrow \Rightarrow T_{Coolant} \uparrow \Rightarrow T_{Fuel} \uparrow \end{aligned} \tag{3}$$

Then (at $\sim 200s$) the fuel and the coolant temperature reaches the same value. We witness a plateau of the temperature caused by an equilibrium between $\rho_{net} < 0$ and $Flow \downarrow$. This situation is destabilized by the transition to natural circulation ($\sim 1000s$). During the transition in both reactors the coolant temperature increase. But in the B&B core this increase leads to a strong positive coolant density reactivity that generates temperature-reactivity oscillations. In this case the net reactivity is stronger and the oscillations are not damped, causing the boiling of the coolant. The passage to natural circulation occurs later, compared to the ABR case, because of the different of the flow at steady-state conditions.

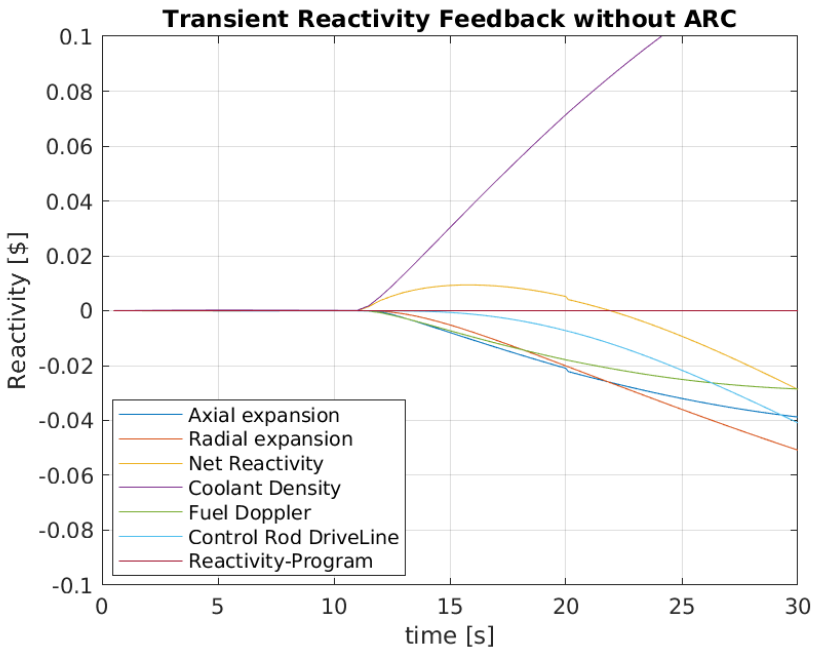

Figure 49: Transient reactivity for ULOF scenario for B&B Core.

In the UTOP transient, see Figure 50, due to the stronger void coefficient, the net reactivity stays positive for the entire transients. Therefore the power continues to increase, causing the boiling of the coolant.

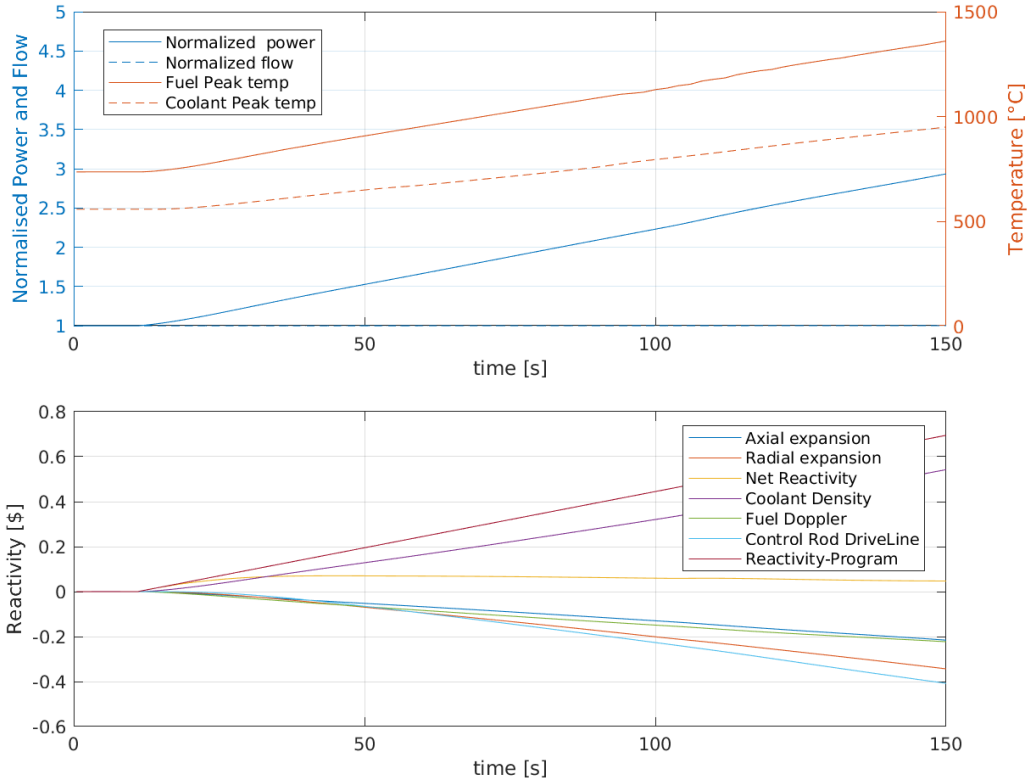

Figure 50: Response to a UTOP accident in the nominal B&B core.

A summary of the boiling time in B&B transients is provided in Table 9.

Table 9: Time of boiling of the three transients for the transients in B&B core

	ULOF	**UTOP**	**ULOHS**
Time of boiling (s)	1284	150	-

In the ULOHS scenario, as the SGs stop the coolant temperature increases. This would lead to a negative net reactivity mainly because of the radial expansion. Contrarily to the ABR case, see Figure 37, the control rod drive line feedback is not the more negative.

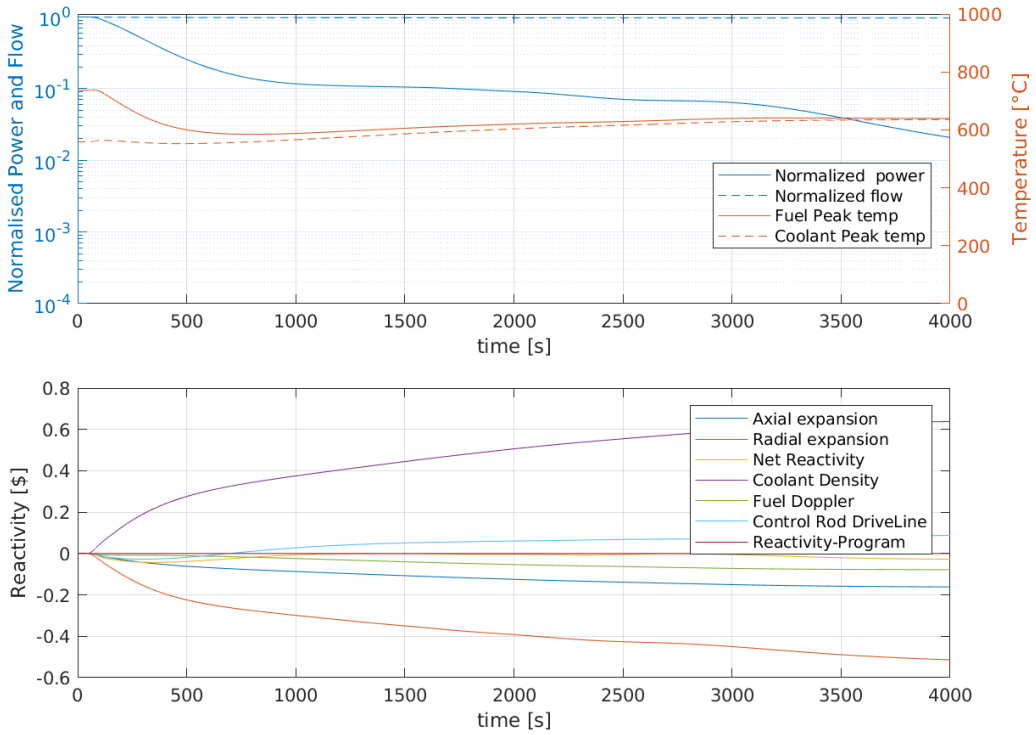

Figure 51: Response to a ULOHS accident in the nominal B&B core.

We can see better this feedback effect in Figure 52, in fact, it starts negative but then becomes positive for the heating of the vessel walls as explained in Section 2.2.2. The vessel wall temperatures strongly depend on the inlet temperature that increases ($\Delta T \sim 300$ in 4000 s) in the ULOHS, while it remains slightly constant ($\Delta T \sim 30$) in the other transients. Finally, we don't see this behavior for the ULOHS in the ABR core because the control rod feedback is modeled differently. As mentioned in Section 5.2, the control rod drive line reactivity is modeled as follows:

$$\delta k_{cr} = a_{cr} \Delta Z_n + b_{cr} \Delta Z_n^2$$

Where a_{cr} and b_{cr} are negative. As we can see in Table 2, in the B&B core $b_{cr} = 0$, therefore it is easier to have a positive reactivity. Then, its value is also limited by the value of a_{cr} . Once the net reactivity is negative, the power decreases and consequently also the peak fuel temperature decreases, but, as we can see in Figure 52, the Doppler stays negative. That's because the peak temperature decrease while the average temperature increase, as we can see in Figure 53. The reason for this behavior is the very

asymmetric axial temperature of the B&B reactor. Later on, the net reactivity reaches a value close to zero mostly because of the coolant density.

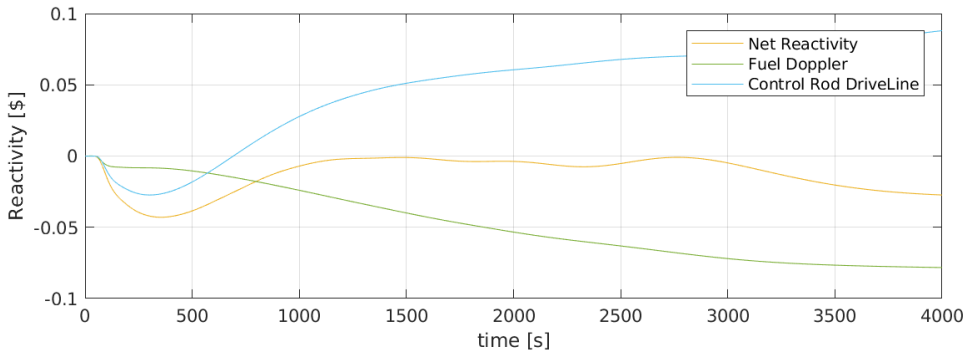

Figure 52: Fuel Doppler and Control Rod feedback for ULOHS transient in B&B core

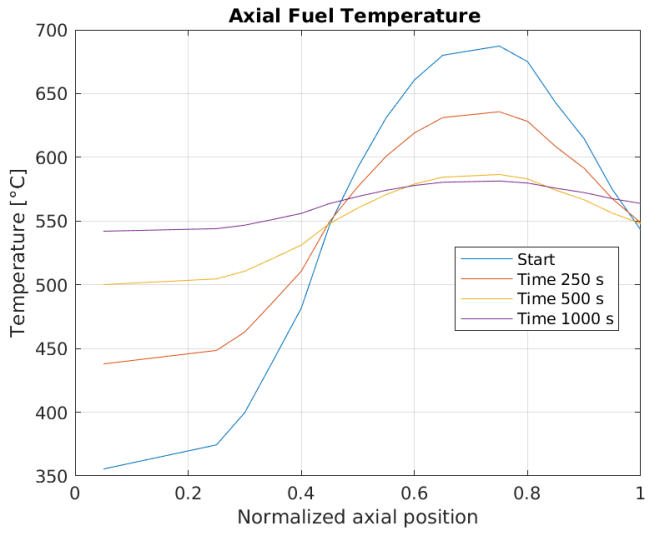

Figure 53: Axial Fuel temperature for ULOHS transient in the nominal B&B core

7.4 B&B-Performance with ARC inclusion

7.4.1 B&B-performance with former ARC inclusion

In previous work, τ was increased to 300 s to avoid the boiling in the UTOP case. However, no ARC system design could be found to avert the boiling in the ULOF. The oscillatory behavior was in fact worsened with the introduction of the ARC system, as we can see in Figure 54

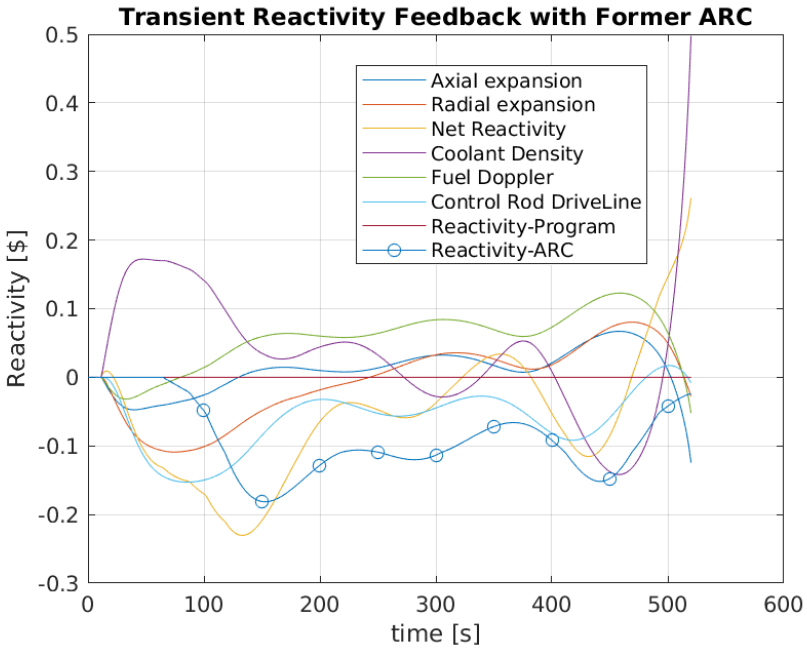

Figure 54: Response to a ULOF accident in B&B core with former ARC inclusion.

As we can see from Figure 54, the boiling occurred earlier than the case without the ARC system, see Figure 48. Therefore, in previous work [5] the final configuration was chosen conducting a parametric study over the margins of the other two accidents. Regarding its total worth, the optimal ARC system design was identified with $w =$ \$1.75,

7.4.2 Parametric study of the modified ARC's parameters in B&B core

As the first analysis, the configuration found for the ABR core was chosen to run the B&B's simulations. The boiling was avoided in UTOP accident and the peak temperature decreased in ULOHS. However, the boiling still occurred in ULOF accident. Further details about the transients will be shown in Section 7.4.3 A parametric study was performed to evaluate if the boiling could be avoided. The value of $K_{for} = 10^4$ and $K_{back} = 10^8$ were kept constants, w was varied from \$ 0.5 to 2 and the cover volume from 5×10^{-5} to 1×10^{-3} m^3. The domain of w was extended till \$ 2 since the coolant boiling continued to occur. As we can see in Figure 55, the coolant boiling couldn't be avoid. From this study, we can also notice the very little sensitivity to the total system worth. Trying to avert the boiling, also the value of τ was varied, keeping $w =$ \$ 1.5, cover volume $= 10^{-4}$ m^3 $K_{for} = 10^4$ and $K_{back} = 10^8$. The results are shown in Table 10, as we can see with the increase of τ the boiling time decreases.

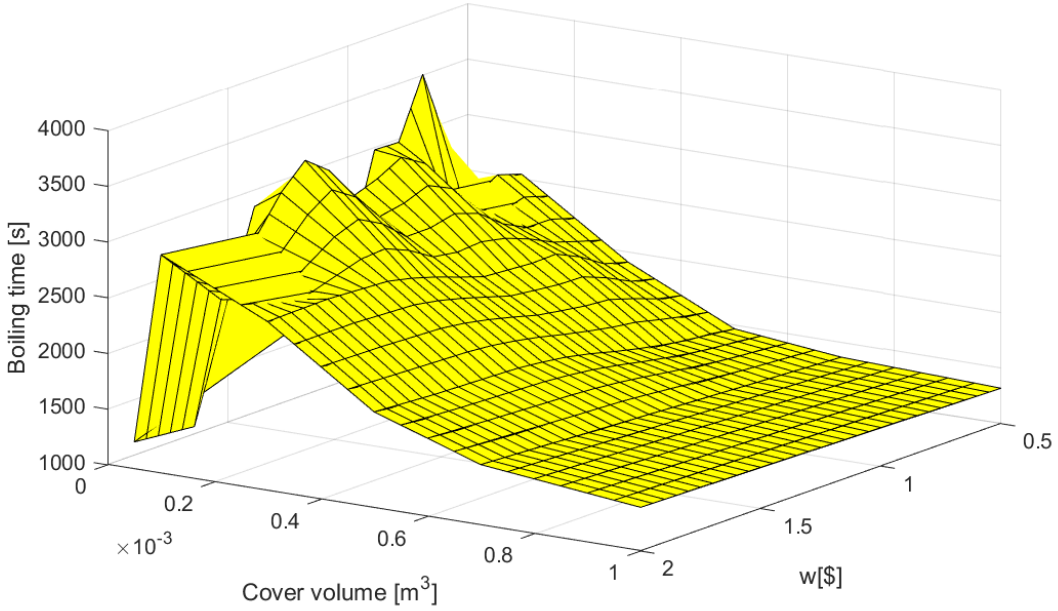

Figure 55: Boiling Time for ULOF transient in B&B core with modified ARC inclusion

Table 10: Boiling Time changing τ for ULOF transient in B&B core with the modified ARC

τ (s)	1.3	8	15	25
Time of boiling (s)	3140	2704	1616	1381

7.4.3 B&B-transients with ARC inclusion

After seeing these results I chose the following configuration to evaluate the transients: w = \$1.5 , cover volume = 10^{-4} m^3, $K_{for} = 10^4$, $K_{back} = 10^8$ and τ = 1.3 s. Whith this configuration the ULOF boiling occurs at 3140 s

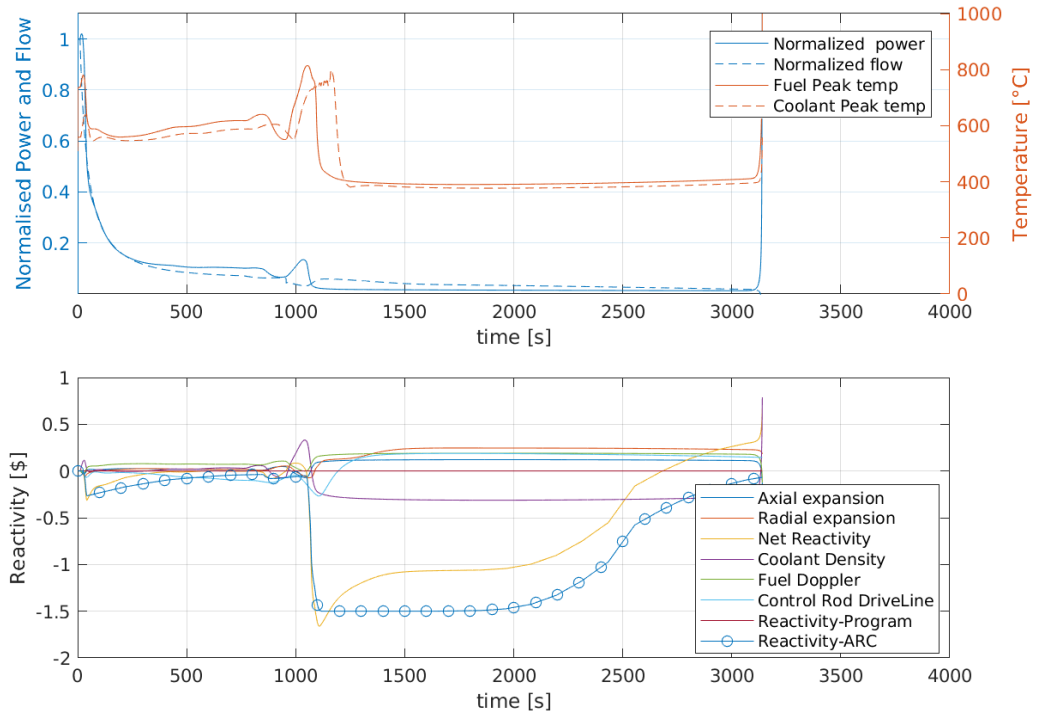

Figure 56: Response to a ULOF accident in B&B core with modified ARC inclusion.

In the ULOF case, see Figure 56, we can notice the increase of temperature caused by the transition to natural circulation ($\sim$ 1000s). With this increase, the ARC is fully activated and it behaves like a SCRAM prevailing over all other feedback effects. So the net reactivity drops to $\sim$ \$ -1.6 , this drop strongly reduces the power and the temperatures. Therefore the ARC system would be disengaged because of the reduction of the coolant temperature. However, we can easily see a strong difference between the engagement and the disengagement of the ARC thanks to the one-way valve that hinders the fluids. We can notice a delay of $\sim$ 1000 s between the drop of the temperature and the disengagement of the ARC. At $\sim$ 2000 s the absorber liquid height starts to reduce below the top of the active core and the net reactivity starts to increase. From figure 56, we can notice the slow disengagement of the ARC and therefore we can see the integral control rod worth shape of the ARC reactivity. As the net reactivity becomes positive ($\sim$ 2700 s) the fission power increases. However, this increase is not observable if we look at the total power curve because of the strong different ($\sim$ 6 order of magnitude) between the decay power and the fission power. The different powers are shown in Figure 57. Once the fission power reaches the decay

power, also the total power starts to increase but with so fast trend that the others feedback have no time to overcome the positive net reactivity, then the temperature increases making the coolant boil. Performing the parametric study the reduction of the cover volume or the increase of τ aimed to delay or slow down the ARC activation, to avoid the SCRAM behavior. On the other hand, if the ARC doesn't act fast enough the boiling is reached for the oscillation induced by the transition to natural circulation. That was the case with a small cover volume of a high τ in which we can witness a boiling time similar to the case without the ARC inclusion.

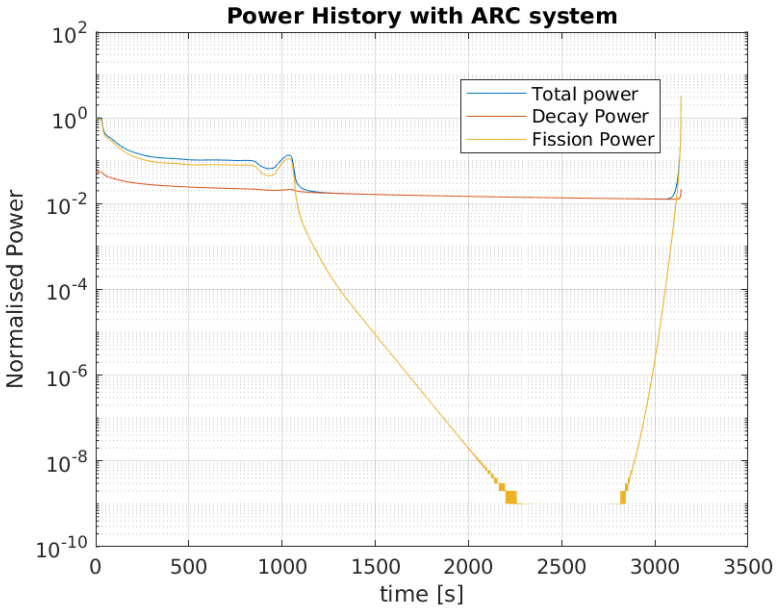

Figure 57: Power History in ULOF accident in B&B core with modified ARC inclusion

Another idea to avoid the boiling was to reduce the reactivity of the ARC system so that the Reactivity-ARC was balanced by other reactivity feedback. In fact, if we compare to the ABR case, see Figure 40, the ARC reactivity is balanced by the Doppler feedback and so, the net reactivity never reaches a value so negative. However, even with $w = \$\ 0.5$ the ARC reactivity prevailed over the other feedback. As mentioned before in the B&B case the Doppler effect is not strong enough to balance the ARC reactivity.

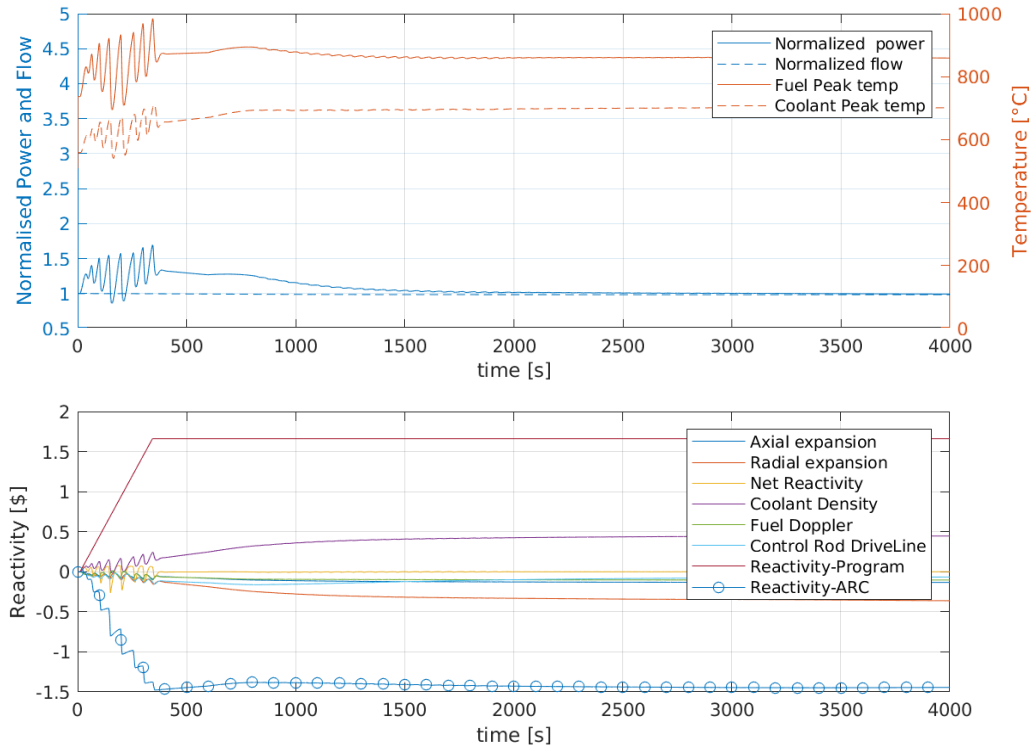

Figure 58: Response to a UTOP accident in B&B core with modified ARC inclusion.

Contrary to ULOF transient, with the introduction of the modified ARC system no boiling occurs in the UTOP transient, see Figure 58. In this case, the withdrawing of the control rod is balanced by the ARC system. We can notice an oscillator behavior similar to the one witnessed in the ABR case, see Figure 43. As mentioned, these oscillations are due to the swing between the ARC actuation and the UTOP transient. Also in this case, the oscillations don't diverge. Comparing the two cores responses (Figure 43 and 58), we can notice greater amplitudes in the fuel temperature oscillations caused by the higher thermal conductivity of the metal fuel present in the B&B reactor, as reported in Table 2.
In the ULOHS case, see Figure 59, due to a slight increase in coolant temperature the ARC starts to act at $\sim 1000s$, therefore its benefits are limited. However, with its activation, the peaks temperature reaches lower values. We can notice that in the ABR case the activation of the ARC is faster, see Figure 45. This difference is because of the slight increase of the coolant temperature in B&B core, due to the decrease of fuel metal temperature, that for his high thermal conductivity limits its increase caused by the stop of SGs. We can notice the difference in the coolant temperature in Figure 60

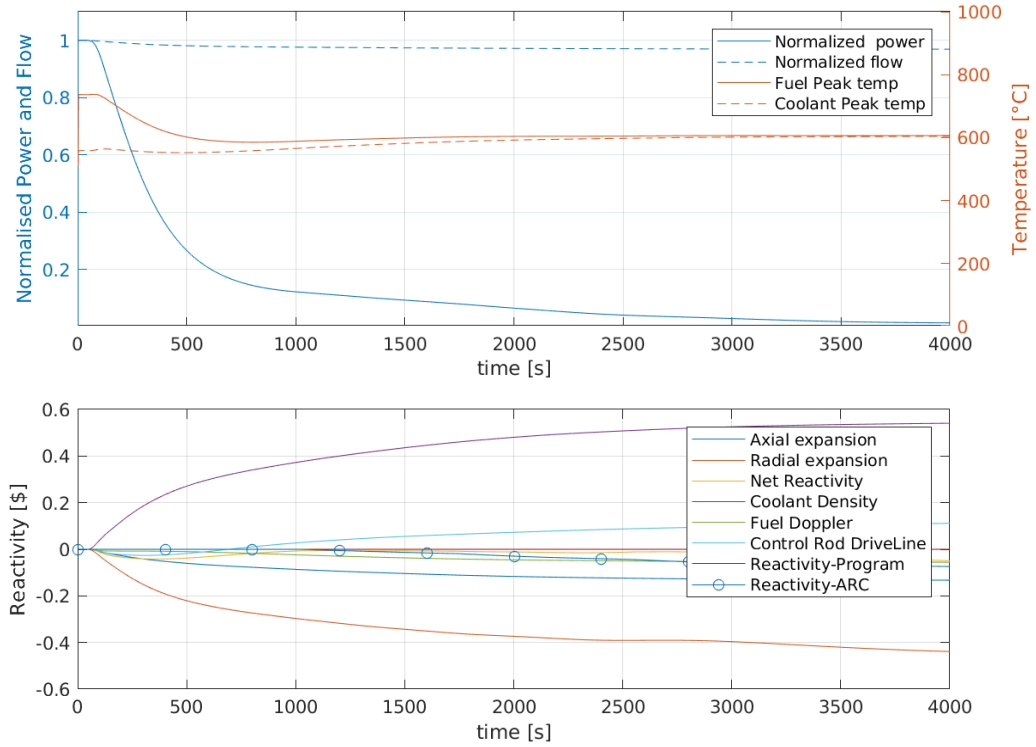

Figure 59: Response to a ULOHS accident in B&B core with modified ARC inclusion.

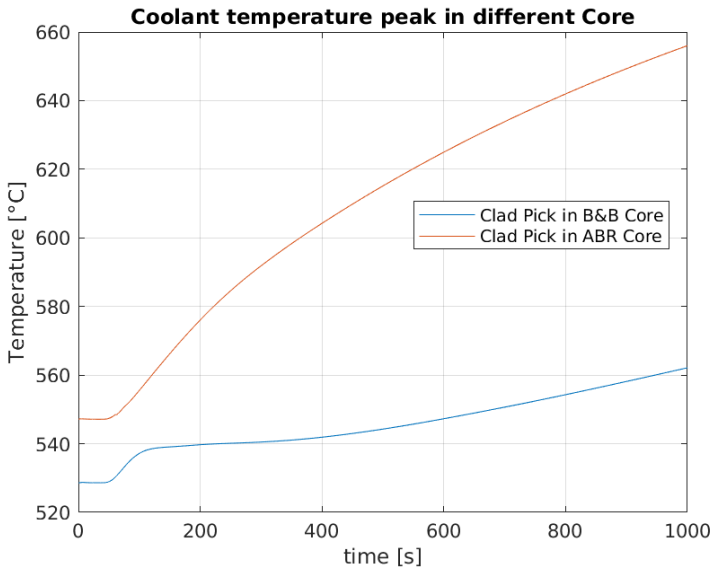

Figure 60: Peak coolant temperature during ULOHS accident in ABR and B&B

7.4.4 B&B Margins calculation

A summary of the transients results with the modified ARC inclusion is provided in Table 11.

Table 11: Peak temperatures in B&B core with modified ARC inclusion.

	Peak coolant temperature[$^{\circ}C$]	Peak fuel temperature[$^{\circ}C$]	Margin to boiling gained [$^{\circ}C$]	Margin to fuel melting [$^{\circ}C$]
ULOHS	604	738	23	-
UTOP	711	984	237	376

Table 12: Peak temperatures in B&B core with former ARC inclusion.

	Peak coolant temp[$^{\circ}C$]	Peak fuel temp[$^{\circ}C$]	Margin to boiling gained [$^{\circ}C$]	Margin to melting gained [$^{\circ}C$]
ULOHS	583	738	42	-
UTOP	720	1002	221	358

In Table 12, I have also reported the highest margins obtained with the former ARC system using the configuration found in previous work [5]. The boiling times for the ULOF transient are reported in Table 13.

Table 13: Time of boiling for the ULOF transient in diffenet configuration

	No ARC	**Former ARC**	**Modified ARC**
ULOF Time of boiling (s)	1284	520	3140

In this work, the yardstick of the parametric study for choosing the ARC configuration was the boiling time in the ULOF accident because with the modified ARC this boiling time could be delayed. That is the reason why the margins in Table 12 are similar to the ones in Table 11. As we can see the ULOHS margin to boiling is even better for the former design.
Then, I ran the simulation with the same configuration, but with $K_{back} = 10^7$. In UTOP no boiling occurs, but in the ULOF case the boiling time was equal to 866 s. As in previous work, the introduction of the ARC system worsened the oscillation behavior. Therefore, contrary to the ABR case, in B&B core the value of K_{back} is fundamental. A one-way valve with a sufficiently high value of K_{back} is needed to obtain these results.
As the last analysis for the B&B core, the ARC system was coupled to Channel 2 and Channel 3 outputs. As mentioned before, in Section 4.1.1, in the B&B core modeled in SAS fuel assemblies were grouped in 4 channels. However comparing Figure 32b and Figure 23, we can notice that Channel 4 group the batches from 7 to 12 that doesn't

produce power, so Channel 4 was not considered in this analysis. I calculated the percentage error between the peak coolant temperatures obtained with the different channels as explained in Section 7.2.4 for the ULOHS and the UTOP transients.

Table 14: Percentage Error of the peak coolant temperature in B&B core

	UTOP	**ULOHS**
Percentage error Channel1-Channel2 [%]	2,8	0.05
Percentage error Channel1-Channel3 [%]	2,7	0.13

For the ULOF, I decided to compare the boiling time. As we can notice from Table 15, the error in the boiling time is between 15-20 %, choosing different channels the boiling time decreases. The transients are the same but as we can see in Figure 61 using Channel 1 the temperature reaches higher value, therefore also the level of the absorber liquid will be higher and so the disengagement requires more time

Table 15: Percentage Error of Boiling time in B&B core

	ULOF
Percentage error Channel1-Channel2 [%]	17
Percentage error Channel1-Channel3 [%]	19

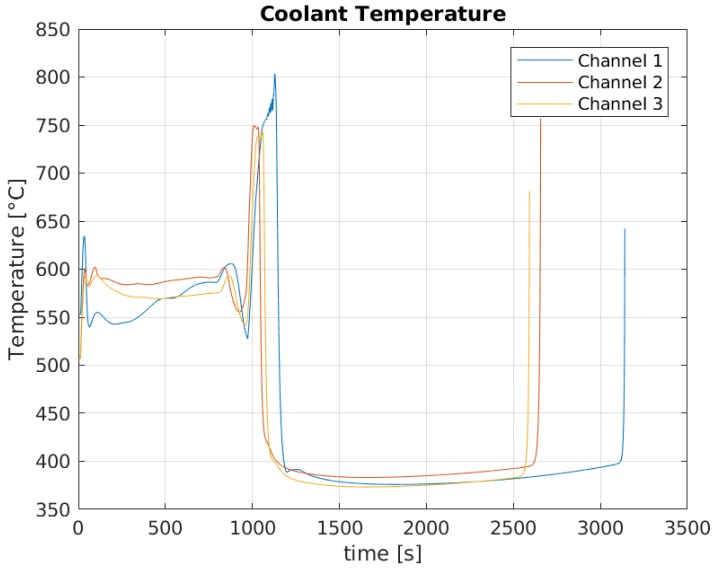

Figure 61: Peak coolant temperature in differeent Channels during ULOF accident in B&B

7.4.5 B&B Numerical accuracy

Regarding the time step used in the coupling, the UTOP and ULOF cases required a smaller time step to evaluate the transients, as we can see in Figure 62.

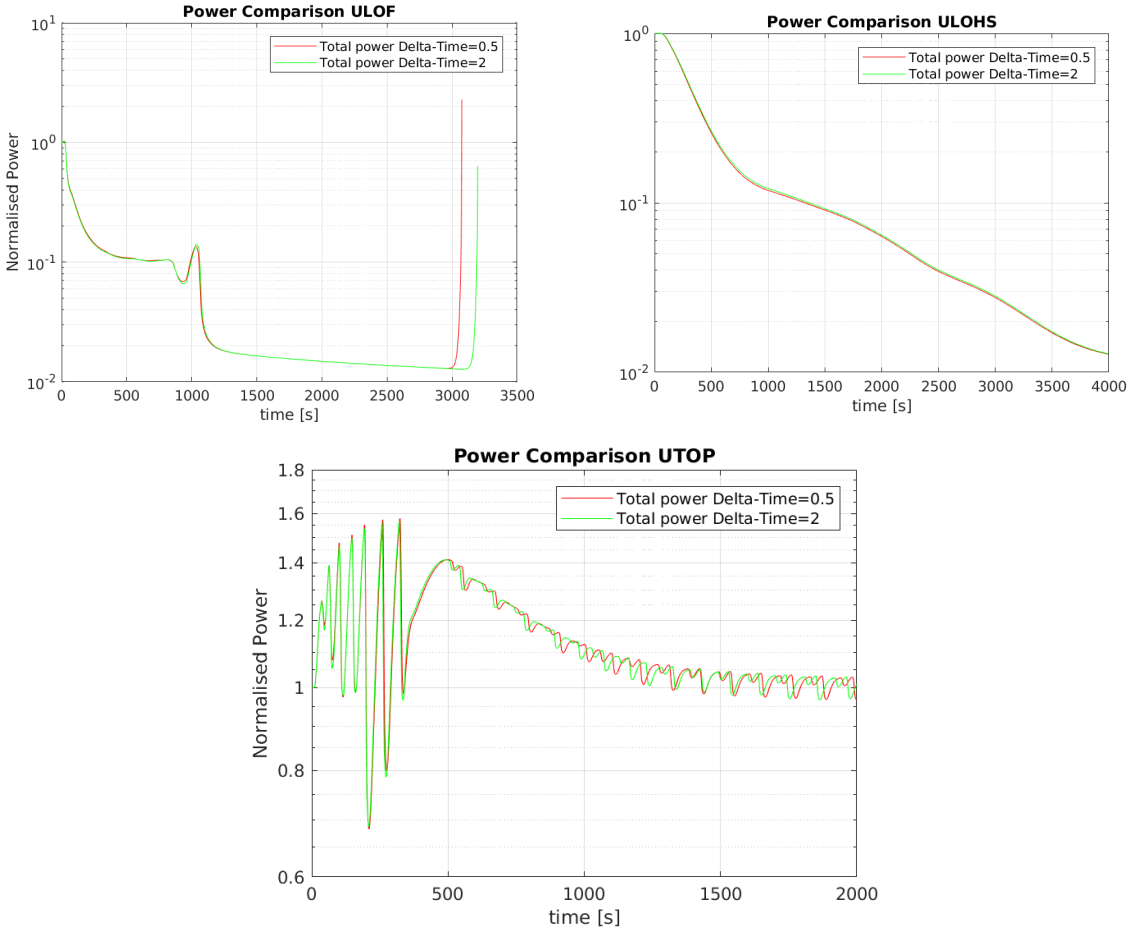

Figure 62: Comparison Delta Time in B&B transients

8 Conclusion

This works aimed to modified the ARC system to reduce the oscillation behavior seen in previous works during different transients. As we have seen through the results, the modifications make the ARC system behaves as we would have wished. In fact, for temperature coolant fluctuations, the absorber liquid stays constant at the same level preventing the consequently ARC-reactivity oscillations. This performance reduces the oscillation behavior witnessed in previous work and prevents the boiling generating form these oscillations. In the ABR case, the modified ARC system has permitted to explore a wider parameter configuration, compared to previous work [5], allowing to obtain higher margins. Future works could extend the domain of the parameters to obtain higher margins. In the B&B core, the modified ARC system has avoided the boiling for the UTOP transients, has increased the margins in the ULOHS. It has increased the boiling time in the ULOF, but no modified configuration has been found to avoid the boiling in this transient. Nevertheless, contrarily to previous work, the boiling was not caused by the oscillation generated at the transition from forced- to natural-circulation but was generated by the disengagement of the ARC system which prevented a steady-state from being achieved. Future work could perform a more precise parametric study, for example choosing different values of τ for different configurations. And if the boiling still occurs, it could be interesting to evaluate the performance of the ARC when the boiling begins. It's known that during subcooled boiling the heat transfer process is extremely efficient, therefore the ARC could operate faster. As mentioned SAS can evaluate the boiling transition.
Finally, we may conclude that in all the transient tested during this work the modifications have provided remarkable benefits. Moreover, this work underlines the possible issues caused by the normal disengagement of the ARC system. The ARC system has been thought to be a passive safety system that provides negative reactivity, but also that withdraws it once the reactor cools down. The ULOF accident in the B&B core was the one where the ARC's disengagement was tested. Therefore, future works could be focused on the study of the ARC's disengagement, for example simulating accidents that last for a limited period of time, to analyze how the transients evolve.
The results obtained during this work will be the subjects of a forthcoming paper for the Conference PHYSOR 2020. The abstract has already been accepted and the deadline for the full paper is 1^{st} October.

References

[1] Glenn F. Knoll, *Radiation detection and measurement, 4th Edition*, Wiley (2017)

[2] A. E. Waltar, D. R. Todd, P. V. Tsvetkov, *Fast spectrum reactory*, New York (2012)

[3] https://nucleus.iaea.org/Pages/evaluated-nuclear-data-file.aspx

[4] J. R. Lamarsh, *Introduction to Nuclear Reactor Theory*, New York (1983).

[5] E. Greenspan, T. Fanning, M. Fratoni, M. Gradeck, C. Keckler, S. Qvist *Enhanced Performance Fast Reactors with Engineered Passive Safety System*, Final report, University of California, Berkeley, (December 2018)

[6] J. Cahalan and T. H. Fanning, *The SAS4A / SASSYS-1 Safety Analysis Code System*, Tech. rep., Argonne National Laboratory, Lemont, IL (2012).

[7] P. Herzog, L. K. Chang, E. M. Dean, E. E. Feldman, D. J. Hill, D. Mohr, H. P. Planchon, *CODE VALIDATION WITH EBR.II TEST DATA*, Argonne National Laboratory, Lemont, IL (1992).

[8] Rui Hu, *SAM User's Guide for Beta Testing*, Tech. rep., Argonne National Laboratory, Lemont, IL (2016).

[9] Rui Hu, *SAM Theory Manual*, Tech. rep., Argonne National Laboratory, Lemont, IL (2017).

[10] Rui Hu, *Verification and Validation Plan for the SFR System Analysis Module*, Tech. rep., Argonne National Laboratory, Lemont, IL (2014).

[11] Louis Patarin, *Le cycle du combustible nucleaire*, Collection Génie Atomique, EDPN Science, (2002).

[12] Staffan Alexander Qvist,*Safety and core design of large liquid-metal cooled fast breeder reactors*, Doctor of Philosophy in Engineering - Nuclear Engineering in the Graduate Division of the University of California, Berkeley, (2013)

[13] H. W. Davinson, *Compilation of thermophysical properties of liquid lithium*, Tech. rep., NASA Lewis Reserch Center, Cleveland, OH (1968).

[14] D. W. Jeppson, J. L. Ballif, W. W. Yuan, and B. E. Chou, *Lithium Literature Review: Lithium's Properties and Interactions* Tech. rep., Hanford Engineering Development Laboratory, Hanford, WA (1978).

[15] C. B. Alcock, M. W. Chase, V. P. Iykin, and M. W. Chase, *Thermodynamic Properties of the Group IA Elements Thermodynamic Properties of the Group IA Elements* Journal of Physical and Chemical Reference Data, 23, 385 (1994).

[16] O. Foust, *Sodium-NaK Engineering Handbook* Gordon and Breach (1972).

[17] Chris Keckler, Thomas Fanning, Massimiliano Fratoni, and Ehud Greenspan, *Protected and Unprotected Transient Performance and Sensitivity in a B&B Core*, Conference: 2019 ANS Annual Conference, At Minneapolis, MN.

[18] I. E. Idelchik, *Handbook of Hydraulic Resistance 3rd edition*, (1994).

[19] C. Keckler, M. Fratoni, and E. Greenspan, *On the importance of control assemble layouts in standing wave B&B Cores* PHYSOR 2018 Cancun Mexico

[20] https://en.wikipedia.org/wiki/Moody-chart